RCA REVIEW

A Quarterly Journal of Radio Progress

Published in July, October, January and April of Each Year by

RCA INSTITUTES TECHNICAL PRESS

A Department of RCA Institutes, Inc.

75 Varick Street New York, N. Y.

VOLUME III October, 1938 NUMBER 2

CONTENTS

PAGE

U-H-F Equipment for Relay Broadcasting 133
W. A. R. BROWN

Review of Ultra-High-Frequency Vacuum-Tube Problems 146
B. J. THOMPSON

A Survey of Ultra-High Frequency Measurements 156
L. S. NERGAARD

Temperature Reduction in High Powered Loudspeakers 196
FRANK MASSA

Microphone Wind Screening 203
WILLIAM D. PHELPS

Selective Side-Band vs. Double Side-Band Transmission of Telegraph and Facsimile Signals 213
J. ERNEST SMITH, BERTRAM TREVOR, PHILIP S. CARTER

Tensor Analysis and Its Application to Equivalent Circuits 239
D. W. EPSTEIN

Our Contributors 255

SUBSCRIPTION:

United States, Canada and Postal Union: One Year \$1.50, Two Years \$2.50, Three Years \$3.50
Other Foreign Countries: One Year \$1.85, Two Years \$3.20, Three Years \$4.55
Single Copies: 50¢ each

Entered as second-class matter July 17, 1936, at the Post Office at New York, New York, under the Act of March 3, 1879.

Printed in U.S.A.

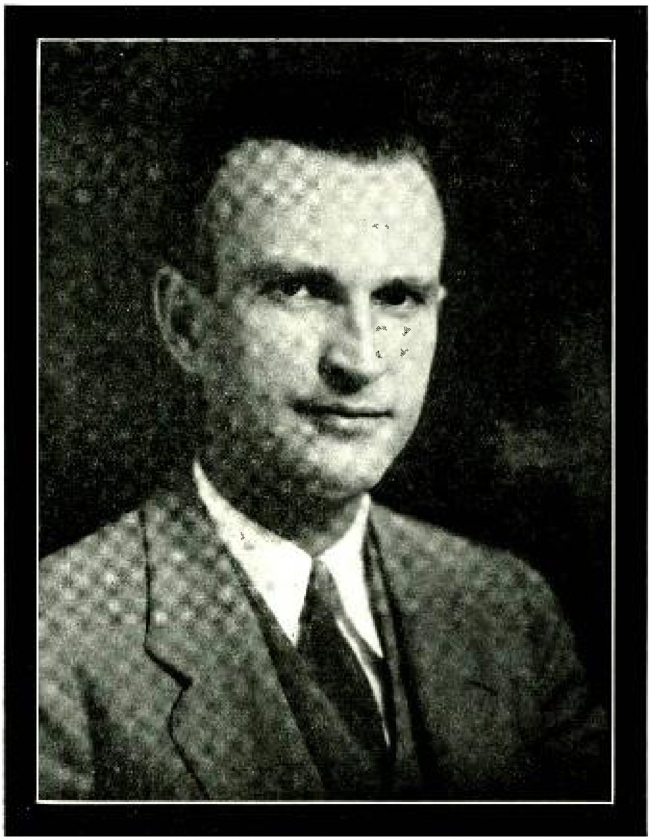

John C. Warner

1896-1938

Vice-President, RCA Manufacturing Company, Radiotron Division
and Member of the Board of Editors, RCA Review

Resolution

The Board of Editors of the RCA REVIEW is grieved to learn of the death of one of its members,

John C. Warner

The members of the Board have long known and esteemed Mr. Warner as a man of most genial, friendly, and manly personality. They have enjoyed the benefit of his wise counsel and capable efforts in his association in the activities of the Board, and they have observed with admiration the success of his chosen career.

The members of the Board wish to convey to his wife and family their sincere condolence and to express their deep grief at the loss of so thoughtful and admirable a colleague and friend.

Passed by the Board of Editors of
RCA REVIEW, October 10, 1938.

U-H-F EQUIPMENT FOR RELAY BROADCASTING

BY

W. A. R. BROWN

Assistant Development Engineer, National Broadcasting Company, Inc.

Summary—*Several types of portable transmitting and receiving equipment, which have recently been developed to meet the increasing demands imposed upon operating facilities by the constantly expanding scope of ultra-high-frequency relay broadcasting are described, and their functions in relay-broadcast operations outlined in this paper.*

RELAY broadcasting is a recent designation for a form of program transmission of some years' standing which has steadily increased until it is now an integral part of radio broadcasting. This interesting and colorful service furnished to the listener is another step in the expansion of broadcasting brought about by the desire of the broadcaster to better serve the public.

A number of intermediate and ultra-high frequencies has been allocated to this service. The ultra-high-frequency allocations in the 30-42 Mc band are particularly suitable for many phases of relay-broadcast operation because they permit the use of radiating systems of comparatively high efficiency, but of small physical dimensions. Readily portable equipment can be used because the efficiencies of many standard tubes are still high at these frequencies. Propagation characteristics are also suitable as attenuation is not excessive and wave interference is not too pronounced.

In relay-broadcast operations the radio link permits the presentation of programs from points where wire facilities are not available or their installation is impractical. These program-origination points may be almost anywhere: aeroplanes, ships, automobiles, golf courses, airports.

Before this service reached its present stage of efficiency a long period of experimental development was necessary. Work in this field up to 1936, and particularly the work at 300 Mc, has been described previously.[1] This paper will describe briefly the u-h-f relay-broadcast

[1] "Micro-waves in NBC Remote Pick-ups," R. M. Morris, RCA REVIEW, July, 1936.

equipment which NBC has since developed and is now standard in all its divisions throughout the country.

Equipment for this service must necessarily be portable, rugged, efficient, easily operated, and reliable in operation. It must also operate under a wide variety of conditions.

The present u-h-f equipment consists of five major units: the 25-watt general-utility transmitter, the 2-watt pack transmitter, the 0.2-watt miniature transmitter, the program receiver, and the cue receiver.

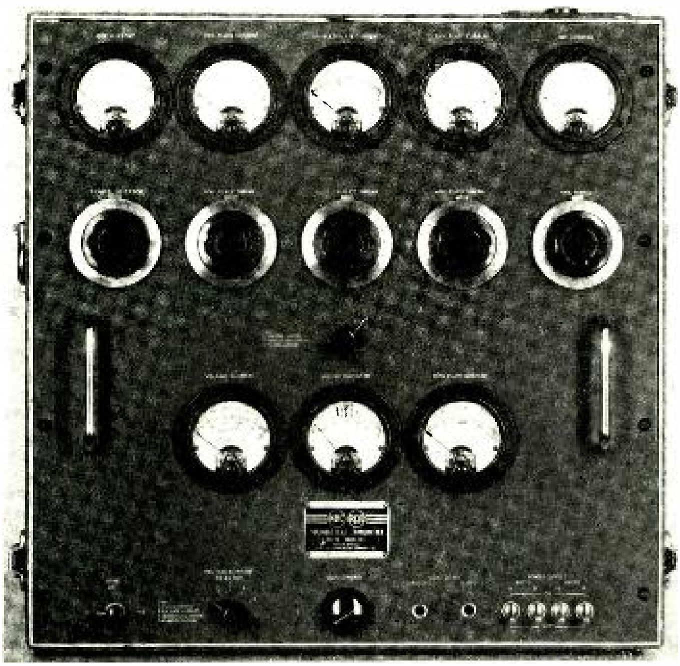

Fig. 1—Utility transmitter.

The utility transmitter, with 25 watts output, is the highest powered portable transmitter of our u-h-f relay-broadcast line. Its power renders it useful for a wide variety of applications, including (a) mobile transmission from automobiles, trains, aeroplanes; (b) as a base transmitter at wire-line terminals for cue transmission and communication to program-origination points in the field; (c) as an automatic relay-transmission point when low-power program-origination transmitters cannot reach the wire-terminal location directly, etc.

The 25 watts power output represents a compromise between tube efficiencies and the necessity for keeping the equipment, including the associated a-c power supply, sufficiently small in size and low in weight to be readily portable. The transmitter, without the power supply, is shown in Figure 1. Its size is 19″ × 19¼″ × 10½″ and its weight is 73 pounds. For operation from 110-volt d-c sources a small auxiliary motor-generator is employed with the power supply. Storage battery operation of the transmitter is accomplished by the use of a dynamotor. This power-supply unit may also be used to provide power for the intermediate-frequency relay-broadcast transmitter which is identical in size and output.

Conventional circuits are utilized in the transmitter. The schematic diagram is shown in Figure 2. Harmonic V-cut crystals with low-temperature coefficients are employed to control the transmitter frequency and there is provision for switching to any of four crystals. Plate modulation is employed and 100 per cent modulation may be obtained with less than 4 per cent harmonic distortion (arithmetical sum).

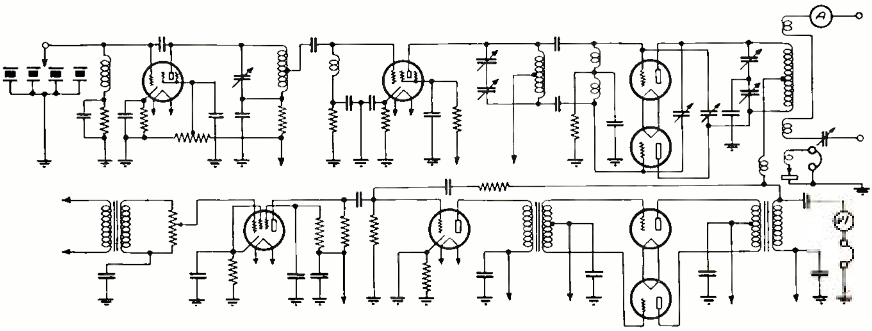

Fig. 2—Schematic of utility transmitter.

The r-f section is contained in the upper half of the assembly and consists of three stages: a crystal oscillator, a doubler, and a push-pull power amplifier. The audio-frequency section is contained in the lower half of the assembly and also consists of three stages: a speech amplifier, a driver, and a push-pull Class AB modulator. About 8 db of negative feedback is utilized to reduce distortion. The frequency characteristic is peaked at 8,000 cycles, to improve the signal-to-noise ratio at the higher audio frequencies, and is down 3 db at 50 cycles.

The antenna-coupling system permits the use of either a grounded quarter-wave radiator or a remotely located radiator fed by a two-wire or concentric transmission line.

Both aural and visual monitoring are obtained from the secondary of the modulation transformer, the former with headphones and the latter with a level indicator. Radio headphone monitoring is obtained from an enclosed crystal detector and pick-up coil. Comprehensive metering facilities are provided, for plate currents of all tubes, grid currents of all r-f tubes, modulator-bias voltage, and filament voltage. Some of these are indicated directly and others by a universal meter and selector switch. Careful consideration was given in the

Fig. 3—Pack transmitter.

design to accessibility of parts to facilitate repairs if necessary while in the field.

The 2-watt pack transmitter, shown in Figure 3, is a highly portable, medium-powered, self-contained unit designed primarily to provide relay-broadcast transmission facilities while carried as a pack. It is normally carried in a leather case securely strapped to the announcer's back and the only piece of external equipment is the microphone, which is carried by hand. Thus the announcer is free to move around wherever necessary. With an output power of 2 watts it is used chiefly for transmission over distances of a few hundred yards to a mile, as for example, from locations on a golf course to the line terminal in the club house. Under more favorable conditions, the range is considerably greater. For instance, when receiving on top of the RCA Building in New York City, at an elevation of 850 feet, this transmitter is frequently employed for program transmission from vessels in the harbor, some four or five miles distant. Under highly favorable transmission conditions, such as from aeroplanes, program transmission ranges of fifteen miles or more are obtained. It is also employed sometimes as a cue transmitter when the relay-broadcast circuits are short.

The design of this pack transmitter is based upon several years experience in this phase of broadcasting. Although the basic circuit is conventional, several features have been incorporated which con-

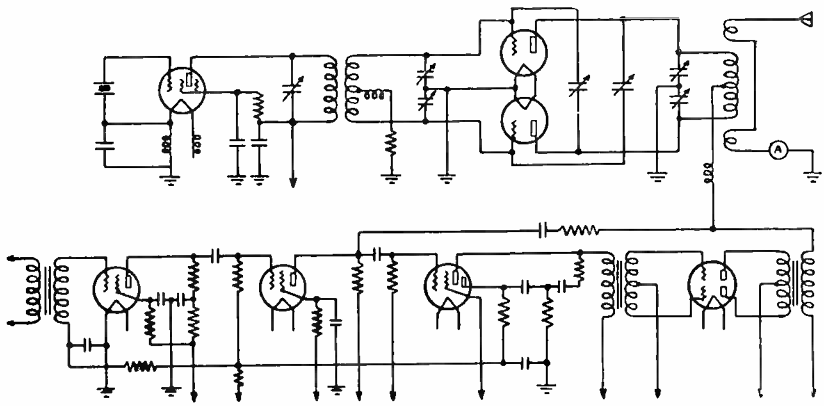

Fig. 4—Schematic of pack transmitter.

tribute to high efficiency and utility and render the unit rather outstanding in its field. A schematic diagram is shown in Figure 4. The power output of 2 watts represents, of course, the inevitable compromise between size, weight, tube capabilities, power supply, etc. The total weight, including the self-contained power supply, is 33 pounds and the dimensions of the transmitter are 17½" high, 12⅝" wide, and 4½" deep. Figure 3 shows the three sections into which the unit is divided mechanically. The upper section contains the r-f equipment, the middle section the a-f equipment, and the lower section the power supply. Any or all of these sections may be readily removed from the chassis. This greatly facilitates maintenance.

For obvious reasons the transmitter is crystal controlled. Plate modulation is employed and 100 per cent modulation is obtained with low harmonic distortion using negative feed-back. One of the distinctive features of this transmitter is automatic audio-gain control. This is a very valuable operating feature as it reduces the extreme vocal dynamic ranges which frequently occur in this type of broadcasting and assures high modulation levels without over or under modulation for all except extremely abnormal voice levels.

The r-f section consists of two stages: a crystal-controlled electron-coupled oscillator-doubler and a push-pull power amplifier. To obtain 2 watts output it is necessary to operate all tubes somewhat above normal filament potentials. Tube life is shortened under these conditions and tubes are discarded after 50 hours operation to provide a wide margin of safety.

The a-f section contains four stages: a two-stage speech amplifier, a driver, and a modulator. These possess sufficient gain, after utilizing degeneration, to permit full modulation with an RCA 50-A inductor microphone. Correct polarization of the audio circuits to obtain maximum undistorted power is another operating feature which contributes to the efficiency of this transmitter. By taking advantage of the phenomenon that the peak amplitudes of most voice waves are highest in one direction, it is possible to secure greater than 100 per cent modulation upward while not exceeding 100 per cent downward. Automatic audio-gain control is obtained by feeding a portion of the rectified-driver output to the input of the speech amplifier through a resistor-condenser combination of suitable delay characteristics. The frequency characteristic is purposely peaked about 3 db from 5,000 to 10,000 cycles and is down 3 db at 60 cycles. This departure from a flat characteristic is an attempt to compensate for difficulties encountered in operation. Our experience has indicated that general crowd noise and wind noise is often most pronounced at frequencies below 80 cycles while the hiss type interference experienced at the receiving point from ignition and diathermy frequently appears most pronounced at the higher audio frequencies.

The antenna construction and installation is particularly convenient for operation. It is a continuously-adjustable four-section semi-flexible telescopic assembly which is an integral part of the transmitter and telescopes into the case when not in use. The system is designed to operate as close to resonance as is necessary to obtain correct loading of the power amplifier.

Two meters are contained in the transmitter assembly. One indicates antenna current and the other, by selective switching, indicates filament and plate voltages, oscillator, power-amplifier, and modulator-plate currents, and power-amplifier grid current.

Standard dry batteries are employed for the power supply which has sufficient capacity for nine hours continuous operation. To obtain this length of service a reserve 45-volt battery is included in the power supply and is switched into service after about six hours transmission. This is an operating convenience which permits considerable test transmission to be conducted prior to a broadcast and still allows a comfortable margin of available power for a lengthy period of program operation. For continuous operation at a fixed location, as for cue-channel transmission, provision has been made for plugging in an external heavy-duty battery supply.

The miniature transmitter, shown in Figure 5, is the smallest and most recent of our u-h-f transmitters. It is a small, entirely self-contained, extremely portable, low-powered transmitter for short-

Fig. 5—Miniature transmitter.

range transmission. Although its small size is productive of considerable novelty appeal the unit was actually developed to fill a definite operating need and has already introduced a new technique in program presentation. It is particularly useful for program origination in crowded areas, or on locations where the size of the equipment must be kept to an absolute minimum or where transmission distances are short. One of its most distinguishing features, and one which at times is a valuable operating convenience, is that it can be readily passed from hand to hand. The working range is dependent upon propagation conditions and the signal-to-noise ratio at the receiver and may vary from a few hundred feet to half a mile.

The transmitter, with built-in microphone and power supply, is housed in an aluminum case 10″ × 4½″ × 5¾″ and weighs 7½ pounds. Despite its small size an output of 0.2 watt is obtained. Crystal control assures frequency stability and automatic audio-gain control maintains proper modulation levels.

The circuits employed are quite conventional and the efficiency of the unit is the result of good detail design. A schematic is shown in Figure 6. The r-f section consists of a crystal oscillator-doubler stage and a power amplifier while the audio-frequency section consists of a single-stage speech amplifier and a modulator. Heising modulation is employed and modulation values of approximately 90 per cent are obtained by the expedient of dropping the power-amplifier plate voltage.

Automatic audio-gain control is particularly effective in the maintenance of proper modulation levels under the conditions frequently encountered in operation of this transmitter. With 12-db peak gain

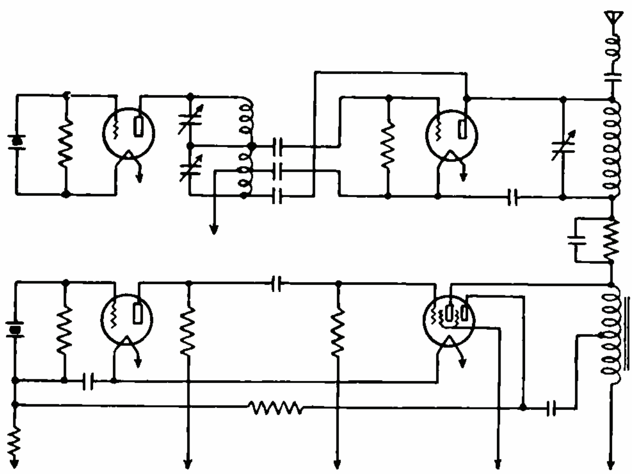

Fig. 6—Schematic of miniature transmitter.

reduction it effectively eliminates overloading of the transmitter except on very pronounced peaks.

A crystal microphone is employed in the interest of weight reduction and is concealed behind a metal grille on the front of the unit. The overall audio-frequency characteristic of the transmitter drops off rapidly above 5500 cycles and is therefore not as good as the larger transmitters. It is quite adequate, however, for voice transmission which is the only type normally employed with this unit.

The antenna is fed through an insulator in the top of the housing. It consists of a short dural rod with a spring coil at the lower end which provides the necessary mechanical flexibility for the antenna and also some electrical loading.

The power supply is a special battery block in which is combined the filament, plate, and bias supplies. This is sufficient for nine hours continuous operation and is so designed that the *A* and *B* capacities are exhausted practically simultaneously.

Jacks and an external meter permit determination of oscillator, power-amplifier, and modulator-plate currents. Tuning is also accomplished externally by the use of a wand which is inserted in small openings in the housing to vary the tuning condensers.

The program receiver shown in Figure 7 is a portable, high-quality, superheterodyne receiver designed primarily for reception of crystal-controlled relay-broadcast transmitters. This type of receiver possesses a number of advantages over the super-regenerative receivers previously used for this service, one of the most important being the

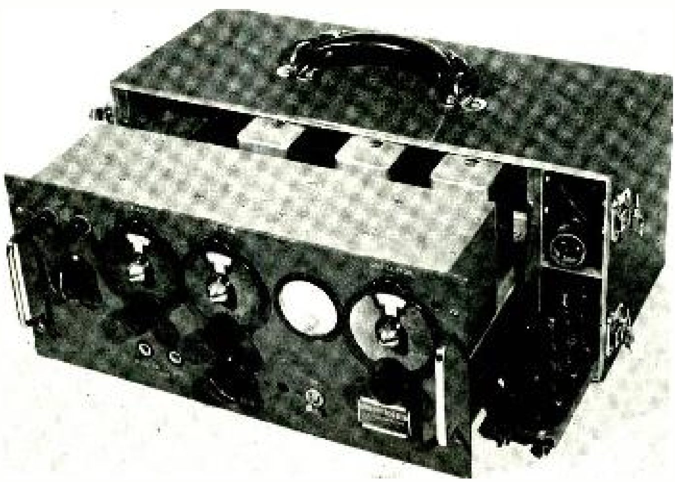

Fig. 7—Program receiver.

absence of re-radiation. The receiver dimensions are $19\frac{1}{4}'' \times 9\frac{3}{4}'' \times 8\frac{1}{2}''$, and its weight, exclusive of the external battery-power supply, is 26 pounds.

Conventional superheterodyne circuits, with avc, are employed, as follows: one stage r-f amplifier, first detector, oscillator, two-stage i-f amplifier, and second detector-audio amplifier. Figure 8 shows the schematic diagram. The oscillator operates 5.9 Mc above the signal frequency. This choice of intermediate frequency was a matter of design convenience to obtain the desired band-width characteristic.

The design and operating characteristics of the receiver were based largely upon the conditions under which the unit would operate in the field. At that time there were still some self-excited transmitters in use and provision was therefore made for variation of the i-f amplifier band width, up to a maximum of 100 kc, by the inclusion of variable coupling in each i-f transformer. With a 60-kc band pass the selectivity is sufficient to reduce an undesired signal 75 kc off resonance by approximately 44 db. The selectivity can be improved considerably when necessary. Image response under above conditions is minus 72 db.

High gain is not essential in this receiver since in normal broadcast operation it would feed into a field-program amplifier with 100 db gain. There is sufficient amplification, however, to give a plus 4-db level at the receiver output with 100 microvolts signal input. With this gain the audio characteristic is practically flat from 30 to 10,000 cycles. It may be of interest to note that a voltage gain of 15 is obtained in the r-f amplifier stage with an RCA acorn tube.

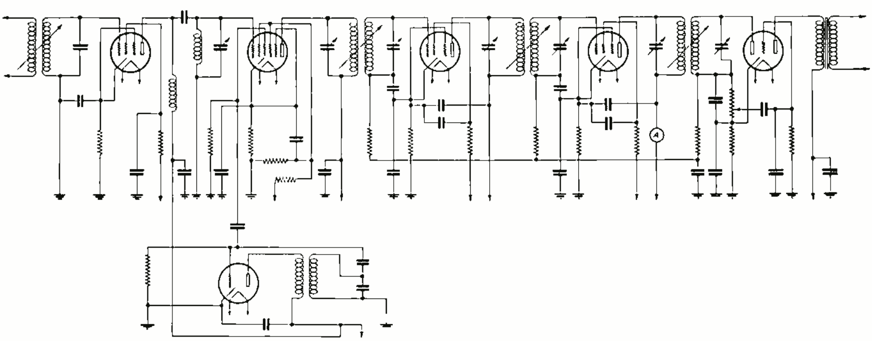

Fig. 8—Schematic of program receiver.

A half-wave antenna is usually employed for reception and the input circuit is designed to operate from a low-impedance two-wire transmission line. Although the minimum useful signal input is about 10 microvolts, in the absence of external noise, the utility of the receiver is dependent upon the signal-to-noise ratio and for satisfactory program use a ratio of about 25 db or more is desirable. Receiving conditions on the roof of the RCA Building in New York City may be cited as a typical example. Here, when the noise input averages about 30 microvolts, signal inputs of about 600 microvolts are considered satisfactory for program use. This corresponds to a signal-to-noise ratio of 26 db.

There are three tuning controls: r-f amplifier, detector, and oscillator. Separate controls eliminate any possible difficulties of gang tuning and simplified design. No operating difficulties are introduced since relay-broadcast frequencies are limited in number and the tuning dials are marked for these frequencies. However, a complete oscillator-dial calibration is provided to assist in tuning other frequencies, if necessary.

A very valuable operating feature is a tuning meter which indicates the i-f amplifier plate current and is calibrated against signal input. This permits easy determination of relative signal strengths at various locations, good and poor transmission areas and also signal-to-noise ratios.

Headphone monitoring facilities are provided and a fixed 20-db pad is incorporated in the receiver for matching impedances when feeding a field amplifier.

Fig. 9—Cue receiver.

The cue receiver shown in Figure 9 is a small, light-weight, entirely self-contained superheterodyne receiver designed primarily for the reception of cues and instructions at relay-broadcast program-origination points. Under these conditions extreme portability and a high degree of sensitivity are frequently essential, but the quality need not be more than sufficient for good speech intelligibility. When used in conjunction with the pack transmitter the engineer who accompanies the announcer carries the receiver in a leather case slung across the chest. All controls are within easy reach and it can be carried for hours without discomfort. The total weight of the complete unit and carrying case is only 13 pounds and its size is but $9\frac{3}{4}'' \times 4\frac{3}{4}'' \times 10\frac{1}{4}''$. The power supply is the same battery block that is used in the miniature transmitter and will provide eight hours continuous service. Battery replacement is convenient and rapid.

Conventional superheterodyne circuits, with avc, but no pre-selection, are employed in the following circuit arrangement: first detector, oscillator, two-stage i-f amplifier, second detector-audio amplifier. The schematic is shown in Figure 10. The elimination of an r-f amplifier stage was dictated by the necessity for a minimum of weight, although it introduced certain disadvantages.

One interesting design feature is the use of a triode tube in parallel with the triode section of a pentagrid converter to increase

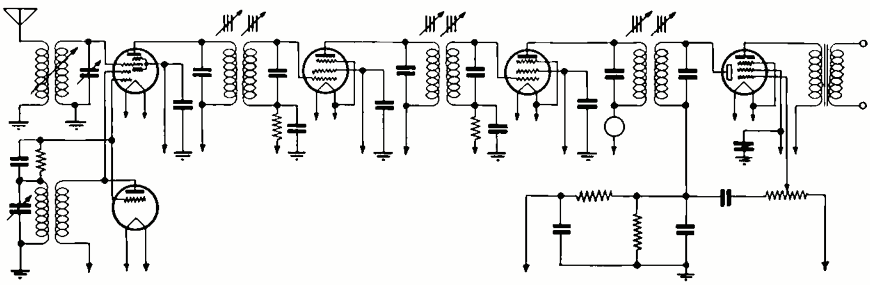

Fig. 10—Schematic of cue receiver.

the mutual conductance of the latter and thereby improve its oscillation performance at the ultra-high frequencies. The oscillator operates 4.1 Mc below the signal frequency. Transformers with adjustable iron cores to facilitate circuit alignment are employed in the i-f amplifier. Although the selectivity is limited somewhat by lack of pre-selection it is sufficient for relay-broadcast operation. A signal 75 kc off resonance is down 23 db. Image response is approximately minus 35 db. The antenna is of the telescoping, flexible, whip type, similar to that used in the pack transmitter. It is an integral part of the unit and telescopes into the receiver when not in use.

Many of the operating features are similar to those of the program receiver and for the same reasons. Two tuning dials are employed: first detector and oscillator. Dial settings for the usual relay-broadcast frequencies and oscillator-dial calibration for spotting other frequencies render operation simple. A tuning meter for indicating relative signal intensities has also been incorporated in this receiver and operates in the same manner as in the program receiver.

The output transformer is specifically designed to work into high-impedance headphones and therefore this receiver is not suitable for feeding an amplifier or line. A manually operated gain control is also provided to keep the phone levels below values where acoustical feed-back to the associated pack transmitter may occur.

At these operating frequencies there are several advantages in favor of horizontally polarized transmission, such as somewhat lower noise levels, and higher average signal strengths. However, in many phases of relay-broadcast operation these advantages cannot be realized because physical limitations permit only vertical transmission. This is particularly true with the pack and miniature transmitters.

With the low power of these transmitters the operating personnel must therefore exercise a high degree of engineering ability to cope successfully with the problems which the varied conditions of operation produce.

Considerable attention has been given to the use of standardized directive receiving antennas, but the problem is not easy of solution because of the widely different conditions which exist at most receiving locations.

Acknowledgment

The transmitting and receiving equipment described above represents the combined efforts of several individuals. Acknowledgment is made to A. A. Walsh, who designed the utility transmitter and the pack transmitter; to J. L. Hathaway, who designed the miniature transmitter; to W. C. Resides, who designed the program receiver and the cue receiver; and to R. M. Morris, Development Engineer, under whose direction the development was conducted.

ADDENDA

The paper, "Figure of Merit for Television Performance," by A. V. Bedford, in the July issue of RCA Review, was delivered before a joint meeting of the Institute of Radio Engineers and the Radio Manufacturers Association, at Rochester, in November, 1937, and was published in part in the November issue of the *R.M.A. Engineer.*

The number of words per minute at present required for an amateur radio license is 13, rather than the previous requirement of 10 as stated in the article on "Amateur Radio," in the July issue of RCA Review.

REVIEW OF ULTRA-HIGH-FREQUENCY VACUUM-TUBE PROBLEMS

BY

B. J. THOMPSON

Research and Engineering Department, RCA Radiotron Division,
RCA Manufacturing Company, Inc., Harrison, New Jersey.

Summary—*The effects of electron transit time and of lead inductance and interelectrode capitance which become of importance at ultra-high frequencies are reviewed. It is shown that, in radio-frequency amplifier tubes for use in receivers, the most serious effect is the high ratio of input conductance to transconductance, which is independent of the transconductance and is proportional to the square of the frequency. This ratio may be reduced by reducing the electron transit time, the lead inductances, and the interelectrode capacitances. In power amplifiers and oscillators for transmitters, the important effects are much the same as in receiving tubes. The solution is complicated, however, by the problem of obtaining sufficient power output in a small structure.*

I. INTRODUCTION

THE intensive use of all longer radio wavelengths by established services has forced new services and expansions of the old into the shorter wavelength portion of the radio spectrum. Fortunately, it has been found that these shorter wavelengths have advantages over the longer for many applications. In fact, the known or expected advantages of the very short wavelengths have brought about the use, or proposed use, of wavelengths from 7 meters to 10 centimeters, even though the spectrum of longer wavelengths is not saturated. Among these advantages are limited transmission range, making possible the multiple use of one wavelength or providing secrecy; wide available band width for a single channel, necessary for television; high directivity attainable with small antenna systems, including the possibility of using "wave guides"; and high resolving power of the waves, making possible, for example, navigational aids for ships and airplanes.

As shorter and shorter wavelengths have been used, it has been found that the vacuum tubes of the transmitters and receivers place a serious limitation on the attainable performance. Ultimately, improved performance can only be attained by radical improvements in vacuum-tube design or by radical departures from conventional modes of vacuum-tube operation. It may be said that the problem of the development of satisfactory apparatus for the ultra-short wavelengths, on which depends the development of this promising field, is identical with the problem of designing better vacuum tubes for ultra-high-frequency operation.

In recent years very considerable advancements have been made in the design of vacuum tubes for high-frequency use. Most noteworthy has been the trend toward the use of conventional modes of operation at frequencies where formerly such operation was not considered feasible. This has been the result of improved design based on increased theoretical knowledge of the limitations to high-frequency tube performance and on the development of new manufacturing techniques. Noteworthy advances have also been made in the performance of some of the unconventional types of vacuum tubes. These advances naturally focus attention on the question of what may be expected in the future.

Foretelling the future is a dangerous though fascinating game. We shall be on surer ground if we confine ourselves to an attempt to understand the nature of the limitations which restrict the design and operation of present ultra-high-frequency tubes. Such an understanding should indicate the directions in which progress may be expected.

II. Fundamental Considerations

At low frequencies any effects of electron transit time or electrode leads are usually ignored. At the higher frequencies which we are discussing, this may no longer be done. The limitations imposed on the performance of high-frequency tubes are so largely the result of lead and transit-time effects that we must consider these in some detail.

The current flowing to an electrode in a vacuum tube is frequently viewed as resulting from the arrival of electrons at the electrode and as being, therefore, proportional to the instantaneous rate of arrival. This viewpoint is fairly satisfactory at frequencies where the electron transit time is a vanishingly small part of the period, but it is completely misleading at higher frequencies where the transit time becomes appreciable.

A useful and satisfactory viewpoint is to consider the current flow to an electrode the result of the motion of charges in the space between electrodes. Consider two infinite parallel-plane electrodes as in Figure 1 with a voltage E applied between them. The electric field F between the electrodes is simply $\frac{E}{d}$ where d is the distance between electrodes. If a small positive electric charge q is placed between the plates very close to the positive plate there will be an increase in the charge of the positive plate of amount $-q$ and no increase in the charge of the negative plate. There will be a force acting on the charge of magnitude Fq tending to move it toward the negative plate. If the charge is allowed to move, the work done on it by the field is equal to Fqx where x is the distance the charge has moved. Now, the work done on the charge is supplied from the battery. The work done by the battery is equal to the product of its voltage E and the change

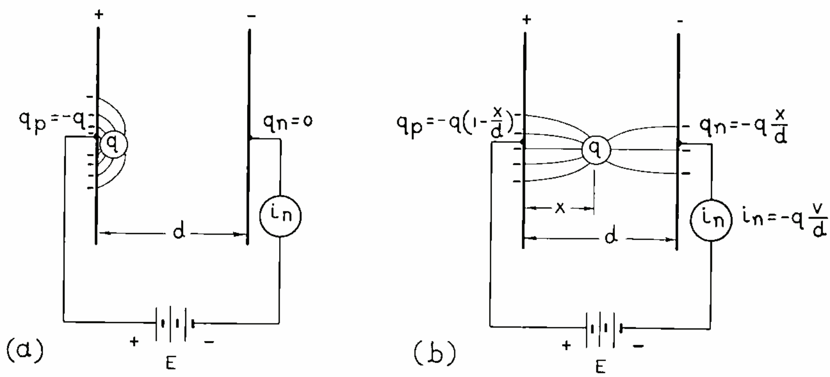

Fig. 1—Distribution of induced charge and current flow between parallel planes as a charge q moves between the planes. (a) illustrates the condition where the charge is an infinitesimal distance from the positive plane. (b) represents the condition where the charge has moved a distance x away from the positive plane and is moving at a velocity v.

in charge induced on one of the plates. If q_n represents the charge induced on the negative plate, we may write

$$-Eq_n = Fqx$$

$$= \frac{Eqx}{d}$$

or

$$q_n = -q\frac{x}{d}.$$

In other words, the charge induced on the negative plate is proportional to the charge in the space and to the fraction of the total distance between plates which the charge has covered. Of course, the charge q_p induced on the positive plate is equal to the difference between the space charge and the charge induced on the negative plate, since the total charge induced on the two plates is always equal in magnitude and opposite in sign to the space charge.

The current flowing to the negative plate as a result of the motion of the charge q is equal to the rate of change of the charge q_n. This is simply

$$i_n = \frac{dq_n}{dt} = -\frac{q}{d}\frac{dx}{dt} = -q\frac{v}{d}.$$

In other words, the current flowing as a result of the motion of a charge between two plates is equal to the product of the charge times its velocity divided by the distance between the plates. Of course, the current flow to the positive plate is always instantaneously equal in magnitude to the current to the negative plate.

The important conclusion which we may draw from this simple analysis is that in a vacuum tube the current produced by the passage of an electron does not flow simply at the instant the electron reaches the electrode, but flows continuously in all adjacent electrodes while the electron is in motion. If the electron moves between parallel plates, the current flow does not depend on the position of the electron, but only on its velocity.

The total current flowing to an electrode may be determined by adding up all the minute currents produced by individual electrons, or more analytically by integrating the currents produced by infinitesimal strips of space charge.

In a steady-state condition, the current flow determined by such integration (or the measured value) is exactly equal to the rate of arrival of electrons at the electrodes. When the current is varying with time—as in the case of an amplifier tube with an alternating voltage applied to the grid,—the rate of arrival of electrons at the electrode may be greater or less than the actual current flowing because of the finite transit time of the electrons. If the current is momentarily increasing, the rate of arrival of electrons is less at any instant than corresponds to the flow of electrons in the space.

These considerations show that the current flowing to an electrode may be different from the rate of arrival of electrons at the electrode. It is also possible to have a current flowing to an electrode at which no electrons arrive, if the number or velocity of the electrons approaching the electrode is instantaneously different from the number or velocity of those receding from it.

From these elementary considerations we may understand qualitatively the various transit-time effects which are observed in high-frequency vacuum tubes.

The transit-time effects in the grid circuit are of most interest to us because they are the only effects in that circuit when no electrons or ions reach the grid. Because of the instantaneous difference between the rates at which electrons approach the grid and recede from it, there is an alternating current flowing to the grid which is proportional to the transconductance, to the alternating grid voltage, to the frequency, and to the electron transit time. This current leads the alternating grid voltage by 90 degrees. Hence, one may say that there is an electronic component of grid capacitance which is proportional to the transconductance and to the transit time. This capacitance is the well-known increase in "hot" capacitance over "cold" capacitance. While it is a transit-time effect, the equivalent capacitance does not vary appreciably with frequency, though, of course, the capacity current is proportional to the frequency.

Because of the electron transit-time, there is a shift in the originally 90-degree phase relation between grid voltage and grid current with increasing frequency. This phase shift results in an equivalent shunt resistance between grid and cathode which is inversely proportional to the transconductance and to the square of the frequency and of the transit time. This resistance, which is normally very high at frequencies of the order of 1 megacycle, may become as low as several thousand ohms at a frequency of 50 megacycles in conventional receiving tubes.

There are also transit-time effects in the plate circuit. First, there is a phase lag between plate current and grid voltage which is proportional to the frequency and to the transit time. The relation between plate current and grid voltage is normally expressed as the transconductance. Of course, properly speaking, conductance can refer only to the component of alternating plate current which is in phase with the grid voltage. The quotient of the total alternating plate current divided by the alternating grid voltage is therefore called the transadmittance.

Second, the magnitude of the transadmittance decreases somewhat as the frequency is increased. This effect is normally quite small at the maximum frequency at which a given tube may be used.

Third, there is a decrease in the internal plate resistance of the tube as the frequency is increased. This is also usually quite small.

These are the principal transit-time effects. Lead effects are also of importance.

Consider the simple triode shown in Figure 2 with inductance in the cathode and plate leads and with capacitance between grid and cathode and grid and plate. The plate has no external load and the frequency of the voltage applied to the grid is well below that at which resonance between lead inductances and interelectrode capacitances occurs. If L_k is equal to L_p, C_{gk} to C_{gp}, and i_1 to i_2, it can readily be seen that i_g is not influenced by the lead inductances, for the triode is then a bridge in perfect balance. But if any one of these qualities is upset (more exactly, if $i_1 L_k C_{gk}$ is not equal to $i_2 L_p C_{gp}$), there appears a conductive component in the grid current i_g. If $i_1 L_k C_{gk}$ is greater

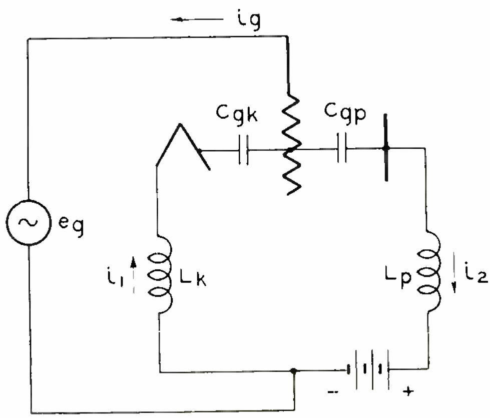

Fig. 2—Schematic diagram of triode without plate-load impedance. L_k and L_p represent the self-inductances of the cathode and plate leads.

than $i_2 L_p C_{gp}$, this component is positive and represents an input loading in addition to the electronic loading. It is most interesting to observe that the effective resistance shunted between grid and cathode which corresponds to this lead-effect loading is inversely proportional to the transconductance and to the square of the frequency, exactly as was the case for electronic loading.

Normally it is not feasible to balance out the two lead effects. Especially is this true in screen-grid tubes where the screen-grid current is a small fraction of the cathode current. Therefore, the lead-effect loading is often very important.

III. Receiving Tubes

For almost any application of ultra-short waves, both transmitting and receiving apparatus are required. While it may seem that transmission logically comes first, the problems of receiving tubes are such that the discussion of them will serve as background for the discussion of transmitting tubes.

It is conventional practice at lower frequencies to amplify the received signal at the radio frequency, then to convert it to a lower intermediate frequency at which additional amplification takes place, and finally to detect the signal, or to omit the intermediate frequency and detect the radio-frequency signal directly. Where intermediate-frequency amplification is used, radio-frequency amplification is desirable to prevent radiation at the local-oscillator frequency from the receiving antenna, to reduce the response to the unwanted frequency which differs from the local-oscillator frequency by the same amount as the wanted frequency, and to increase the signal-to-noise ratio for weak signals. Where intermediate-frequency amplification is not used, radio-frequency amplification is required to achieve selectivity and sensitivity with high signal-to-noise ratio. While special applications of ultra-short waves may not impose such severe requirements on the receiver, it is reasonable to suppose that equivalent performance will be desired in other applications. We shall, therefore, wish to discuss all pertinent limitations of receiving tubes.

The maximum voltage amplification per stage which may be obtained from a vacuum-tube amplifier depends on the magnitudes of the transadmittance, the internal grid conductance, the internal plate resistance, the grid and plate capacitances to ground, and the band width to be passed by the amplifier. The phase angle of the transadmittance is unimportant in an amplifier. There is ordinarily no serious problem in obtaining suitable external circuits at even the highest frequencies. Where ordinary lumped circuits may not be used, distributed circuits, such as concentric transmission lines, are suitable.

As was stated earlier, the reduction in magnitude of transadmittance with increasing frequency is usually not serious. The internal plate resistance may or may not be importantly reduced at high frequencies. When it is, the trouble is not usually fundamental, but is likely to be a matter of bulb effects such as electron bombardment or surface film resistance. Such effects may be hard to isolate and to eliminate, but they will certainly not be an ultimate limitation.

For wide-band amplification, the interelectrode capacitances may be a limiting factor in determining the maximum attainable amplification at moderately high frequencies. However, as the frequency is increased, the input conductance becomes rapidly larger until the effective impedance of the circuit connected to the grid becomes lower, in general, than the value required for wide-band amplification. The problem of increasing the frequency at which some voltage amplification may be obtained is, therefore, the problem of increasing the ratio of transadmittance to input conductance.

Because for given spacings and operating voltages the ratio of transadmittance to input conductance at a definite frequency is fixed, increase in this ratio may be attained in a straightforward manner only by reducing spacings or increasing voltages. As the latter method is usually impractical, reduced spacings is the obvious alternative. This is the method followed in the design of acorn tubes. There are possibilities of more or less radically new kinds of amplifying tubes which may give better performance without smaller structures. Speculation as to the nature of such tubes is beyond the scope of the present paper; one may be sure, however, that the improvement will be in the ratio of transadmittance to input conductance.

Satisfactory performance at higher frequencies than those at which vacuum-tube amplifiers will give a voltage gain appears to be possible only if one is satisfied to do without radio-frequency amplification. Detectors will operate at much higher frequencies than present amplifiers or oscillators. Superheterodyne operation at as high as 3,000 megacycles does not seem impossible with the use of a harmonic of a lower-frequency local oscillator.

IV. Transmitting Tubes

The performance requirements for transmitting tubes for ultra-high-frequency operation are substantially the same as those for lower frequencies. Only where such requirements cannot be met will inferior performance be accepted. These requirements stated briefly are: oscillators having good frequency stability; efficient power amplifiers which have good modulation characteristics; and as much power output as can be attained. It appears that the requirements of power amplification and good modulation characteristics may not readily be met by such tubes as magnetrons and Barkhausen-Kurz oscillators. It is not surprising, therefore, that the trend has been toward conventional negative-grid tubes at all frequencies much below 3,000 megacycles.

The fundamental electronic theory of the operation of negative-grid transmitting tubes at high frequencies is, naturally, the same as that of receiving tubes. If power output were not a consideration, transmitting tubes would not differ from receiving tubes. The demand for large power outputs with low interelectrode capacitance and close spacings, three requirements mutually in opposition, naturally requires a compromise in design about which one might not be optimistic. Actually, however, the situation is not so bad as it might appear at first. Because transmitting tubes are normally operated with much higher voltages than receiving tubes and, further, because the grid usually swings quite positive over a portion of the cycle to cause the current to flow for a half-cycle or less, the electron velocity is much higher and therefore the spacings may be greater than in the case of receiving tubes. The fact that current flows for only part of a cycle causes the average grid conductance over the cycle to be lower.

Oscillators have one important advantage over power amplifiers. Lead-inductance effects are not serious because the feed-back from cathode to grid may be more than compensated by feed-back from plate to grid. They also have a disadvantage in that the phase angle of the transconductance is of importance in the simple feed-back circuits which are most convenient to use. The net result is that properly designed power amplifiers may be expected ultimately to equal or to exceed the performance of oscillators with respect to obtainable power output at a given frequency.

The limitation in power output at a given frequency of either oscillators or power amplifiers is set by the limitation in cathode-emission density and in anode and grid-dissipating ability which are properties of the materials used or of the methods of cooling. If unlimited emission could be obtained in a small space and the resultant unlimited-power dissipation accommodated, the problem would become simply one of handling the output power in the plate lead.

The limitation in frequency for a given power output is set by the transit times which result from the operating voltages, anode area, and spacings determined by the permissible anode dissipation per unit area and interelectrode capacitance.

The limitation in highest operating frequency without regard for power output is set by how small and how closely spaced it is considered feasible to make tubes, exactly the same limitation as for receiving tubes.

Improvements in both power output and maximum frequency may be expected from further refinements of design and construction. Greater improvements may be expected to result if new anode, grid, and cathode materials are found which will withstand greater dissipation density and afford greater emission density. As it is not to be expected that very great improvements may be attained in this direction, it appears that other means of generation must be found if power outputs as great as will be demanded are to be obtained.

The substantial progress which has been made in ultra-high-frequency vacuum-tube performance in the past few years is very encouraging. It will be interesting to watch the developments in the next few years. The requirements are definite and the demands pressing; the limitations are great and well recognized. Engineering and scientific ingenuity seem to be most active under such circumstances.

Bibliography

D. O. North, "Analysis of the Effects of Space Charge on Grid Impedance", *Proc. I.R.E.*, Vol. 24, No. 1, pp. 108-136; January (1936).

W. R. Ferris, "Input Resistance of Vacuum Tubes as Ultra-High-Frequency Amplifiers", *Proc. I.R.E.*, Vol. 24, No. 1, pp. 82-107; January (1936).

F. B. Llewellyn, "Phase Angle of Vacuum-Tube Transconductance at Very High Frequencies", *Proc. I.R.E.*, Vol. 22, No. 8, pp. 947-956; August (1934).

M. J. O. Strutt and A. van der Ziel, "The Causes for the Increase of the Admittances of Modern High-Frequency Amplifier Tubes on Short Waves", *Proc. I.R.E.*, Vol. 26, No. 8, pp. 1011-1032; August (1938).

B. J. Thompson and G. M. Rose, Jr., "Vacuum Tubes of Small Dimensions for Use at Extremely High Frequencies", *Proc. I.R.E.*, Vol. 21, No. 12, pp. 1707-1721; December (1933).

B. Salzberg and D. G. Burnside, "Recent Developments in Miniature Tubes", *Proc. I.R.E.*, Vol. 23, No. 10, pp. 1142-1157; October (1935).

C. E. Fay and A. L. Samuel, "Vacuum Tubes for Generating Frequencies Above One Hundred Megacycles", *Proc. I.R.E.*, Vol. 23, No. 3, pp. 199-212; March (1935).

A. L. Samuel, "Extending the Frequency Range of the Negative Grid Tube", *Journal of Applied Physics*, Vol. 8, No. 10, pp. 677-688; October (1937).

W. G. Wagener, "The Developmental Problems and Operating Characteristics of Two New Ultra-High-Frequency Triodes", *Proc. I.R.E.*, Vol. 26, No. 4, pp. 401-414; April (1938).

L. S. Nergaard, "Electrical Measurements at Wavelengths Less Than Two Meters", *Proc. I.R.E.*, Vol. 24, No. 9, pp. 1207-1229; September (1936).

A SURVEY OF ULTRA-HIGH-FREQUENCY MEASUREMENTS

By

L. S. Nergaard

RCA Radiotron Division, RCA Manufacturing Company, Harrison, N. J.

Summary—*A simple magnetron signal generator is described. The more useful transmission-line and skin-effect formulas are listed. In connection with transmission lines, it is pointed out that even at very high frequencies the quadrature component of the characteristic impedance cannot be neglected. Methods which have been used for the measurement of the following quantities are described:*

(1) Wavelength—Wavelength has been measured by reflection of waves in free-space and transmission-line wavemeters. A method of determining the end correction of a transmission-line wavemeter is described.

(2) Power—Thermocouples for the measurement of small powers are described. The use of incandescent lamps for the measurement of large powers is discussed.

(3) Voltage—Diode voltmeters and thermocouples have been used for the measurement of voltage. The errors of these voltmeters are discussed.

(4) Reactance—Reactance has been measured by tuning the unknown reactance to resonance with a transmission line of known characteristics. The method is illustrated by two examples: the determination of the resonant wavelength, the inductance and capacitance of a diode, and the calibration of a variable condenser.

(5) Resistance—Resistance has been measured by the substitution method, the resistance-variation method, and the reactance-variation method. The reactance-variation method has been used in all of its forms, namely, capacitance variation, line-length variation, and frequency variation. The pertinent formulas and examples of the methods are given. A transmission line and condenser for the measurement of resistance by the capacitance-variation method are described.

(6) Current—The measurement of current with thermocouples is discussed.

I. Introduction

THE last five years have brought ever-increasing activity in the ultra-short-wave field and a gradual shift of the work on the more conventional tubes and circuits from a research to an engineering basis. This shift is, in a large measure, due to the development of a measurement technique for the ultra-high-frequency region. This development is by no means complete. Much remains to be done, both in improving the precision of the measurements and in extending the frequency range over which reliable measurements can be made. However, it is sometimes advantageous to pause and take stock of the methods available. It was with this thought in mind that the present paper was undertaken.

This paper is a survey of those methods of measurements which have proved most useful in this laboratory. The writer is well aware that, in limiting himself to a report of the methods used in a single laboratory, he is excluding the very valuable work done elsewhere. His apology for this exclusion is that it permits him to describe only those methods of which he has first-hand knowledge, i.e., the methods whose value he is best able to appraise.

II. Signal Generators

A good source of radio-frequency power is essential to radio-frequency measurements. The requirements of a signal generator are much the same at any frequency and include (1) adequate output, (2) a wide frequency range, (3) freedom from harmonics, (4) frequency and voltage stability, and (5) good shielding. It is also desirable that the generator be flexible so that the frequency and output can be varied widely with ease.

Two types of oscillators are commonly used, namely: (1) the negative-grid triode and (2) the magnetron. Triode oscillators can be made to operate down to a wavelength of 20 cm with an output of 2 watts.[1] For wavelengths above 80 cm, the RCA-955 and the RCA-834 have been used in this laboratory. Below 80-cm wavelength, the feed-back becomes critical of adjustment, and it is usually necessary to tune the filament circuit. Therefore, a triode oscillator for wavelengths less than 80 cm requires a minimum of two circuit adjustments to change wavelength and becomes less flexible than is desirable.

Magnetrons operating in the negative-resistance mode will deliver as much as 80 watts at a wavelength of 19 cm.[2] This output was obtained from a water-cooled internal-circuit tube. Because of the fixed internal circuit, such a tube lacks the flexibility desirable in a signal generator. Messrs. G. R. Kilgore and T. H. Clark of this laboratory have designed a small split-anode magnetron having an anode diameter of 2.5 mm and very short anode leads.* This tube delivers 1 watt at a wavelength of 40 cm with 300 volts on the anodes and a field

* With the exception of the RCA-955 and the RCA-834, all of the tubes and thermocouples described in this paper have been constructed for measurements incidental to our short-wave research.

strength of 1500 gausses. The wavelength can be varied from 40 cm to 200 cm by merely varying the length of the anode transmission line. The output is readily controlled by varying the filament current. Three signal generators employing these tubes are now in use in this laboratory and are proving very usable and useful. The completely shielded signal generator described in the writer's previous measurement paper[11] now uses this type of tube. For many rough measurements the oscillator need not be shielded. Figure 1 shows a simple signal generator of the unshielded type.

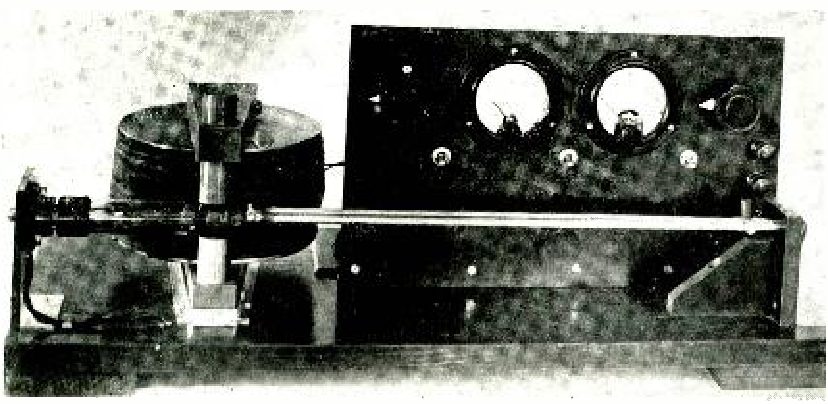

Fig. 1—An unshielded magnetron signal generator.

III. Circuits

At short wavelengths, transmission lines have almost entirely supplanted the lumped circuit elements used at long wavelengths. This change has taken place for two reasons; namely, lumped circuit elements for short wavelengths are difficult to construct because of their small physical size, and are also difficult to adjust once they have been constructed.

The following example illustrates the difference in physical size of a lumped circuit and a transmission line, both to tune to a wavelength of 50 cm. Suppose the condenser of the lumped circuit consists of coaxial circular plates 2 cm in diameter and spaced 0.1 cm. apart. The capacitance of the condenser is approximately 2.8 $\mu\mu f$ and the required inductance is approximately $1/\omega^2 C$, or 2.5×10^{-8} henry. A circular loop of No. 14 wire, 2 cm in diameter, has approximately the required inductance. For a transmission line open at one end and short-circuited at the other end, the length of the line for resonance is 12.5 cm. It is interesting to note that the current in the lumped inductance is uniform within 10 per cent, whereas the current in the transmission line is zero at the open end and a maximum at the short-circuited end.

Because of the great utility of transmission lines, a few of the more important formulas† will be listed in the forms in which they have been found most useful. Let

l = length of line in cm
r_o = total resistance per unit length of line in ohm · cm^{-1}
L_o = inductance per unit length of line in henrys · cm^{-1}
C_o = capacitance per unit length of line in farads · cm^{-1}
G_o = leakage conductance per unit length of line in mhos · cm^{-1}
α = attenuation constant in cm^{-1}
β = phase constant in cm^{-1}
m = propagation constant in $cm^{-1} = \alpha + j\beta$
γ = resistive component of the characteristic impedance in ohms
δ = reactive component of the characteristic impedance in ohms
Z_o = characteristic impedance of the line in ohms $= \gamma - j\delta$
$j = \sqrt{-1}$
$\omega = 2\pi f$
f = frequency in cycles per sec
λ = wavelength in cm
E_s = voltage across sending end of line in volts
E_r = voltage across receiving end of line in volts
I_s = current at sending end of line in amperes
I_r = current at receiving end of line in amperes
Z_r = impedance across the receiving end in ohms
Z_s = impedance looking into sending end of line in ohms

The properties of a transmission line are most conveniently expressed in terms of the characteristic impedance, the propagation constant, and the length of the line. Because the expressions relating the characteristic impedance and the propagation constant to the resistance, inductance, conductance, and capacitance per unit length of line are unwieldy, it is advantageous to have approximate expressions which are simple, yet adequately accurate. The exact expressions for the real and imaginary parts of the propagation constant and characteristic impedance are:

$$\alpha = \omega \sqrt{L_o C_o} \cdot \left\{ \frac{1}{2} \left[1 + \left(\frac{r_o}{\omega L_o} \right)^2 \right]^{\frac{1}{2}} \cdot \left[1 + \left(\frac{G_o}{\omega C_o} \right)^2 \right]^{\frac{1}{2}} \right.$$

(Formula continued on next page)

† A consistent notation is used throughout the paper. For convenience, a table of the symbols used is given in Appendix A.

$$-\frac{1}{2}\left[1-\frac{G_o r_o}{\omega^2 L_o C_o}\right]\Biggr\}^{\frac{1}{2}}$$

$$\beta = \omega\sqrt{L_o C_o}\cdot\Biggl\{\frac{1}{2}\left[1+\left(\frac{r_o}{\omega L_o}\right)^2\right]^{\frac{1}{2}}\cdot\left[1+\left(\frac{G_o}{\omega C_o}\right)^2\right]^{\frac{1}{2}}$$
$$-\frac{1}{2}\left[1+\frac{G_o r_o}{\omega^2 L_o C_o}\right]\Biggr\}^{\frac{1}{2}}$$

$$\gamma = \sqrt{\frac{L_o}{C_o}}\cdot\left[1+\left(\frac{G_o}{\omega C_o}\right)^2\right]^{-\frac{1}{2}}\cdot\Biggl\{\frac{1}{2}\left[1+\left(\frac{r_o}{\omega L_o}\right)^2\right]^{\frac{1}{2}}\cdot$$
$$\left[1+\left(\frac{G_o}{\omega C_o}\right)^2\right]^{\frac{1}{2}}+\frac{1}{2}\left[1+\frac{G_o r_o}{\omega^2 L_o C_o}\right]\Biggr\}^{\frac{1}{2}}$$

$$\delta = \sqrt{\frac{L_o}{C_o}}\cdot\left[1+\left(\frac{G_o}{\omega C_o}\right)^2\right]^{-\frac{1}{2}}\cdot\Biggl\{\frac{1}{2}\left[1+\left(\frac{r_o}{\omega L_o}\right)^2\right]^{\frac{1}{2}}\cdot$$
$$\left[1+\left(\frac{G_o}{\omega C_o}\right)^2\right]^{\frac{1}{2}}-\frac{1}{2}\left[1+\frac{G_o r_o}{\omega^2 L_o C_o}\right]\Biggr\}^{\frac{1}{2}}$$

In practical short-wave transmission lines, $G_o = 0$ and $r_o/\omega L_o << 1$. Therefore, the above relations can be written in the following simple forms which are sufficiently accurate for all practical short-wave transmission lines.

$$\alpha = \frac{r_o}{2}\sqrt{\frac{C_o}{L_o}} = \frac{r_o}{2\omega L_o}\beta, \quad \beta = \omega\sqrt{L_o C_o} = \frac{2\pi}{\lambda}, \quad \gamma = \sqrt{\frac{L_o}{C_o}}$$

and

$$\delta = \frac{r_o}{2\omega L_o}\sqrt{\frac{L_o}{C_o}} = \frac{r_o}{2\omega L_o}\gamma \qquad \text{(III-1)}$$

Hence,

$$m = \left(\frac{r_o}{2\omega L_o} + j\right)\cdot\frac{2\pi}{\lambda}$$

$$Z_o = \left(1 - j\frac{r_o}{2\omega L_o}\right)\sqrt{\frac{L_o}{C_o}} \qquad \text{(III-2)}$$

It apparently has been customary to neglect the quadrature component of the characteristic impedance in short-wave transmission-line calculations. This procedure may lead to 50 per cent error in calculating the input impedance of a transmission line with the receiving end short-circuited. That this statement is true is readily verified for the case when the length approaches zero.

The following relations have been found useful:

$$Z_s = Z_o \frac{Z_r \cosh ml + Z_o \sinh ml}{Z_r \sinh ml + Z_o \cosh ml} \qquad \text{(III-3)}$$

$$\frac{I_r}{I_s} = \frac{Z_o}{Z_r \sinh ml + Z_o \cosh ml} \qquad \text{(III-4)}$$

$$\frac{E_r}{E_s} = \frac{I_r Z_r}{E_s} = \frac{Z_o}{Z_r \cosh ml + Z_o \sinh ml} \qquad \text{(III-5)}$$

Two special cases are of particular interest:

a) If the receiving end of the line is short-circuited ($Z_r = 0$), the sending-end impedance is $Z_o \tanh ml$

or

$$Z_s = \frac{\dfrac{r_o l}{2}\left[1 + \dfrac{\sin \dfrac{4\pi l}{\lambda}}{\dfrac{4\pi l}{\lambda}}\right] + j\sqrt{\dfrac{L_o}{C_o}} \sin\dfrac{2\pi l}{\lambda} \cdot \cos\dfrac{2\pi l}{\lambda}}{\cos^2\dfrac{2\pi l}{\lambda} + \left(\dfrac{r_o l}{2}\sqrt{\dfrac{C_o}{L_o}}\right)^2 \sin^2\dfrac{2\pi l}{\lambda}} \qquad \text{(III-6)}$$

When $l = \dfrac{\lambda}{2}$, then $Z_s = \dfrac{r_o \lambda}{4}$ (III-7)

and the circuit acts as a resonant circuit.

When $l = \dfrac{\lambda}{4}$, then $Z_s = \dfrac{8L_o}{r_o \lambda C_o}$ (III-8)

and the circuit acts as an anti-resonant circuit.

When

$$\cos \frac{2\pi l}{\lambda} >> \frac{r_o l}{2} \sqrt{\frac{C_o}{L_o}} \sin \frac{2\pi l}{\lambda}, \quad \text{then}$$

$$Z_s = \frac{r_o l}{2} \left[1 + \frac{\sin \frac{4\pi l}{\lambda}}{\frac{4\pi l}{\lambda}} \right] \sec^2 \frac{2\pi l}{\lambda} + j \sqrt{\frac{L_o}{C_o}} \tan \frac{2\pi l}{\lambda} \tag{III-9}$$

The imaginary term here is much greater than the real, so that the circuit acts as an inductance with a small loss. In the limiting case when $l \rightarrow 0$

$$Z_s \rightarrow (r_o + j\,\omega L_o)\, l \tag{III-10}$$

b) If the receiving end of the line is open ($Z_r = \infty$), the sending-end impedance is $Z_o \coth ml$

or

$$Z_s = \frac{\frac{r_o l}{2} \left[1 - \frac{\sin \frac{4\pi l}{\lambda}}{\frac{4\pi l}{\lambda}} \right] - j \sqrt{\frac{L_o}{C_o}} \sin \frac{2\pi l}{\lambda} \cdot \cos \frac{2\pi l}{\lambda}}{\sin^2 \frac{2\pi l}{\lambda} + \left(\frac{r_o l}{2} \sqrt{\frac{C_o}{L_o}} \right)^2 \cos^2 \frac{2\pi l}{\lambda}} \tag{III-11}$$

When $$l = \frac{\lambda}{2}, \quad \text{then} \quad Z_s = \frac{4L_o}{r_o \lambda C_o} \tag{III-12}$$

and the circuit acts as an anti-resonant circuit.

When $$l = \frac{\lambda}{4}, \quad \text{then} \quad Z_s = \frac{r_o \lambda}{8} \tag{III-13}$$

and the circuit acts as a resonant circuit.

When $$\sin \frac{2\pi l}{\lambda} >> \frac{r_o l}{2} \sqrt{\frac{C_o}{L_o}} \cos \frac{2\pi l}{\lambda} \quad \text{then}$$

$$Z_s = \frac{r_o l}{2}\left[1 - \frac{\sin\frac{4\pi l}{\lambda}}{\frac{4\pi l}{\lambda}}\right]\csc^2\frac{2\pi l}{\lambda} - j\sqrt{\frac{L_o}{C_o}}\cot\frac{2\pi l}{\lambda} \qquad \text{(III-14)}$$

and the circuit acts as an imperfect condenser. In the limiting case

$$\text{when} \quad l \rightarrow 0, \quad \text{then} \quad Z_s \rightarrow \frac{1}{j\omega C_o l} \qquad \text{(III-15)}$$

Therefore, transmission lines can be used as resonant and anti-resonant circuits, and as inductances and capacitances.

In the lumped circuits used at long wavelengths, the circuit losses are chiefly in the nature of ohmic losses. At short wavelengths where transmission lines are used as circuit elements and the spacings between conductors of the lines are an appreciable fraction of a wavelength, radiation resistance becomes appreciable. In some short-wave transmission lines, the radiation resistance amounts to half of the total resistance. Furthermore, skin-effect, which results in minor corrections to the ohmic resistance at long wavelengths, becomes an important factor in resistances at short wavelengths.

The resistance per unit length of a solid cylindrical conductor is[4, 5, 6]

$$R_o = R_e \frac{P\rho}{2\pi a} \times 10^{-6} \frac{J_o(Pa)}{J_1(Pa)} \qquad \text{(III-16)}$$

in which

R_o = resistance in ohms per cm length
R_e = "real part of"
J_n = Bessel function of order n
a = radius of conductor in cm
ρ = resistivity of the conductor in microhm · cm
$P = 2\pi\sqrt{\frac{\mu f}{\rho \times 10^3}}(1 - j)$
μ = magnetic permeability
f = frequency in cycles per second
$j = \sqrt{-1}$

Conductors at short wavelengths generally fall into one of two classes:

(1) Those for which the skin effect is small. These generally have very high resistivities or very small diameters. Thermocouple heaters are of this class. In this case, Formula (III-16) reduces to

$$R_o = \frac{\rho \times 10^{-6}}{\pi a^2} \left\{ 1 + \frac{1}{3} \left[\pi a \sqrt{\frac{\mu f}{\rho \times 10^3}} \right]^4 \right\} \qquad \text{(III-17)}$$

which is valid when

$$a \sqrt{\frac{\mu f}{\rho}} < 10$$

(2) Those for which the skin effect is very large. This class includes all of the good conductors normally used in transmission lines. In this case, Formula (III-16) becomes

$$R_o = \frac{3.16 \times 10^{-8}}{a} \sqrt{\rho \mu f} \qquad \text{(III-18)}$$

which is valid when

$$a \sqrt{\frac{\mu f}{\rho}} \geqslant 180$$

Because of the skin effect at short wavelengths, the current in a good conductor flows almost entirely on the surface of the conductor. Therefore, the internal inductance becomes negligible compared with the external inductance. This leads to a very simple and useful formula for the real part of the characteristic impedance of a transmission line. When the internal inductance is negligible and $r_o/\omega L_o << 1$, the phase velocity

$$v = \frac{1}{\sqrt{L_o C_o}} \qquad \text{(III-19)}$$

is equal to the velocity of propagation of light in free space for all practical purposes. Therefore,

$$\sqrt{\frac{L_o}{C_o}} = \frac{1}{v C_o} = \frac{10^{-10}}{3 C_o} \qquad \text{(III-20)}$$

Hence, the real part of the characteristic impedance can be calculated from the capacitance per unit length of line.

The two types of transmission lines commonly used are the parallel-wire line and the concentric transmission line. The concentric line has the lower attenuation of the two and, therefore, gives the higher impedance when used as an anti-resonant circuit. Its lower attenuation is due to its negligible radiation resistance and to the relatively low resistance of the outer conductor. Whether or not a concentric line has any radiation resistance at all except that due to an open end is a controversial point.[7,8,9] However, the concentric lines used in this laboratory have always given higher anti-resonant impedances than equivalent parallel-wire lines, and no radiation from a concentric line with closed ends has ever been detected. In some cases it is necessary to use parallel-wire lines. For example, the split-anode magnetron requires such a line. Push-pull devices in general fit naturally into lines which are balanced with respect to ground. When it has been desirable to shield a parallel line, the line has been enclosed in a metallic cylinder. The cylinder reduces the radiation resistance, but increases the ohmic resistance because of circulating currents in the cylinder.

IV. Measurement of Wavelength

Wavelength is usually measured by reflection of the waves in free space or by a transmission line. To measure wavelength by reflection in free space an indicator such as a crystal detector and microammeter in series is set up in the vicinity of the source. Then as a plane metallic reflector is moved in a direction normal to its surface and roughly in the direction of the indicator, the positions of the reflector for maximum readings of the microammeter are noted. The distance between positions for successive maxima is a half wavelength.

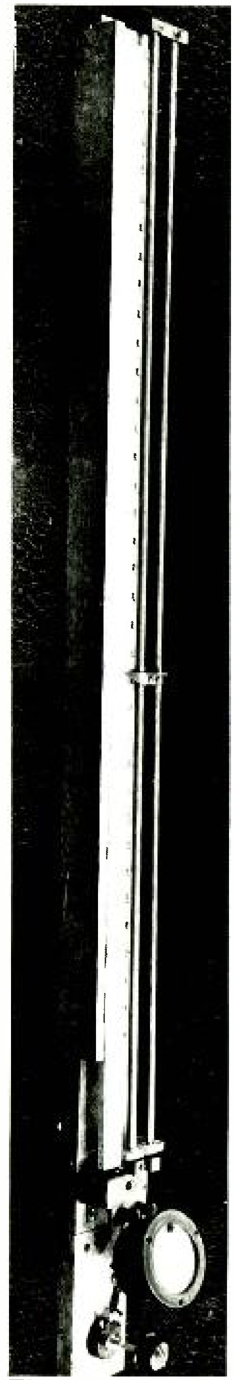

Fig. 2—Transmission-line wavemeter.

The measurement of wavelength with a transmission line consists in measuring the distance between the positions of a movable short-circuit on the line for successive maximum readings of an indicator loosely coupled to the line. The wavelength is then[10]

$$\lambda = 2\Delta l \left[1 + \left(\frac{r_o}{2\omega L_o} \right)^2 \right] \tag{IV-1}$$

where Δl = distance between positions for successive maxima

$$\text{Usually} \left(\frac{r_o}{2\omega L_o} \right) << 1$$

so that

$$\lambda = 2\Delta l \tag{IV-2}$$

Frequently, it is desirable to keep the length of the line to be used as a wavemeter as short as possible. Then, ideally, the line length is just a quarter wavelength. In practice, the short-circuit on the line has a small inductance L, so that the condition for resonance is

$$\omega L - \sqrt{\frac{L_o}{C_o}} \cot \frac{2\pi l_o}{\lambda} = 0 \tag{IV-3}$$

Because L is small, it is permissible to write

$$\omega L \sqrt{\frac{C_o}{L_o}} = \tan \omega L \sqrt{\frac{C_o}{L_o}}$$

in which case (IV-3) becomes

$$\cot \left(\frac{2\pi l_o}{\lambda} + \omega L \sqrt{\frac{C_o}{L_o}} \right) = \cot \frac{2\pi}{\lambda} \left(l_o + \frac{L}{L_o} \right) = 0 \tag{IV-4}$$

Then the wavelength is

$$\lambda = 4 \left(l_o + \frac{L}{L_o} \right) \tag{IV-5}$$

Figure 2 is a photograph of a wavemeter using this principle. A crystal detector and microammeter in series, capacitively coupled to the open end of the line, are used as an indicator. Figure 3 is the calibration curve of this wavemeter. Notice the correction resulting from the inductance of the short-circuit. The inductance in this case is $L = 8.8 \times 10^{-9}$ henry.

V. Measurement of Power

In general, the requirements of a device for measuring power at short wavelengths are:

(1) It should have adequate sensitivity.

(2) Its resistance should be high so that substantially all the power is dissipated in the device and a negligible amount in other circuit resistances.

(3) It should be free from stray capacitances and inductances which make it difficult to match the impedance of the device to the impedance of the source.

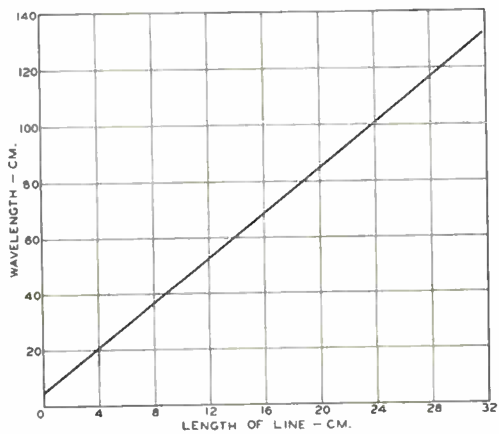

Fig. 3—Calibration of the transmission-line wavemeter.

(4) The calibration should be independent of frequency so that calibration at a low frequency, say 60 cycles per second, is possible.

For powers less than one watt the vacuum thermocouple has been found to be the most satisfactory power-measuring device. Thermocouples for this purpose have been built.[11] The salient features of these thermocouples are:

(1) The heaters are short and straight so that the current is uniform along the length of the heater within 1 per cent for wavelengths above $\lambda = 18$ cm.

(2) The heater resistances are large compared to the circuit resistances likely to be encountered in practical circuits. The resistances range between 5 and 1000 ohms depending on the type of heater used.

(3) The couple and its leads are arranged in an acute V perpendicular to the axis of the heater to minimize coupling between the heater and couple circuits.

(4) The couple and heater are supported by the leads through the radial seal of the acorn-type bulb. No glass beads or spacers are used to support the elements. The most troublesome shunting capacitance is thereby eliminated. The thermocouples having a heater resistance of 1000 ohms described in an earlier paper[11] had glass beads to support the elements. These couples have now been made without beads.

(5) These thermocouples have been made with sufficient sensitivity to measure 0.1 milliwatt.

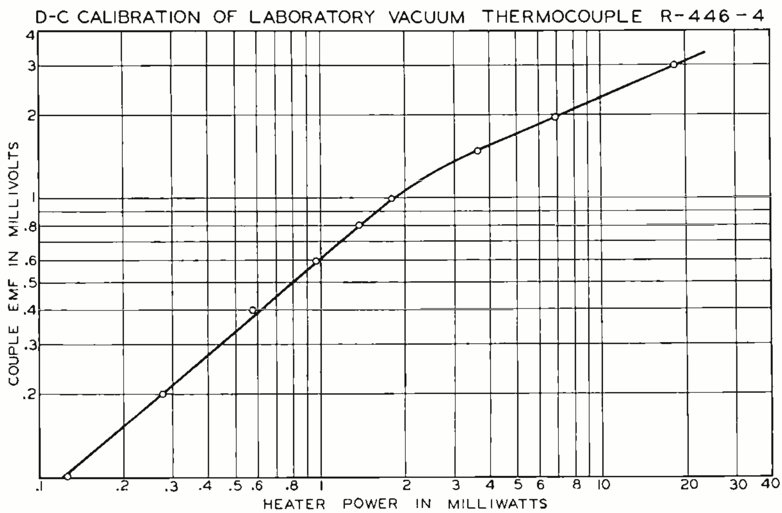

Fig. 4—D-C calibration of laboratory vacuum thermocouple R-446-4. The couple e.m.f. was read on a meter of 10 ohms resistance.

Figure 4 is the calibration curve of one of the more sensitive thermocouples. This thermocouple has a carbon heater of 0.0003-inch diameter and an iron and gold-palladium couple, both the iron and gold-palladium wires having a diameter of 0.0005 inch. The heater resistance is 1000 ohms.

Vacuum thermocouples of the type just described cannot be constructed to dissipate powers in excess of one watt without sacrificing their desirable characteristics. To dissipate considerable power without burning out the heater and couple, the area of the heater must be made large. This can be accomplished by using an undesirably low heater resistance, or by making the heater long and of small diameter, in which case the current is no longer uniform throughout the length of the heater and the use of a low-frequency calibration is impossible. To overcome these difficulties, indirectly heated thermocouples have been built. These "thermocouples" have a long heater of fine wire enclosed in a metal box of high thermal conductivity. The box then absorbs all the heat dissipated by the heater, whatever the current distribution on the heater, and assumes a temperature depending on the amount of heat dissipated. A thermocouple attached to the outside of the box measures its temperature. These "thermocouples" require about 15 minutes to reach a steady-state temperature so they are not particularly useful when time is a consideration. Figure 5 shows the calibration curve of such a thermocouple.

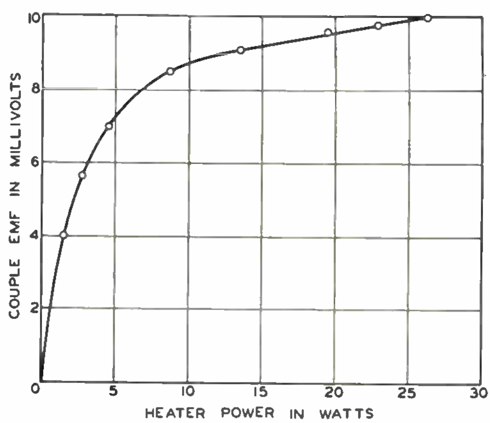

Fig. 5—D-C calibration of laboratory thermocouple R-356. The couple e.m.f. was read on a meter of 10 ohms resistance.

For the measurement of powers of the order of one watt, small diodes can also be used. In these the power is dissipated in the filament and the temperature-limited emission serves as a measure of the power dissipated in the filament. The filament can be made short to insure a uniform current distribution, and the resistance can be made of the order of 50 ohms. The anode voltage must be high enough to insure temperature limitation of the current at all times. The anode dissipation is, therefore, a limitation which considerably restricts the range of power which can be measured with such a diode.

For the measurement of powers between 2 watts and 100 watts, incandescent lamps are quite commonly used. The power to be measured is dissipated in a lamp and a second lamp run from a 60-cycle source is adjusted until the two have the same brilliancy. The adjustment is made visually and with considerable accuracy. To check the accuracy of the method, measurements were made independently by three observers and were found to agree within 5 per cent. Considerable inaccuracy doubtless results from non-uniform heating of the lamp filament at short wavelengths. However, there is something very convincing about seeing a lamp brilliantly lighted. A refinement of this method consists in measuring the light output of a lamp with a phototube. The lamp and cell as a unit are calibrated at 60 cycles per second. Figure 6 shows the calibration curve of such a lamp and phototube.

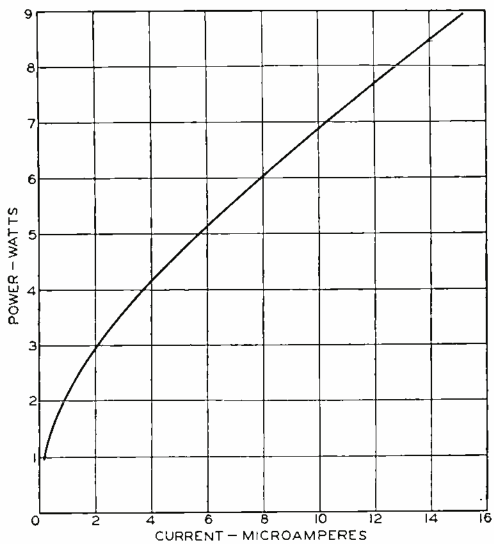

Fig. 6—Low-frequency calibration of an incandescent lamp and phototube used for power measurements.

VI. The Measurement of Voltage

The requirements of a good voltmeter are:

(1) It should have adequate sensitivity.

(2) Its input impedance should be high so that it does not perturb the circuit to which it is connected.

(3) Its calibration should be independent of frequency.

Triode voltmeters have these attributes at long wavelengths so it was natural to try to use them at ultra-short wavelengths. It was soon found that they loaded tuned circuits very considerably. As a matter of fact, their input resistance appeared to be less than 10^4 ohms at a wavelength of 100 cm. Because the calibrations of the existing voltmeters were not known, only estimates of impedances could be made at the time. Diode voltmeters of the type shown in the inset of Figure 7 were then tried. The diodes used had an anode diameter of 0.012 inch and a cathode diameter of 0.0026 inch. These voltmeters were found to have an input impedance of the order of 10^5 ohms.

In comparing diode voltmeters at various wavelengths, two sources of error were found:

(1) A voltage step-up between the external terminals and the diode electrodes due to series resonance between the lead inductances and the interelectrode capacitance of the tube. This error is usually referred to as the resonance error.

(2) A non-linearity in calibration due to the transit time of electrons between cathode and anode.

The resonance error is usually the larger of the two. Fortunately, it is easier to correct because it is independent of the applied voltage.

Let

L_d = the inductance of the leads of the diode
C_d = the interelectrode capacitance of the diode
$\lambda_r = 2\pi v \sqrt{L_d C_d}$ = the resonant wavelength of the diode
$v = 3 \times 10^{10}$ cm per second
λ = the operating wavelength
E_2 = the voltage across the terminals of the diode
E_1 = the voltage across the electrodes of the diode

Now L and C are in series, so

$$\frac{E_1}{E_2} = \frac{1}{1 - \omega^2 L_d C_d} = \frac{1}{1 - \left(\frac{\lambda_r}{\lambda}\right)^2} \qquad \text{(VI-1)}$$

This equation assumes, of course, that λ is sufficiently remote from λ_r so that the resistance of the leads may be neglected. Once the resonant wavelength λ_r has been measured, the reading of the voltmeter is easily corrected for this error by multiplying the indicated voltage by $1 - (\lambda_r/\lambda)^2$. The determination of the resonant wavelength will be discussed in the section devoted to the measurement of reactance.

The nature of the transit-time error can be seen from the following argument: Consider a diode and condenser connected across a source of constant high-frequency voltage. When the voltage is applied, the diode will pass current on the positive peaks of voltage and charge the condenser. As the charge on the condenser increases, the peak positive swing across the diode electrodes decreases. If the time of transit of the electrons were zero, the condenser would charge up to the peak value of the alternating voltage, i.e., until the electrons at the cathode felt no accelerating force at any part of the cycle. Actually, the transit time is not zero so the condenser will charge only to such a voltage that electrons just fail to reach the anode before their velocity becomes zero because of the retarding field on the inverse half-cycle. Since the condenser does not charge to the peak of the alternating voltage when the transit time is appreciable, the voltmeter reads low. Actual voltmeters have a resistance across the condenser. However, when the time constant of the resistance-condenser combination is large compared to the period of the applied voltage, the resistance changes the picture inappreciably. This point has been checked by using an electrometer in place of the resistor and microammeter. Because the finite transit-time makes the diode cut off at a lower voltage at short wavelengths than at long wavelengths, this effect is sometimes called *premature cut-off*.

The transit-time error was first studied theoretically.[11,12,13] The analysis led to the following approximate formula for the error in cylindrical diodes.

$$\frac{\Delta E}{E} = -\frac{\Gamma K d}{\lambda \sqrt{E}} \qquad \text{(VI-2)}$$

in which

ΔE = the error in peak volts
E = the applied peak voltage
d = the spacing between cathode and anode in cm
λ = the wavelength in cm
Γ = a constant to be determined experimentally
K = a function of the ratio of anode diameter to cathode diameter which, in effect, reduces a cylindrical diode to an equivalent parallel-plane diode[14]

Because all voltmeters suffer transit-time errors, no standard voltage could be established. Therefore, the formula had to be verified and the constant Γ determined by comparing voltmeters of different spacings. To accomplish this a series of diodes of different spacings was built. To verify the dependence of error with wavelength and voltage, the discrepancy in readings of a pair of voltmeters employing two of the diodes was measured as a function of wavelength and voltage. To verify the variation of error with spacing and to determine the constant Γ, the discrepancy in readings between each diode of the series and a "standard" diode was measured. This procedure made it possible to plot Γ in Equation (VI-2) as a function of *Kd*. A straight line resulted. The slope Γ had the value of 562 volts$^{1/2}$.

In Figure 7 are shown the calibration curves at two wavelengths of a diode voltmeter employing a diode having an anode diameter of

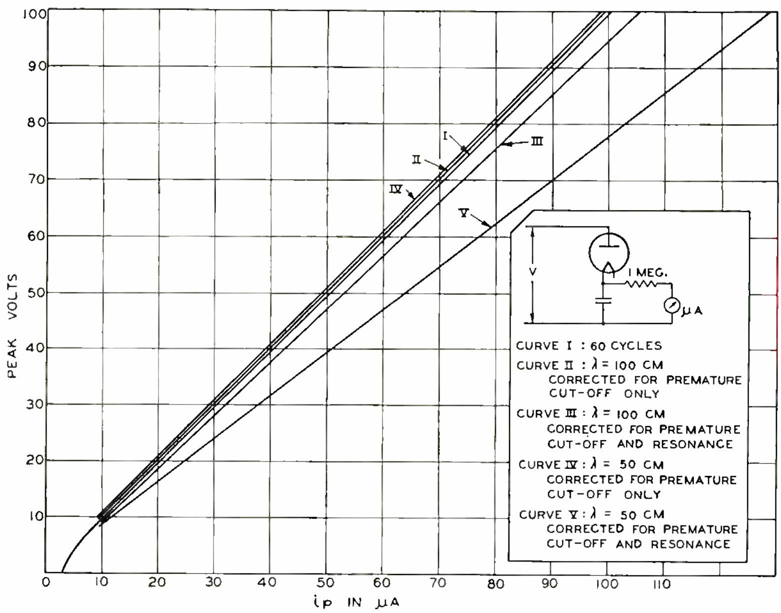

Fig. 7—Calibration of laboratory diode R-353 as a peak voltmeter.

0.009 inch and cathode diameter of 0.0026 inch. Note that the resonance error is by far the larger of the two errors. For this diode the resonance correction is $1-(25/\lambda)^2$ and the premature cut-off correction is $\Delta E = -7.5\sqrt{E}/\lambda$.

In making voltage measurements on parallel-wire transmission lines, it is advantageous to have a balanced voltmeter. Figure 8 shows the schematic circuit diagram of such a voltmeter. It will be noticed that each cathode return has its own resistor. If the diodes were perfectly matched and the line perfectly balanced, the cathodes could be returned to ground through a common resistor. However, if these conditions do not obtain, one of the diodes will cut off before the other and the indicated voltage will be merely the voltage from one side of the line to ground. When separate resistors are used, this difficulty is overcome and the indicated voltage is the total voltage between the lines.

The RCA-955 "acorn" triode with grid and anode tied together is frequently used as a diode voltmeter. Its resonance and premature cut-off corrections, respectively, are approximately $1-(40/\lambda)^2$ and $\Delta E = -30\sqrt{E}/\lambda$. While the RCA-955 is not quite as satisfactory as a diode built for the purpose of measuring voltage, its ruggedness and ready availability make it very useful for this purpose.

A thermocouple in series with a resistance has also been used as a voltmeter. The thermocouple had a short heater of 0.002-inch carbon wire and, therefore, had no appreciable skin-effect. Hence, the low-frequency calibration could be used to determine the current through

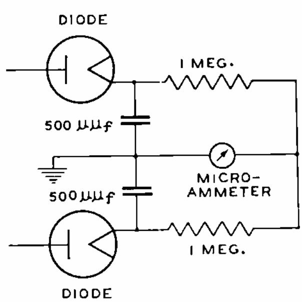

Fig. 8—Schematic diagram of a balanced diode voltmeter.

the heater. This voltmeter was checked against a diode voltmeter at $\lambda = 184$ cm and the current through the heater was found to be a linear function of the applied voltage. Whereas the measured value of the resistance in series with the thermocouple was 40,000 ohms for direct current, the apparent resistance of the voltmeter obtained by dividing the applied voltage by the current through the thermocouple was only 14,300 ohms. This decrease in resistance is due to the stray capacitances of the resistor. The writer would hesitate to use such a voltmeter without a calibration made with the resistance and thermocouple in the exact positions in which they are to be used. With such a voltmeter extreme care must be taken to prevent stray fields from reaching the couple circuit. Because the couple circuit has a very low resistance compared to the heater circuit, a stray field which does not affect the heater circuit appreciably can cause large circulating currents in the couple circuit. Such currents greatly disturb the calibration of the instrument and may have dire effects on the thermocouple.

The writer recently burned out three thermocouples in ten minutes before he obtained shielding enough to make operation safe for the thermocouples.

It is sometimes necessary to obtain known voltages whose magnitudes are smaller than those which can be measured with existing voltmeters. For instance, it may be necessary to calibrate a crystal detector to be used in field-strength measurements. To provide such voltages, a capacitance attenuator has been built. This attenuator consists of two parallel, circular condenser plates enclosed in a concentric cylinder. The capacitance between plates in such a condenser varies as[15] exp $(-K_1 z/a)$ when $z/a > 1$

where

$z =$ spacing between plates in cm
$a =$ radius of enclosing cylinder in cm
$K_1 =$ first root of the zero-order Bessel function
$= 2.405$

The spacing between plates in the attenuator is varied by means of a micrometer screw. The radius of the enclosing cylinder and the pitch of the micrometer thread were so chosen that the capacitance changes by a factor of ten for ten turns of the micrometer head. The dimensions were made small so that an attenuation range of 100 to 1 can be obtained at a wavelength of 50 cm with a spacing between condenser plates less than a tenth of a wavelength. This prevents errors due to the radiation field which attenuates less rapidly than the induction field. The attenuator has been calibrated at wavelengths of 151, 129, and 112 cm and the attenuation has been found to agree with the calculated attenuation.

VII. The Measurement of Reactance

Reactance is usually measured by connecting the unknown reactance across one end of a transmission line, coupling the line loosely to a generator, and tuning the circuit to resonance by varying the length of the transmission line. If the unknown reactance X is tuned to resonance with a short-circuited line, the reactance is

$$X = -\sqrt{\frac{L_o}{C_o}} \tan \frac{2\pi l_o}{\lambda} \qquad \text{(VII-1)}$$

It may be necessary to take into account the inductance of the "short circuit". This can be done as described in the section on the measurement of wavelength. If an open-ended line is used, the reactance is

$$X = \sqrt{\frac{L_o}{C_o}} \cot \frac{2\pi l_o}{\lambda} \qquad \text{(VII-1-a)}$$

This method is usually simple and straightforward and is perhaps best demonstrated by example.

As a first example, consider the measurement of the resonant wavelength of a diode of the type described in the discussion of voltmeters. Before apparatus is set up, it is usually advantageous to theorize briefly in order to determine what is required of the apparatus. The reactance of a diode is

$$X = \omega L_d - \frac{1}{\omega C_d}$$

Therefore, the condition for resonance when a short-circuited line is used is

$$\omega L_d - \frac{1}{\omega C_d} = -\sqrt{\frac{L_o}{C_o}} \tan \frac{2\pi}{\lambda} \left(l_o + \frac{L}{L_o} \right) \qquad \text{(VII-2)}$$

The correction for the inductance of the "short-circuit" has been included.

Now we can write

$$\omega L_d - \frac{1}{\omega C_d} = \omega L_d \left[1 - \frac{1}{\omega^2 L_d C_d} \right] = \frac{2\pi v L_d}{\lambda} \left[1 - \left(\frac{\lambda}{\lambda_r} \right)^2 \right]$$

On substituting this relation in Equation (VII-2), we obtain

$$\lambda \tan \frac{2\pi}{\lambda} \left(l_o + \frac{L}{L_o} \right) = -2\pi v L_d \cdot \sqrt{\frac{C_o}{L_o}} \left[1 - \left(\frac{\lambda}{\lambda_r} \right)^2 \right]$$

$$= +2\pi \frac{L_d}{L_o} \left[\left(\frac{\lambda}{\lambda_r} \right)^2 - 1 \right] \qquad \text{(VII-3)}$$

Therefore, if we plot $(\lambda \tan 2\pi/\lambda)(l_o + L/L_o)$ versus λ^2, we should obtain a straight line.

The intercept on the λ^2 axis is λ_r^2, and the slope is

$$S = \frac{2\pi}{\lambda_r^2} \frac{L_d}{L_o}$$

Hence, the series inductance of the diode is

$$L_d = \frac{\lambda_r^2}{2\pi} S L_o \qquad \text{(VII-4)}$$

Finally, we can obtain the interelectrode capacitance of the diode from the relation

$$C_d = \frac{\lambda_r^2}{(2\pi v)^2 L_d} \qquad \text{(VII-5)}$$

To determine λ_r, L_d, and C_d, we require the following data:

(1) The inductance per unit length L_o of the line

(2) The inductance L of the "short circuit"

(3) The length of line l_o for resonance for a series of values of the wavelength λ

To obtain these data, a transmission line consisting of two ⅜-inch copper tubes with a center-to-center spacing of ¾ inch was used. For this line

$$C_o = 2.11 \times 10^{-13} \text{ farad per cm}$$

$$L_o = 5.26 \times 10^{-9} \text{ henry per cm}$$

The length of the line could be varied by moving a movable short-circuit. The inductance of the short circuit was determined in the manner described in connection with wavemeters, and was found to be $L = 5.89 \times 10^{-8}$ henry. Then, the correction in length for this inductance was $L/L_o = 1.12$ cm. The diode was connected to the open end of the line. In this case it was convenient to use the diode as an indicator of resonance. In order to avoid extraneous effects due to the filament leads of the diode, these leads were brought through one of the copper conductors of the transmission line to the inactive part of the line which was essentially at ground potential. The length of the line for resonance as a function of wavelength was then measured, and $(\lambda \tan 2\pi/\lambda)(l_o + L/L_o)$ plotted against λ^2. Figure 9 shows this plot. The intercept on the λ^2 axis is 550. Therefore, the resonant wavelength is $\lambda_r = \sqrt{550} = 23.4$ cm. The slope of the line is $S = 4.67 \times 10^{-2}$ cm^{-1}. Hence, from Equation (VII-4), the diode inductance is

$$L_d = \frac{(23.4)^2}{2\pi} \times 4.67 \times 10^{-2} \times 5.26 \times 10^{-9} = 2.15 \times 10^{-8} \text{ henry}$$

and the capacitance, from Equation (VII-5) is

$$C_d = \frac{(23.4)^2}{(2\pi \times 3 \times 10^{10})^2 \times 2.15 \times 10^{-8}} = 0.719 \times 10^{-12} \text{ farad}$$

Summarizing these results, we have

$\lambda_r = 23.4$ cm = resonant wavelength of diode
$L_d = 2.15 \times 10^{-8}$ henry = inductance of diode leads
$C_d = 0.719 \times 10^{-12}$ farad = interelectrode capacitance

As a second example, we shall consider the calibration of a symmetrical variable condenser used in resistance measurements.

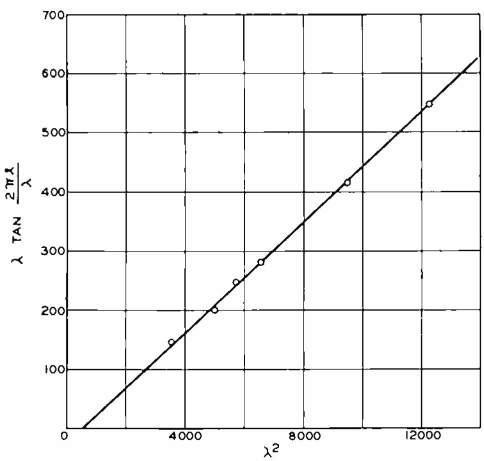

Fig. 9—Determination of the resonant wavelength of a diode.

The condenser is essentially a concentric cylinder condenser with the outer conductor split symmetrically into two electrodes. The inner cylinder has a diameter of 5/16 inch; and the outer conductor has a diameter of 3/8 inch. The angular aperture of the slits dividing the outer conductor into two segments is 60 degrees. The capacitance between the two segments is varied by moving the central cylinder axially with a micrometer screw. When the segments of the outer cylinder are connected across a symmetrical circuit, the central conductor, which is not connected to either segment, assumes ground potential and may be connected to ground if advantageous.

The purpose of the measurement to be described was to determine the change in capacitance between electrodes per division on the micrometer head. Figure 10 is a photograph of this condenser. The condenser was mounted at the end of the transmission line used in the previous example. The voltmeter was left in place to indicate resonance. The capacitance of the condenser can be written

$$C_1 + t \cdot C_2 \qquad \text{(VII-6)}$$

in which

C_1 = the zero capacitance
C_2 = the capacitance per division of the micrometer head of the condenser
t = reading of the micrometer

Fig. 10—Balanced condenser for the measurement of resistance by the reactance-variation method.

The diode voltmeter was in parallel with the condenser, so the reactance of the combination was

$$X = \frac{1}{-\omega(C_1 + t \cdot C_2) + \dfrac{1}{\omega L_d - \dfrac{1}{\omega C_d}}} \qquad \text{(VII-7)}$$

During the calibration at a given wavelength, all of the quantities except t in this expression are constant. Hence, for convenience, Equation (VII-7) can be written

$$X = \frac{1}{-\omega C_2 (t + A)} \qquad \text{(VII-8)}$$

Then the equation (VII-1) for resonance becomes

$$\frac{1}{\omega C_2 (t + A)} = \sqrt{\frac{L_o}{C_o}} \tan \frac{2\pi}{\lambda} \left(l_o + \frac{L}{L_o} \right)$$

or

$$\cot \frac{2\pi}{\lambda} \left(l_o + \frac{L}{L_o} \right) = \omega C_2 \sqrt{\frac{L_o}{C_o}} (t + A) = \frac{2\pi}{\lambda} \frac{C_2}{C_o} (t + A) \qquad \text{(VII-9)}$$

Therefore, when $\cot 2\pi (l_o + L/L_o)/\lambda$ is plotted against t, a straight line results, the slope of which is

$$S = \frac{2\pi}{\lambda} \frac{C_2}{C_o}$$

Then the required capacitance is

$$C_2 = \frac{\lambda S}{2\pi} C_o \qquad \text{(VII-10)}$$

The measurement consists in measuring l as a function of t. Figure 11 is a plot of $\cot 2\pi (l_o + L/L_o)/\lambda$ versus t at a wavelength of 98.4 cm. The slope of the line is

$$S = 1.46 \times 10^{-4}$$

Therefore, the capacitance per division on the micrometer head is

$$C_2 = \frac{98.4 \times 1.46 \times 10^{-4}}{2\pi} \times 2.11 \times 10^{-13} = 4.82 \times 10^{-16} \text{ farads}$$

A calibration was made at a wavelength of 308 cm; the result checked the value found above within one per cent, which is within the experimental accuracy.

VIII. The Measurement of Resistance

Resistance has been measured by three methods:

(1) Substitution method
(2) Resistance-variation method
(3) Reactance-variation method

At short wavelengths all of these methods employ a tuned circuit loosely coupled to a generator. This arrangement is equivalent to connecting the tuned circuit in series with a very high impedance across

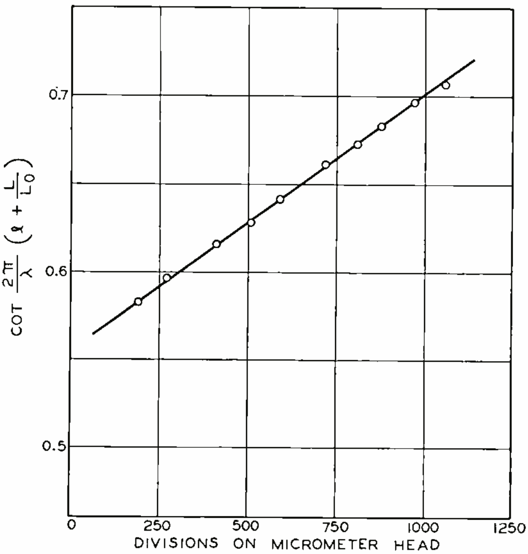

Fig. 11—Determination of the calibration of the balanced condenser.

a constant-voltage generator. Then the voltage developed across the tuned circuit is proportional to its impedance.

J. M. Miller and B. Salzberg of this laboratory have used the substitution method to study commercial resistors at frequencies up to 250 megacycles and to measure dielectric losses.[16] In this case, the tuned circuit consists of a transmission line of low characteristic impedance, terminated by a short circuit at one end and by a capacitance at the other end. The voltage distribution along the line is then

$$E = E_1 \frac{\sin \dfrac{2\pi l}{\lambda}}{\sin \dfrac{2\pi l_1}{\lambda}} \tag{VIII-1}$$

where

l_1 = the total length of line
E_1 = the voltage at l_1
l = the distance from the short circuit to any point on the line
E = the voltage at l

If a resistance R is placed across the line at l and the current through the resistor is inappreciable compared to the circulating current in the line at that point, the voltage distribution will not be altered. When the circuit is resonant, the circulating current is very high so that resistances as low as 8,000 ohms can be placed across the line without disturbing the voltage distribution. The power dissipated in the resistor is

$$W = \frac{E^2}{R} = \frac{E_1{}^2}{R}\left[\frac{\sin\frac{2\pi l}{\lambda}}{\sin\frac{2\pi l_1}{\lambda}}\right]^2$$

The same power would be dissipated in a resistor R_1 at the end of the line if

$$R_1 = R\left[\frac{\sin\frac{2\pi l_1}{\lambda}}{\sin\frac{2\pi l}{\lambda}}\right]^2 \qquad \text{(VIII-2)}$$

Therefore, placing a resistor R at l is equivalent to placing a resistor R_1 at the end of the line. This assumes that the equivalent resistance R_1 is small compared to the resonant impedance of the line alone. In the line used by Miller and Salzberg, $l_1 << \lambda/4$ so that

$$R_1 = R\left(\frac{l_1}{l}\right)^2 \qquad \text{(VIII-3)}$$

A series of resistors of various values were placed across the line at such positions that R_1 remained constant, as evidenced by the constant reading of a vacuum-tube voltmeter across the line. For low values of the particular type of resistor used, they found the resistance measured at low frequencies in agreement with Equation (VIII-3). Since it is quite unlikely that these resistors should all have the same percentage error, they assumed that the high-frequency values were the same as the low frequency. Having thus established a number of standard resistances, other resistors were measured by comparing them with the standards through relation (VIII-3). It was possible by this means to measure very high values of resistance. It is of interest to note that certain ½-watt resistors of the ceramic type, in the resistance range from 10,000 to 100,000 ohms, show less than 10 per cent deviation from their low-frequency values up to 250 megacycles.

The resistance-variation method consists in placing the unknown resistance and a voltmeter across a resonant circuit which is loosely coupled to a generator. The voltage across the tuned circuit is then read. A known resistance is added across the circuit and the voltage is again read. Since the voltage across a loosely coupled circuit is proportional to the impedance, the unknown resistance has a value

$$R_x = R_s \left(\frac{E_x}{E_s} - 1 \right) \tag{VIII-4}$$

in which

R_x = the unknown resistance
R_s = the known resistance
E_x = the voltage with the unknown resistance across the circuit
E_s = the voltage with the known and unknown resistances in parallel across the circuit

If the resonant impedance of the tuned circuit is comparable to the unknown resistance, the circuit impedance must be taken into account. The resonant impedance can be measured by the same method. This method has been useful for wavelengths greater than 120 cm ($f < 250$ Mc) where the work of Miller and Salzberg has provided a series of known resistances.

The reactance-variation method takes three forms at short wavelengths:

(1) The capacitance-variation method
(2) The line-length-variation method
(3) The wavelength-variation method

In all these forms, the unknown resistance is placed across a tuned circuit, usually a transmission line terminated at one end by a short circuit and at the other by a capacitance. The tuned circuit is loosely coupled to a generator and the voltage across the line at some point is read.

The capacitance-variation method is perhaps the simplest method to use. A variable condenser of known calibration is connected across the circuit. Then the admittance of the circuit is

$$Y = G + j(B + \omega C) \qquad \text{(VIII-5)}$$

in which

G = the parallel conductance of the line and unknown impedance
B = the parallel susceptance of the line and unknown impedance
ωC = the susceptance of the condenser

Let

$$\omega C = \omega C' + \omega \Delta C$$

where C' = the capacitance which makes the circuit resonant.

Then

$$Y = G + j\,[B + \omega C' + \omega \Delta C] = G + j\omega \Delta C \qquad \text{(VIII-6)}$$

Now the voltmeter reading is proportional to the magnitude of the impedance. Therefore

$$\frac{1}{E^2} = k\,[G^2 + (\omega \Delta C)^2] \qquad \text{(VIII-7)}$$

where k is a proportionality factor. At resonance, $\Delta C = 0$ and the voltage E_o is given by

$$\frac{1}{E_o^2} = kG^2$$

Then

$$\frac{E_o^2}{E^2} = 1 + \left(\frac{\omega \Delta C}{G} \right)^2 \qquad \text{(VIII-8)}$$

Therefore, when the circuit is detuned until the voltage drops to 0.707 times the voltage at resonance, the resistance of the circuit is equal to the change in capacitance reactance:

$$R = \frac{1}{G} = \frac{1}{\omega \Delta C} \qquad \text{(VIII-9)}$$

The condenser described in Section VII as built for measuring resistances by this method. Because of its symmetrical form, it is particularly useful for measuring the resonant impedances of parallel-wire transmission lines.

A special transmission line and condenser system has been built for measuring resistance. This is shown schematically in Figure 12. Figure 13 is a photograph of the instrument. The system consists of a concentric transmission line with one end terminated in a short-circuit and the other terminated in a concentric-cylinder condenser. The short-circuit is mounted on a brass cylinder which is driven by a lead screw to make adjustments of line length. A second short-circuit

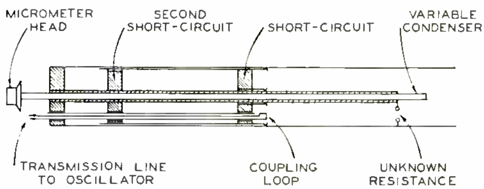

Fig. 12—Schematic diagram of a transmission line and condenser for the measurement of resistance by the reactance-variation method.

is provided to suppress standing waves on the inactive part of the line. The inner conductor of the variable condenser is brought back to the inactive part of the transmission line through the central conductor of the line. A micrometer screw controls the variable condenser. The change in capacitance of the condenser per turn of the micrometer head is $C_T = 4 \times 10^{-14}$ farad when the length of the inner conductor is very small compared to a wavelength. Since this is usually not true, the voltage distribution on the condenser must be taken into account. When this is done the change in capacitance per turn is

$C_T = 4 \sec^2 \dfrac{2\pi l}{\lambda} \times 10^{-14}$ where l is the length of the inner conductor

of the condenser. The line is excited by a small coupling loop near the short-circuit.

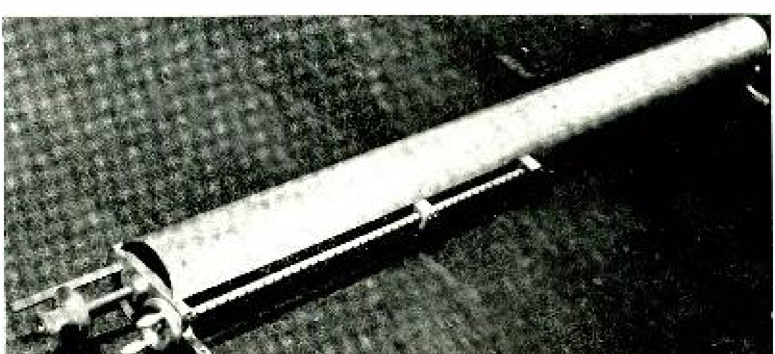

Fig. 13—The transmission line and condenser for the measurement of resistance.

Figure 14 shows the resonance curve of a diode voltmeter at a wavelength of 184 cm measured with this apparatus. R in the figure is the reading of the micrometer in turns. This curve appears symmetrical and of the normal form. However, to check the constancy of the voltage supply and coupling, the reciprocal of the voltage squared was plotted against the square of the increment of R from the value at resonance. This is essentially a plot of Equation (VIII-7). The curve is shown in Figure 15. This method of plotting gives an excellent check on the performance of the apparatus. Since the squares of the pertinent quantities are plotted, any irregularities are doubled.

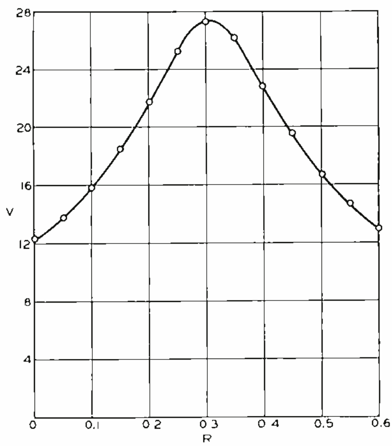

Fig. 14—Resonance curve of a diode voltmeter across the transmission line for the measurement of resistance.

From the curve it is seen that the intercept is

$$\frac{1}{E^2} = 0.00135$$

When $\frac{1}{E^2}$ has twice this value

$$R = \sqrt{0.0225} = 0.150$$

The length of the inner conductor of the condenser was 5.5 cm. Hence, the resistance of the voltmeter and line is

$$R = \frac{\cos^2 \frac{2\pi l}{\lambda}}{\omega C_T \cdot \triangle R} = \frac{\cos^2 \frac{2\pi \times 5.5}{184}}{\frac{2\pi}{184} \times 3 \times 10^{10} \times 4 \times 10^{-14} \times 0.150}$$

$$= 157{,}000 \text{ ohms}$$

The length-of-line variation method is very similar to the capacitance-variation method except that the length of a transmission line instead of the capacitance of a condenser is varied. Let

G = the parallel conductance of the unknown resistor
G_L = the parallel conductance of the line
B = the parallel susceptance of the unknown resistor

Then the total admittance of the line and resistor is

$$Y = G + G_L + j\left[B - \sqrt{\frac{C_o}{L_o}} \cot \frac{2\pi l}{\lambda} \right] \qquad \text{(VIII-10)}$$

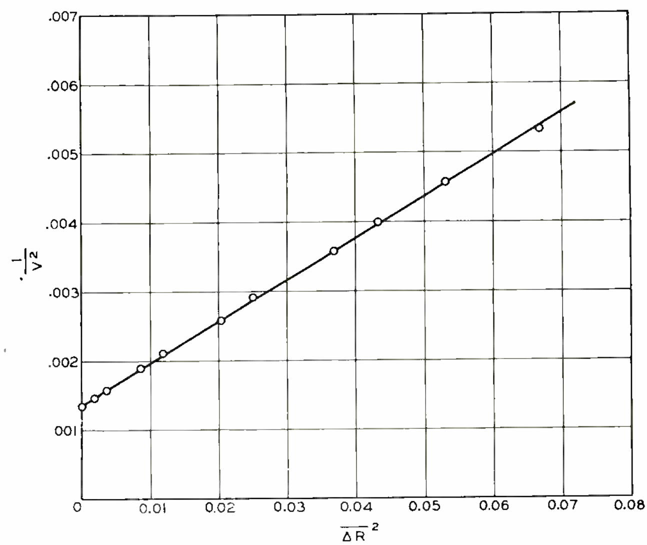

Fig. 15—Determination of the input resistance of a diode voltmeter.

G_L is a function of l/λ. However, since G_L is small, less than 5×10^{-5} mho for practical transmission lines, its variation with l/λ causes no difficulty in measurements. The reasons will be detailed in connection with particular applications of the formula. The condition for resonance is

$$B = \sqrt{\frac{C_o}{L_o}} \cot \frac{2\pi l_o}{\lambda} \qquad \text{(VIII-11)}$$

where l_o = the length, which satisfies (VIII-11). Hence, B is determined by measuring the length for a maximum voltage reading.

The measurement of G separates conveniently into two cases:

(a) The first case is that in which $G >> G_L$. Then G_L can be neglected and Equation (VIII-10) becomes:

$$Y = G + j\left[B - \sqrt{\frac{C_o}{L_o}}\cot\frac{2\pi l}{\lambda}\right] \qquad \text{(VIII-12)}$$

B in this relation is first measured as outlined above. Then the line length is changed until the voltage drops to 0.707 times its resonant value, and the line length l_1 for this condition is measured. The conductance is then

$$G = \left\{B - \sqrt{\frac{C_o}{L_o}}\cot\frac{2\pi l_1}{\lambda}\right\} \qquad \text{(VIII-13)}$$

This method has been used to measure the resistance of thermocouples.

(b) The second case is that in which G and G_L are of the same order of magnitude. Then because both G and G_L are small, l can be written

$$l = l_o + \Delta l, \qquad \frac{\Delta l}{l_o} << 1$$

where l_o = length of line for resonance. Equation (VIII-10) then reduces to

$$Y = G + G_L + j\sqrt{\frac{C_o}{L_o}}\,\frac{2\pi\Delta l}{\lambda}\csc^2\frac{2\pi l_o}{\lambda} \qquad \text{(VIII-14)}$$

The conductance of the line and resistor are determined by changing the length such an amount Δl_o that the voltage drops to 0.707 times its resonant value. Then

$$G + G_L = \sqrt{\frac{C_o}{L_o}}\cdot\frac{2\pi\Delta l_o}{\lambda}\csc^2\frac{2\pi l_o}{\lambda} \qquad \text{(VIII-15)}$$

During the detuning G_L also changes. However, the real and imaginary parts of Equation (VIII-14) are of the same order of magnitude. Therefore, the change in G_L will be of the order of G_L^2, which may be neglected in view of the small magnitude of G_L.

The latter method is used extensively to determine the impedance of quarter-wave transmission lines. For such lines Equation (VIII-15) becomes

$$G = \frac{\pi}{2} \sqrt{\frac{C_o}{L_o}} \frac{\Delta l_o}{l_o} \qquad \text{(VIII-16)}$$

P. D. Zottu of this laboratory has used this method to determine the resistance of circular conductors.[17] In essence, his method is the following. The inner conductor of a quarter-wave concentric transmission line was made of the material whose resistance was to be measured. The impedance of the line was determined from the appropriate measurements and Equation (VIII-16). The resistance per unit length of line was determined from Equation (III-8). The resistance per unit length of the outer conductor of the line, previously determined, was subtracted from this result. The remainder was the required resistance. His results are in good agreement with the asymptotic skin-effect formula (III-18).

The wavelength-variation method is so similar to the other methods that it will not be described in detail. It is sufficient to say that when the wavelength has been shifted from the resonant wavelength by an amount such that the line voltage has dropped to 0.707 times its resonant value

$$G + G_L = \sqrt{\frac{C_o}{L_o}} \frac{2\pi l}{\lambda_o} \cdot \frac{\Delta\lambda_o}{\lambda_o} \left[1 + \frac{\sin \frac{4\pi l}{\lambda_o}}{\frac{4\pi l}{\lambda_o}} \right] \csc^2 \frac{2\pi l}{\lambda_o} \qquad \text{(VIII-17)}$$

in which

G = the conductance of the unknown
G_L = the conductance of the line
λ_o = the resonant wavelength
$\Delta\lambda_o$ = the change in wavelength from λ_o to reduce the voltage to 0.707 times its value at resonance.

This formula assumes that G and G_L are small, i.e., less than 10^{-3} mho.[18]

Mr. G. R. Kilgore of this laboratory has used this method to measure the resonant impedance of the anode circuit of a magnetron. An oscillator was loosely coupled to the anode circuit. A second fixed-frequency oscillator was set up sufficiently remote from the circuit to induce no perceptible voltage across the circuit. To measure the difference in frequency between the two oscillators, a crystal detector was connected between the ground and antenna terminals of a broadcast receiver and the difference in frequency read on the calibrated tuning dial. The frequency of the oscillator coupled to the magnetron circuit was varied and the frequency shift from resonance necessary to reduce the resonant voltage across the line to the 0.707 point was measured. In this work, Mr. Kilgore found that a slight amount of unbalance in a parallel-wire line greatly reduces the resonant impedance, as much as 50 per cent in some cases. This reduction in impedance is apparently due to the increase in the radiation resistance of the line with unbalance.

In the course of his experimental work on the measurement of impedance, the writer encountered an anomoly which may considerably trouble others. He found that resonance curves in some instances were asymmetrical near the resonance point. The theory was carefully checked and no trace of such an asymmetry was disclosed. The difficulty finally was traced to the circuit coupling the generator to the measuring circuit. The coupling circuit had a very high resonant impedance. Therefore, when it was tuned slightly off-resonance where the slope of the curve was very steep, any slight reaction of the measuring line on the circuit detuned it sufficiently to reduce its circulating current appreciably. When the coupling circuit was loaded with resistance and tuned to resonance, the difficulty was completely eliminated.

IX. The Measurement of Current

The writer and his associates have had little occasion to measure current at ultra-short wavelengths. In the past, measurements of voltage, reactance, and resistance have given all the required information. Therefore, the measurement of current lacks the background of experience which the other measurements have. However, it is apparent that instruments and a technique for measuring current will be convenient if not necessary in the future. With this in mind, some work on the measurement of current has been done.

The attributes of a satisfactory device for the measurement of current are:

(1) It should have adequate sensitivity

(2) It should have a low resistance

(3) The calibration should be independent of frequency so that the device may be calibrated at 60 cycles per second

The vacuum thermocouple has these attributes in the low-current range. The most sensitive short-wave thermocouple described in Section V will measure a current of 1 milliampere. The resistance of this thermocouple is 1000 ohms, which is not low. However, if a similar thermocouple were built for current measurement, the resistance could be reduced about 50 per cent without seriously reducing the sensitivity. For higher-current ranges, the sensitivity and low-resistance requirements are easily met.

The factors which make the calibration of a thermocouple dependent upon the wavelength of operation are:

(1) The current distribution along the heater

(2) The change in heater resistance due to skin effect

The effect of current distribution along the heater can be taken care of in the same manner in which it was taken care of in the case of power-measuring thermocouples, namely, by making the heater short. Since it is desirable to have a low heater resistance in the case of current-measuring thermocouples, the problem is simpler than in the case of power-measuring thermocouples in which a high heater resistance is desirable. Past experience indicates that a thermocouple with 1-ma sensitivity and a heater length of 4 mm can be built. Such a thermocouple would have less than one per cent error due to current distribution for $\lambda > 9$ cm.

For the measurement of current it is particularly desirable that the thermocouple heater have no skin-effect. A thermocouple depends on the temperature rise of the junction for its operation. Therefore, the resistivity of the heater varies widely over the operating range of the device. The resistance of a conductor having appreciable skin-effect does not vary linearly with the resistivity. Hence, the skin-effect correction varies not only with frequency, but also with the amount of power being dissipated in the conductor. Consequently, a thermocouple to be used for current measurement which has appreciable skin-effect must have its resistance measured over the entire operating range at each frequency at which it is to be used. Such an instrument would be quite inconvenient to calibrate.

From Equation (III-17) it can be readily shown that in order that skin-effect in a solid cylindrical conductor give rise to less than 1 per cent increase in resistance over the d-c value, the following relation must obtain

$$a\sqrt{\frac{\mu f}{\rho}} < 4.27 \qquad \text{(IX-1)}$$

For the materials used as heaters in thermocouples

$$\mu = 1$$

so Equation (IX-1) can be written

$$a^2 \frac{f}{\rho} < 18.2 \qquad \text{(IX-2)}$$

Now the resistance per unit length of a cylindrical conductor is

$$R_o = \frac{\rho}{\pi a^2} \times 10^{-6} \text{ ohms cm}^{-1} \qquad \text{(IX-3)}$$

The substitution of this relation in Equation (IX-2) gives

$$R_o > 1.75\, f \times 10^{-8} \text{ ohm cm}^{-1} \qquad \text{(IX-4)}$$

as the condition that skin-effect be negligible. Therefore, the condition that the resistance of a cylindrical conductor differ by less than one per cent from the d-c value at any wavelength above 1 cm is that

$$R_o > 525 \text{ ohm cm}^{-1} \qquad \text{(IX-5)}$$

i.e., that the resistance per unit length exceed 525 ohms per cm.[19] This condition is satisfied by most carbon conductors of less than 0.002 inch diameter. Therefore, skin-effect is a minor problem in low-current thermocouples.

As noted in Section VIII, the resistance of a few thermocouples at short wavelengths has been measured. Some of these thermocouples had carbon heaters. For these thermocouples no deviation from the d-c resistance was found. Perhaps the results should be construed as a check on the method of measurement.

For currents exceeding 100 ma, the skin-effect in solid conductors becomes troublesome. Circuits carrying high currents are usually low-resistance circuits. Therefore, the resistance of a thermocouple to be placed in such a circuit must be very low if it is not to perturb the circuit. It is readily seen from relation (IX-4) that a solid conductor must have a high resistance per unit length if skin-effect is to be inappreciable. Hence, the solid conductor is inherently unsuited for low values of resistance without skin-effect.

The best solution to the problem of measuring currents exceeding 100 ma appears to be the measurement of the voltage drop across a low resistance placed in the circuit. Thermocouples having heater resistances of the order of 100 ohms with no appreciable skin-effect will readily measure voltages of the order of 0.1 volt. It is therefore feasible to measure currents as low as 100 ma by this method with an added series resistance of only one ohm.

X. Conclusion

Methods for the measurement of wavelength, voltage, current, power, resistance, and reactance have been described. All of these methods with the exception of that for the measurement of current have been in daily use for several years. Therefore, they represent a large background of practical experience. No doubt the future will bring many improvements in both methods and technique. However, the writer feels that the methods of the future will be fundamentally the same as those of the present. After all, they are merely adaptations of the methods described in that familiar measurement classic, Bulletin 74 of the Bureau of Standards.

The writer gratefully acknowledges that he has drawn freely on the ideas and experience of his colleagues, Dr. J. M. Miller, Dr. A. V. Haeff, Mr. G. R. Kilgore, and Mr. P. D. Zottu. The specific references to their work in no way define the extent of their contributions to the work reported in this paper.

Appendix A

List of Symbols

- A = a constant
- a = radius of a conductor in cm
- B = susceptance in mhos
- C_d = interelectrode capacitance of a diode
- C_o = capacitance per unit length of transmission line in farads · cm^{-1}
- C_T = capacitance per turn of a micrometer condenser
- d = interelectrode spacing of a diode in cm
- E_r = voltage across the receiving end of a transmission line in volts
- E_s = voltage across the sending end of a transmission line in volts
- G = conductance in mhos
- G_L = sending-end conductance of a transmission line in mhos
- G_o = leakage conductance per unit length of transmission line in mhos cm^{-1}
- I_r = current at the receiving end of a transmission line in amperes
- I_s = current at the sending end of a transmission line in amperes
- $J_n(x)$ = Bessel function of order n
- K = a function of the ratio of anode diameter to cathode diameter which, in effect, reduces a cylindrical diode to a parallel-plane diode
- K_1 = first root of zero-order Bessel function = 2.405
- L_d = inductance of the leads of a diode in henrys
- L_o = inductance per unit length of transmission line in henrys · cm^{-1}
- l = length of a transmission line in cm

l_o = that length of transmission line which makes a circuit resonant

m = propagation constant of a transmission line in $cm^{-1} = \alpha + j\beta$

$$P = 2\pi \sqrt{\frac{\mu f}{\rho \times 10^3}} (1 - j) \text{ cm}^{-1}$$

R_e = "real part of"

R_o = resistance per unit length of a conductor in ohm cm^{-1}

r_o = total resistance per unit length of transmission line (per loop cm) in ohms $\cdot$ cm^{-1}

S = the slope of a curve

v = phase velocity of a wave on a transmission line in cm $\cdot$ sec^{-1}

Z_o = characteristic impedance of a transmission line in ohms $= \gamma - j\delta$

Z_r = impedance across the receiving end of a transmission line in ohms

Z_s = impedance looking into the sending end of a transmission line in ohms

z = spacing between condenser plates of attenuator (Section VI) in cm

α = attenuation constant of a transmission line in cm^{-1}

β = phase constant of a transmission line in cm^{-1}

Γ = diode voltmeter transit-time error constant (Section VI) in $volts^{1/2}$

γ = real component of the characteristic impedance of a transmission line in ohms

$\triangle$ = an increment, for example, $\triangle l$ = increment in length

δ = reactive component of the characteristic impedance of a transmission line in ohms

ε = base of Napierian logarithms

λ = wavelength in cm

λ_r = resonant wavelength of a circuit in cm

μ = magnetic permeability; when used as prefix, denotes micro-

ρ = resistivity in microhm cm

$\omega = 2\pi f$

BIBLIOGRAPHY

[1] A. L. Samuel, "A Negative Grid Triode Oscillator and Amplifier for Ultra-High Frequencies", *Proc. I.R.E.*, Vol. 25, No. 10, p. 1243, October (1937).

[2] O. Pfetscher and W. Puhlmann, "On Habann Tubes of Large Power for Ultra-High Frequencies", *Hochfrequenz und Elektroakus*, Vol. 47, pp. 105-115, (1936).

[3] E. J. Sterba and C. B. Feldman, "Transmission Lines for Short-Wave Radio Systems", *Proc. I.R.E.*, Vol. 20, No. 7, p. 1163, July (1932).

[4] Russell, "Skin Effect in Concentric Mains", *Phil. Mag.*, Vol. 17, p. 524, (1909).

[5] "Radio Measurements and Instruments", *Bulletin 74, Bureau of Standards.*

[6] "Funktionentafeln", Jahnke und Emde, *Teubner*, p. 142.

[7] Lester E. Reukema, "Transmission Lines at Very High Frequencies", *Elect. Eng.*, Vol. 56, No. 3, p. 1002, August (1937).

[8] Discussion on "Transmission Lines at Very High Frequencies", *Elect. Eng.*, Vol. 57, No. 2, p. 104, February (1937).

[9] S. A. Schelkunoff, "Some Equivalence Theorems of Electromagnetics and Their Application to Radiation Problems", *BSTJ*, Vol. 15, No. 1, p. 92, January (1936).

[10] August Hund, "Theory of the Determination of Ultra-Radio Frequencies by Standing Waves on Wires", *Scientific Papers of the Bureau of Standards*, No. 491.

[11] L. S. Nergaard, "Electrical Measurements at Wavelengths Less than Two Meters", *Proc. I.R.E.*, Vol. 24, No. 9, p. 1207, September (1936).

[12] C. L. Fortescue, "Thermionic Voltmeters for Use at Very High Frequencies", *Jour. I.E.E.*, Vol. 77, No. 456, p. 429, September (1935).

[13] E. C. S. Megaw, "Voltage Measurement at Very High Frequencies", *Wireless Engineer*,

Part I, Vol. 13, No. 149, p. 65, February (1936).
Part II, Vol. 13, No. 150, p. 135, March (1936).
Part II, Vol. 13, No. 151, p. 201, April (1936).

[14] W. R. Ferris, "Input Resistance of Vacuum Tubes as Ultra-High-Frequency Amplifiers", *Proc. I.R.E.*, Vol. 24, No. 1, p. 82, January (1936).

[15] The potential distribution between the inside of a cylinder and a disc electrode within the cylinder was studied by W. Schottky and J. v. Issendorf, *Zeit. f. Physik*, Vol. 31, pp. 163-201, (1925). They obtained the relation

$$V = V_o J_o \left(K_1 \frac{r}{a} \right) e^{-K_1 \frac{Z}{a}}$$

for the potential V at any point (r, Z) in terms of the potential V_o at point (0, 0). The particular type of attenuator described in the present paper was described to me by J. F. Dreyer, Jr., formerly of this Company, in 1934. He had used it some years previously in measurement work. Similar attenuators are described in a paper entitled, "The Design and Testing of Multi-range Receivers", by D. E. Harnett and N. P. Case, *Proc. I.R.E.*, Vol. 23, No. 6, p. 578, June (1935).

[16] J. M. Miller and B. Salzberg, "Measurements on Resistors and Insulators at Ultra-High Frequencies", to be published later.

[17] P. D. Zottu, "Resistance and Permeability Measurements at Ultra-High Frequencies", presented at *U.R.S.I.* meeting, April, 1938.

[18] This formula also assumes that $B = \omega C$ or $B = -1/\omega L$.

[19] These considerations were discussed in 1934 by P. D. Zottu in an unpublished paper entitled "Memorandum on High-Frequency Resistance with Negligible Skin-Effect".

TEMPERATURE REDUCTION IN HIGH-POWERED LOUDSPEAKERS

BY

FRANK MASSA

RCA Manufacturing Company, Inc., Camden, N. J.

Summary—*An ideal loudspeaker designed for high-power output is ultimately limited in its rating by the maximum permissible temperature that can be safely tolerated by the voice-coil structure which is generally the hottest operating portion of the speaker. The high voice-coil temperature results from the insulating film of air which separates the voice coil from the magnetic structure. Data are presented showing the reduction in temperature rise which resulted when the air in the air gap of two speakers was replaced by helium and hydrogen, each gas having a higher thermal conductivity than air. The reduced voice-coil temperature permits either the lowering of the voice-coil dimensions with a corresponding decrease in weight of the magnetic structure, or operation of a given structure at greatly reduced temperature. A small-weight high-powered speaker is particularly desirable for special applications, such as public address from aircraft. If weight is of no importance, the cooler operation due to the use of helium or hydrogen in the gap will permit an increased operating efficiency of the speaker.*

INTRODUCTION

IN a well-designed loudspeaker, as well as in most all other types of electrical apparatus, the power rating is ultimately limited by the maximum temperature that can safely be reached within the structure. For a moving-coil loudspeaker, the maximum temperature rise during operation generally occurs at the voice coil, due, in a large part, to the insulating air film which separates the coil from the metal parts of the magnetic structure. By reducing the thickness of the air film, through the use of smaller air gap clearances, the conduction of heat from the voice coil to the metal parts is facilitated, but a limit is soon reached beyond which further reduction becomes impractical because of the mechanical requirements that must be met to make the coil operative without striking the pole pieces.

To keep the voice coil within safe temperature limits after having adjusted the air-gap clearance to the smallest permissible limit, it is necessary to increase the surface area of the coil as the power rating is increased. If a loudspeaker is designed for high power-handling capacity and no special cooling means are provided, it becomes necessary to resort to large-diameter voice coils with the resulting greatly increased weight for the magnetic circuit. For some special applications such as announcing from aircraft, excessively heavy apparatus is definitely undesirable, therefore some auxiliary means for cooling a loudspeaker voice coil offers a practical means for the solution of the problem. In other cases where small weight is of no great necessity, improved efficiency for high-powered speakers may be realized by providing cooling means for the voice coil.

One obvious method of cooling a loudspeaker voice coil is to circulate cool air through the air gap. For the applications in which the speaker weight should be as small as possible, the auxiliary pumping

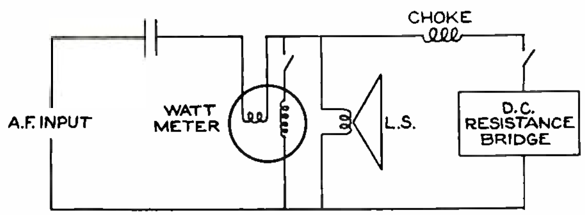

Fig. 1—Experimental set-up for obtaining voice-coil temperature-rise data while the loudspeaker is operating under normal conditions.

and filtering equipment necessary for providing clean circulating air would neutralize the advantages of the reduced speaker weight. To avoid the use of auxiliary mechanical equipment for cooling the voice coil, some experimental tests were carried on to learn what improvement could be realized by providing a fluid of higher thermal conductivity in the air gap in order to increase the rate of heat conduction through the heat-insulating film. Both helium and hydrogen have higher thermal conductivities than air (6.3 and 7.1 times, respectively) therefore both gases were employed in the tests for which the data will be presented.

Measurement of Temperature Rise

It appeared that the simplest and most accurate means for determining the voice-coil temperature rise would be to measure the d-c resistance of the voice coil during actual conditions of operation. The temperature rise could then be simply computed from the temperature coefficient of the voice-coil conductor and the observed increase in voice-coil resistance.

For the sake of simplicity, the first series of measurements was made with the voice coil supplied with direct current and the field unexcited and demagnetized. Under these conditions no sound is radiated and the entire electrical input is converted into heat, which means that higher temperatures may be expected than under normal operation. A voltmeter and ammeter were used to read voice-coil voltage and current, from which both the power input and voice-coil resistance could be directly determined. The temperature rise was then calculated at the various power levels from the various values of the computed resistance.

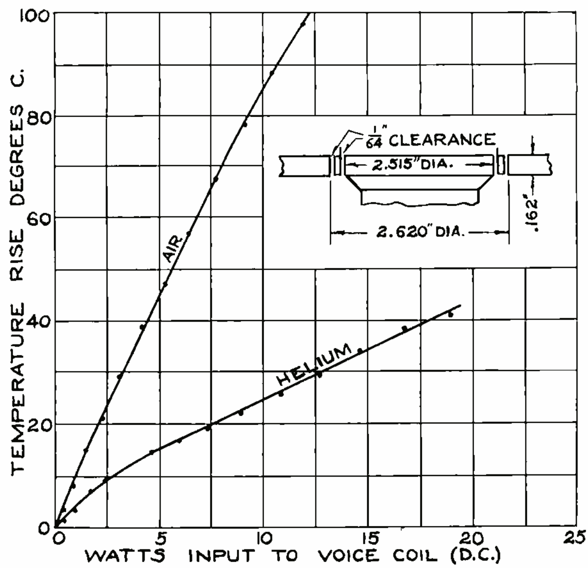

Fig. 2—Experimental data showing temperature rise versus power input to voice coil (speaker No. 1) for both air and helium atmospheres. Tests were made with d.c.

The successful results obtained from the d-c tests led to the development of the circuit shown in Figure 1 for carrying on additional investigations of the advantages of helium and hydrogen under actual operating conditions. The audio signal was applied to the voice coil through a large condenser, and a wattmeter was connected to measure the power input as shown. A d-c resistance bridge was connected across the voice coil through a suitable choke for the purpose of determining the resistance while the coil was operating. From the resistance and wattmeter readings the temperature-rise characteristics under normal operation were thus determined.

Helium or hydrogen was substituted for the air in the gap by supplying the gas through a suitable inlet into an air-tight magnetic structure, while a second outlet from the structure permitted the air to be forced out. When the substitution was completed, the data with the desired gas filling the clearance space between the voice coil and the magnetic structure were obtained.

Experimental Results

Two dynamically driven horn-type loudspeakers were employed in the experiments; speaker No. 1 rated normally at approximately 50

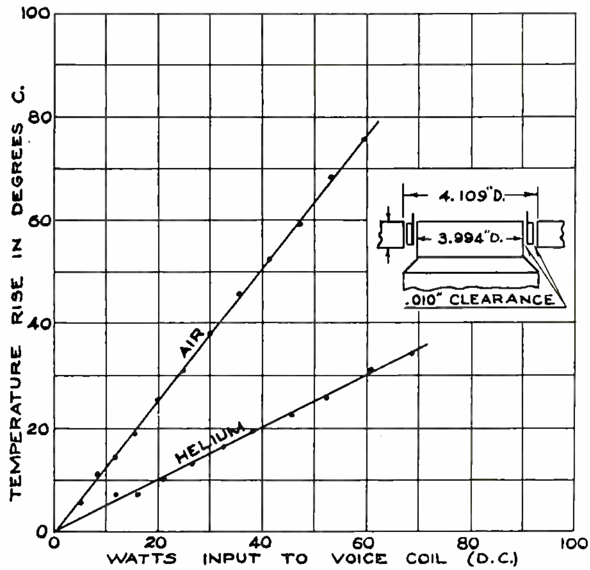

Fig. 3—Experimental data showing temperature rise versus power input to voice coil (speaker No. 2) for both air and helium atmospheres. Tests were made with d.c. on voice coil and no field excitation.

watts input, and speaker No. 2 rated at 250 watts audio input. The measured d-c temperature-rise data with air and helium atmospheres for speaker No. 1 are shown in Figure 2. The voice coil consists of enamelled aluminum wire wound on a paper collar which was attached to an aluminum diaphragm. The voice-coil, air-gap, and clearance dimensions are shown in the insert sketch.

Temperature-rise data for speaker No. 2 under d-c input conditions are shown in Figure 3. The voice-coil structure of this high-powered speaker consists of enamelled aluminum wire wound on an aluminum collar which is riveted to an aluminum cone. The air-gap dimensions and clearance are shown in the insert sketch in Figure 3. In this speaker the voice-coil area is larger than that of speaker No. 1 and also the air-film thickness (air-gap clearance) is smaller.

In view of the large reduction in temperature rise that was measured with d.c. applied to the voice coil and helium present in the gap, the circuit of Figure 1 was developed for testing the advantages of helium and hydrogen under actual conditions of operation. The same two speakers were set up for normal sound reproduction and a 1000-cycle signal of adjustable intensity was applied to the voice coil. The temperature-rise data obtained under normal operation for speakers

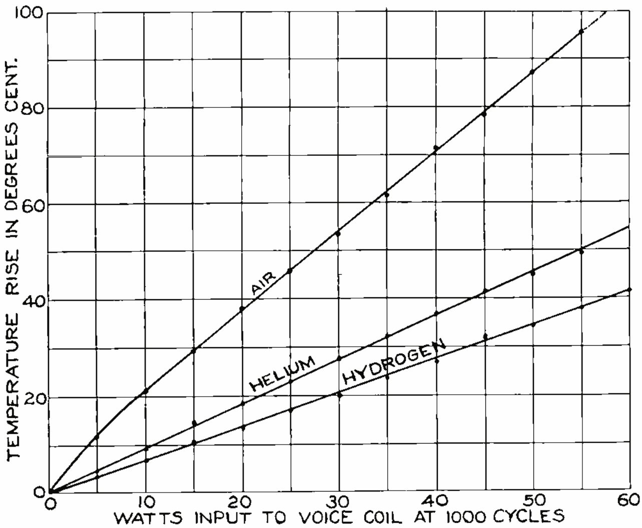

Fig. 4—Experimental data showing temperature rise versus power input to voice coil (speaker No. 1) for the various atmospheres marked on the curves. Tests were made with the speaker operating at 1000 cycles under normal conditions.

No. 1 and No. 2 with air, helium, and hydrogen atmospheres are shown in Figures 4 and 5.

Conclusions

It has been shown from the data presented that a considerable reduction in voice-coil temperature rise is possible in loudspeakers if an atmosphere of gas of higher thermal conductivity than air is provided in the air gap. For the high-powered speaker that was tested (see Figure 5) it was found that at 250 watts input the voice-coil temperature rise with air in the gap was approximately 150° C, while with helium the rise was reduced to 55° C, and with hydrogen to 50° C. These figures show that either the voice coil may be kept much cooler by providing a helium or hydrogen atmosphere in the gap, or, for the same temperature rise, the voice-coil area may be considerably reduced with a corresponding reduction in cross-sectional area of magnetic circuit. This decrease of dimensions would result in greatly reduced weight, which would be particularly desirable for special applications where speakers must be of high-power rating and as light as possible.

If the advantage of a helium or hydrogen atmosphere is utilized for the purpose of keeping the voice coil cooler rather than reducing the weight of the speaker, an appreciable improvement in efficiency will be possible. It was shown elsewhere[1] that one of the fundamental

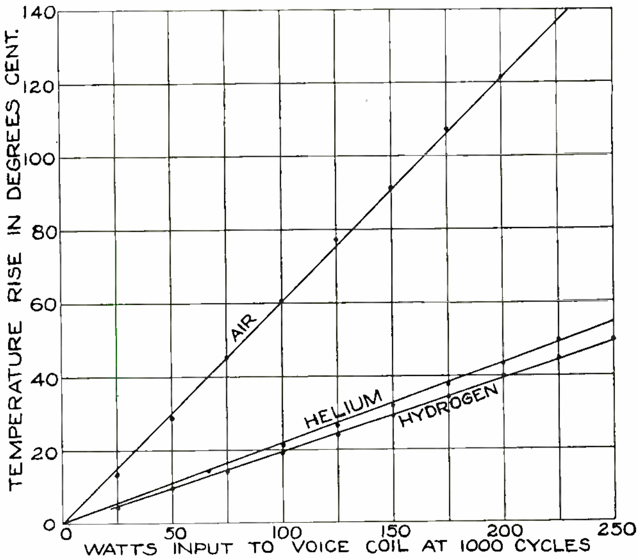

Fig. 5—Experimental data showing temperature rise versus power input to voice coil (speaker No. 2) for the various atmospheres marked on the curves. Tests were made with the speaker operating at 1000 cycles under normal conditions.

factors affecting the efficiency of a horn loudspeaker was the resistivity of the voice-coil conductor. High efficiencies, especially at the higher frequencies, demand that the resistivity be as low as possible. Since both aluminum and copper, the two most generally used conductor materials, have temperature coefficients such that their resistivities are increased approximately .4% per degree centigrade increase in temperature, it is obvious that loudspeaker efficiency may be sometimes greatly improved by limiting the voice coil temperature.

It has also been found that in some cases high-powered speakers are charred at the voice coil if full-load input is impressed on them

[1] Frank Massa, "Efficiency of Horn Loudspeakers", *Electronics,* April. 1937.

for an appreciable time. This abnormal temperature acts not only to reduce efficiency as described above, but also to weaken the voice-coil assembly mechanically, especially when paper collars are employed. The reduction in temperature which is possible with helium or hydrogen would correct many cases displaying these troubles.

If an atmosphere of helium or hydrogen is to be maintained in an air gap, the major problem is to provide a hermetically sealed enclosure surrounding the coil. An air-tight magnetic structure and a non-porous diaphragm material are desirable requisites. Suitable valves may be mounted on the structure to permit the admittance of the gas and the exhaustion of air. It would also be advisable to provide an auxiliary flexible diaphragm for permitting automatic equalization of the gas pressure in the enclosure with the variations in atmospheric pressure.

If the advantages of a helium or hydrogen atmosphere are incorporated for the purpose of reducing the weight of the speaker, it would be desirable to provide radiating fins on the outer surface of the magnet so that the heat may be more readily transmitted to the atmosphere, thereby keeping the ambient temperature at a minimum.

MICROPHONE WIND SCREENING

By

William D. Phelps

RCA Manufacturing Company, Inc., Camden, N. J.

Summary—*Some principles of hydrodynamics applicable to the problem of screening a microphone from pressure fluctuations due to wind are considered. An expression is derived for the wind pressure on a sphere assuming the air to act as a perfect, incompressible fluid in irrotational motion. The pressure is found to vary both in phase and magnitude over the surface of the sphere. The Bernouilli wind screen is described which takes advantage of the pressure and phase difference existing over the surface of a microphone to reduce the wind pressure effective at the diaphragm. The effect of resistance in the vents of the screen is shown. A comparison of the wind-pressure directional characteristic of the Bernouilli screen is made with that of a relatively large ellipsoidal screen.*

Introduction

EARLY[1] efforts made to shield a microphone from pressure fluctuations due to wind were based on the fact that silk greatly reduces the speed of wind, but transmits sound waves with negligible attenuation. The wind screen was simply a large silk-covered enclosure housing the microphone. More recently wind screens have been streamlined to minimize turbulence created at the screen.[2]

Quantitative data on wind screening a microphone are very meager. Jones and Giles[3] show the response of the WE 618-A as a function of velocity for three angular positions of the microphone when placed in a wind of uniform velocity.

There are three possible sources of excitation which a microphone is subject to when placed in a wind. (1) There may be pressure fluctuations due to velocity fluctuations present in the wind even though

[1] Thorne, U. S. Pat. No. 588,034; Olson and Massa, *Applied Acoustics*, p. 282.

[2] Spotts, U. S. Pat. No. 1,901,065.

[3] "A Moving-Coil Microphone for High Quality Reproduction," *J.S.M.P.E.* 17, 977 (1931).

the microphone is absent. (2) There may be pressure fluctuations due to turbulence produced by the microphone in a wind otherwise free from pressure fluctuations, i.e., in a wind of uniform velocity. (3) There may be radiation from the first two sources. The effect of the first source may be reduced by screening which takes advantage of the wind-pressure distribution over the microphone, the effect of the second by streamlining the microphone, and the third is minimized by reductions in the first and second sources. With the apparatus used for the measurements reported herein the predominant excitation comes from the first source.

It is the purpose of this paper to consider principles of hydrodynamics applicable to the problem of microphone wind screening, and to show results on a wind screen embodying these principles.

THEORY

If the magnitude and phase of the wind pressure were known at all points over the surface of the microphone, then it would be possible to minimize the pressure effective at the microphone diaphragm by designing the wind screen to take advantage of existing phase and pressure differences between points on the microphone. Under certain conditions it is possible to compute the pressure on a body immersed in air in motion. If the air is assumed to act as a perfect incompressible fluid, and rotational motion or turbulence is neglected, the general expression relating pressure and velocity at a point in the air is given by the equation[4,5]

$$\frac{p}{\rho} + \frac{1}{2} V^2 + T = \frac{\partial \phi}{\partial t} + F(t) \qquad (1)$$

where p is the pressure, ρ the density of the air, V the velocity, ϕ the velocity potential, and $F(t)$ is independent of x, y, and z.

To apply equation (1) to the case of a sphere it is necessary to know V, T, and $F(t)$ over the sphere and in space. T may be taken as zero everywhere. At a distance from the sphere assume the wind velocity takes the form

$$V = V_o + V_1(t) \qquad (2)$$

where $V_1(t)$ is some function of time.

[4] Page, "Introduction to Theoretical Physics," p. 193.
[5] Lamb, "Hydrodynamics".

For points near the sphere V may be found from the continuity equation

$$\nabla^2\phi = O \tag{3}$$

Expressed in spherical coordinates equation (3) becomes

$$\frac{\partial}{\partial r}\left(r^2\frac{\partial\phi}{\partial r}\right)+\frac{1}{\sin\theta}\frac{\partial}{\partial\theta}\left(\sin\theta\frac{\partial\phi}{\partial\theta}\right)=O \tag{4}$$

since ϕ is symmetrical about the line OX in Figure 1.

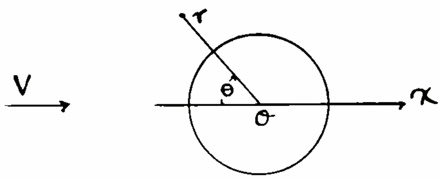

Fig. 1—Axes for determining the wind pressure on a sphere.

The solution of equation (4) is given by

$$\phi = Ar\cos\theta + \frac{B}{r^2}\cos\theta \tag{5}$$

Applying the boundary conditions, $\left(-\frac{\partial\phi}{\partial r}\right)_{r=a} = O$ and $\left(-\frac{\partial\phi}{\partial r}\right)_{r\ \text{large}} = \text{V}\cos\theta$, it follows that

$$\phi = V\cos\theta\left(r+\frac{a^3}{2r^2}\right) \tag{6}$$

where a is the radius of the sphere.

Hence the velocity everywhere is given by

$$\left[\left(\frac{\partial\phi}{\partial r}\right)^2+\left(\frac{1}{r}\frac{\partial\phi}{\partial\theta}\right)^2\right]^{\frac{1}{2}} = V\left[\cos^2\theta\left(1-\frac{a^3}{r^3}\right)^2+\sin^2\theta\left(1+\frac{a^3}{2r^3}\right)^2\right]^{\frac{1}{2}} \tag{7}$$

Substituting in equation (1) gives the pressure

$$p(r, \theta, t) = -\frac{\rho}{2} V^2 \left[\cos^2\theta \left(1 - \frac{a^3}{r^3}\right)^2 + \sin^2\theta \left(1 + \frac{a^3}{2r^3}\right)^2 \right]$$

$$+ \rho \frac{\partial V}{\partial t} \cos\theta \left(r + \frac{a^3}{2r^2} \right) + \rho F(t) \qquad (8)$$

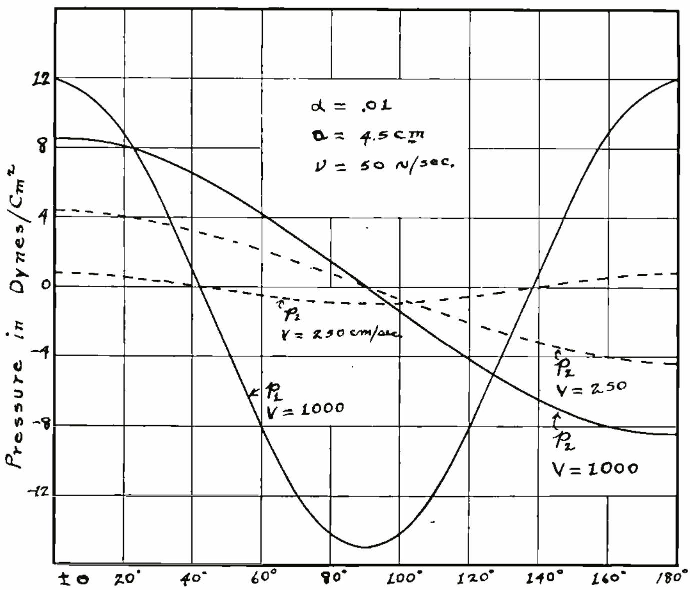

Fig. 2—The pressure components p_1 and p_2 as a function of θ on the sphere at two values of V_o.

Now the assumption of incompressibility contained in equation (3) introduces the term $\rho r \frac{\partial V}{\partial t} \cos\theta$ in the expression for the pressure which would not be found in the propagation of waves in wind. Hence it will be omitted in the subsequent expressions for the pressure. On the sphere of radius a the pressure becomes

$$p(\theta, t) = \rho \frac{V^2}{8} [9 \cos^2\theta - 5] + \frac{1}{2} \rho a \cos\theta \frac{\partial V}{\partial t} + \frac{P}{\rho} \qquad (9)$$

where P is the pressure at $\theta = \frac{\pi}{2}$, $r >> a$.

The part of $p(\theta, t)$ which depends on time is given by

$$p_1(\theta, t) = \rho \frac{V_0 V_1(t)}{4} [9 \cos^2 \theta - 5] + \frac{1}{2} \rho a \cos \theta \frac{\partial V_1}{\partial t} + P_1(t) \quad (10)$$

assuming $V_0 >> V_1(t)$.

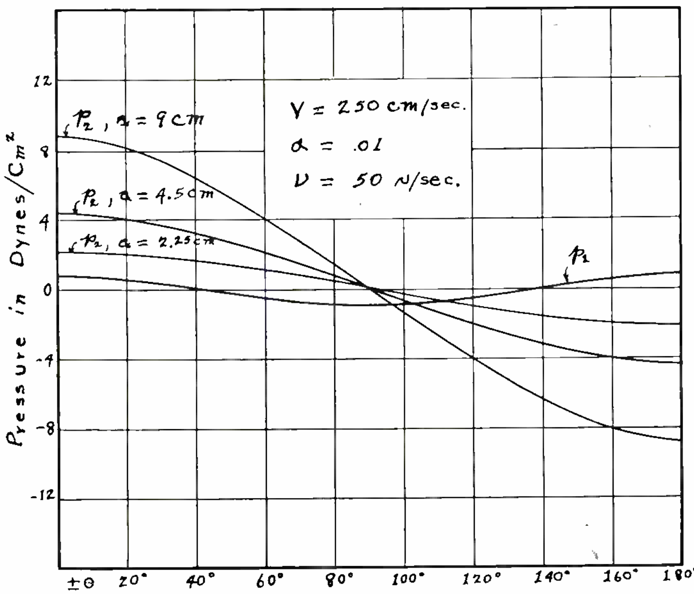

Fig. 3—The pressure components p_1 and p_2 as a function of θ on the sphere at three values of the radius a.

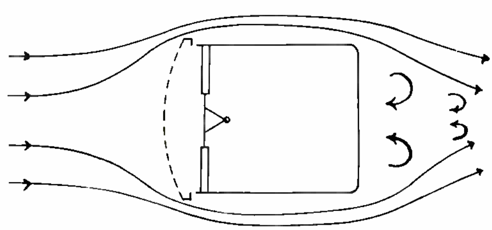

Fig. 4—Schematic diagram of the Bernouilli wind screen and the RCA 50-A microphone in 0° wind.

From equation (10) one notes that the first term in the expression for the excitation pressure, $p_1(\theta, t)$, changes phase over the surface of the sphere being positive at $\theta = 0°$ and 180°, zero at $\theta = 41.8°$ and 138.2°, and negative at $\theta = 90°$. Likewise, the second term changes phase over the sphere through a cosine term. Moreover the phase change in both terms is independent of the particular form the function $V_1(t)$ takes. The term $P_1(t)$ has the same value over the sphere.

In order to compute $p_1(\theta, t)$ for the case of sinusoidal velocity variations set

$$V = V_o(1 + \alpha \sin \omega t) \qquad (11)$$

Then

$$p(\theta, t) = \frac{\rho V_o^2 \alpha}{4} (9 \cos^2 \theta - 5) \sin \omega t + \frac{\rho V_o \alpha a \omega}{2} \cos \theta \cos \omega t + P_1(t) \qquad (12)$$

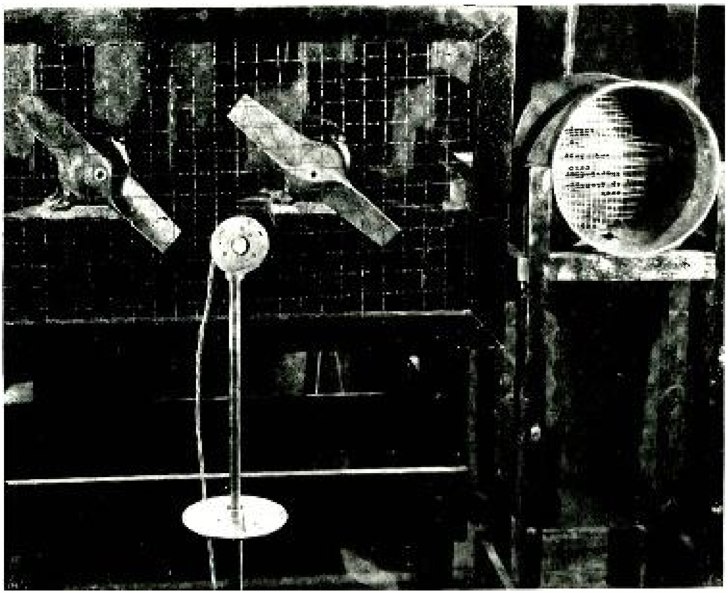

Fig. 5—Wind source and pressure microphone.

Write

$$\frac{\rho V_o^2 \alpha}{4} (9 \cos^2 \theta - 5) = p_1 \qquad (13)$$

and

$$\frac{\rho V_o \alpha a \omega}{2} \cos \theta = p_2 \qquad (14)$$

In Figures 2 and 3 are shown curves of the components p_1 and p_2 for different values of V_o and a. As in the more general case both change in phase and magnitude over the surface of the sphere.

The Bernouilli wind screen, shown schematically with the RCA 50-A microphone in Figure 4, provides a relatively simple means of taking advantage of the phase and pressure differences existing over the surface of a microphone in order to reduce the wind pressure effective at the diaphragm. The front of the wind screen is perforated

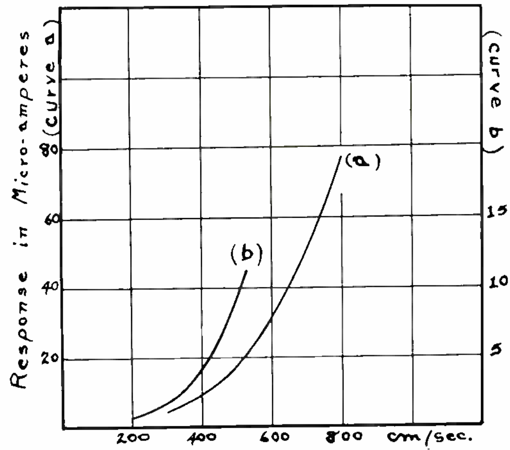

Fig. 6—Response to wind of the microphone with baffle as a function of velocity when (a) outside the wind tunnel section 24 inches from the propellers, and (b) inside the tunnel, the tunnel entrance being 24 inches from the propellers. The velocity was measured at the microphone.

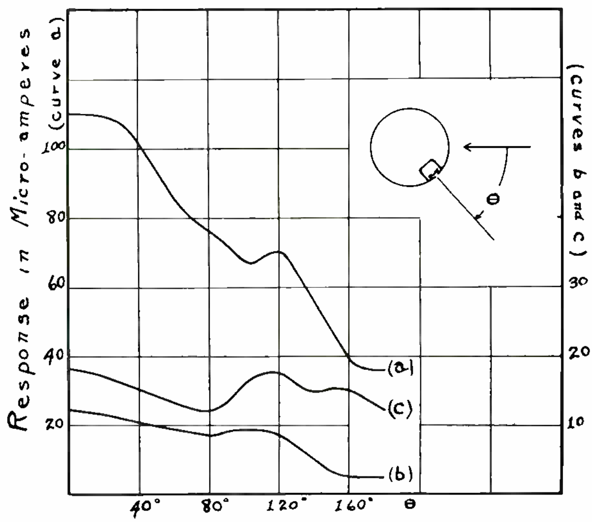

Fig. 7—Wind pressure distribution on a great circle of a sphere 9 centimeters in diameter when (a) and (b) outside the wind tunnel and (c) inside the tunnel. The velocities for curves (a), (b), and (c) are respectively 800, 350, and 530 centimeters per second.

and covered with silk while the side portion is provided with a narrow flange and vents immediately behind the flange. The vents are covered with one layer of silk.

Apparatus

The apparatus used in the measurements on wind screens is shown in Figure 5. The wind was produced by two wooden propellers of opposite hand 15 inches in diameter, driven by one-quarter hp variable

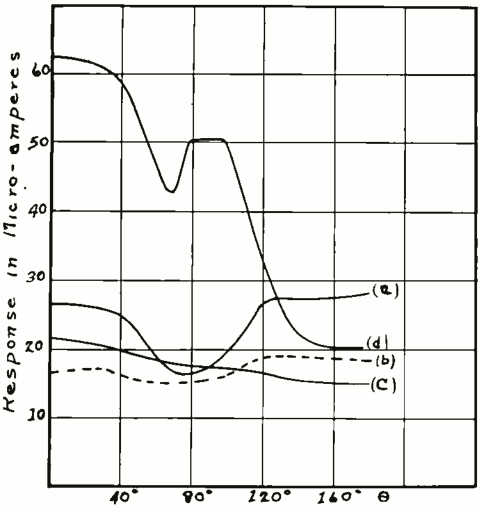

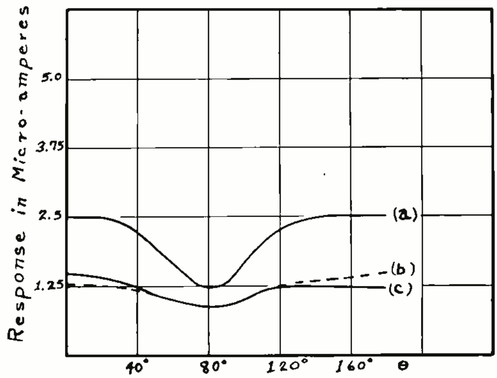

Fig. 9—Wind pressure directional characteristics of the Bernouilli wind screen with the vents (a) open, (b) covered with one layer of silk and (c) covered with two layers of silk. $V = 350$ centimeters per second.

Fig. 8—Wind pressure directional characteristics of the Bernouilli wind screen with the vents (a) open, (b) covered with one layer of silk, and (c) covered with two layers of silk. Curve (d) is the characteristic of the microphone with screen removed. $V = 800$ centimeters per second.

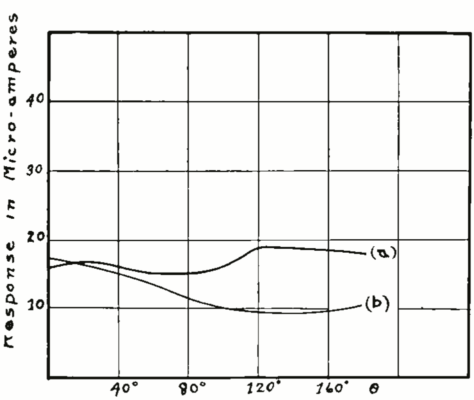

Fig. 10—Wind pressure directional characteristics of (a) the Bernouilli screen with the optimum vent resistance and (b) the large ellipsoidal screen. $V = 800$ centimeters per second.

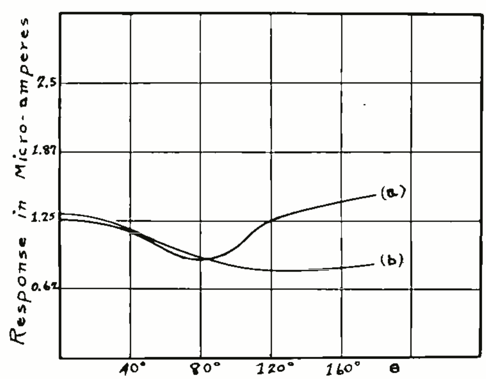

Fig. 11—Wind pressure directional characteristics of (a) the Bernouilli screen with the optimum vent resistance, and (b) the large ellipsoidal screen. $V = 350$ centimeters per second.

speed motors. The velocity of the wind at 24 inches from the propellers could be varied from 350 to 800 centimeters per second. A wind tunnel was used in some of the measurements to show the presence of

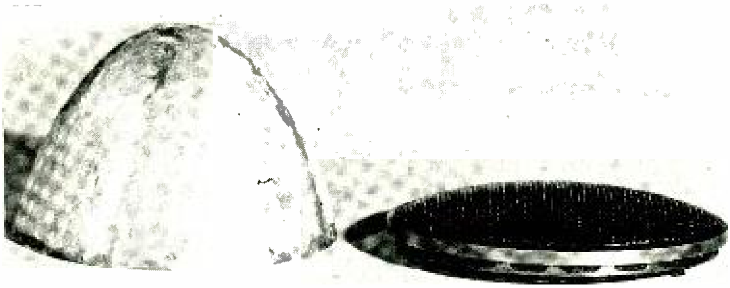

Fig. 12—A comparison of the relative size of the Bernouilli and ellipsoidal wind screens.

rotational motion or turbulence in the wind. In Figure 6 are shown curves of the microphone response to wind as a function of velocity outside and inside the wind tunnel. The presence of turbulence is also evident by a comparison of the curves of wind pressure distribution on a great circle of a sphere 3.5 inches in diameter when placed outside and inside the wind tunnel. These are shown in Figure 7.

TABLE I

Effectiveness of the Vents, $\theta = 0°$

Number of layers of silk	($V = 800$ cm/sec.) Relative Response	($V = 350$ cm/sec.) Relative Response
∞ (vents closed)	1.0*	1.0*
2	0.47	0.70
1	0.35	0.63
0	0.61	0.93

* Not the same response.

RESULTS

The effect of resistance in the vents of the Bernouilli screen on the wind-pressure directional characteristic of the screen attached to a dynamic-pressure microphone with baffle is shown in Figures 8 and

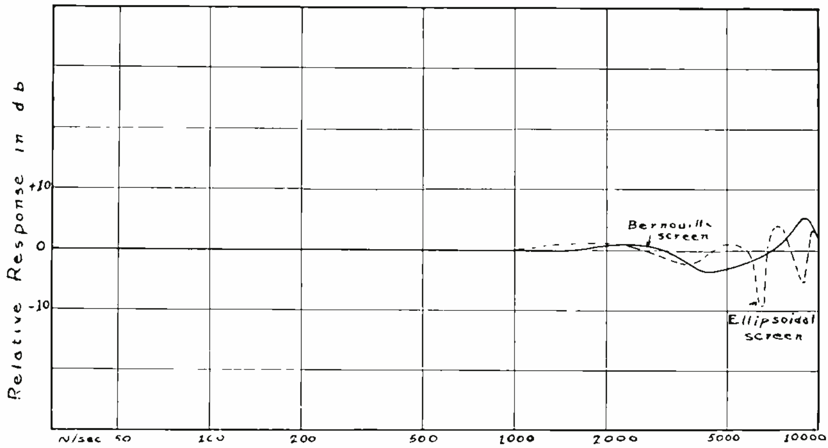

Fig. 13—Alteration of the response of the microphone with baffle at the various frequencies introduced by the Bernouilli and ellipsoidal wind screens for 0° sound.

9 for two values of the wind velocity. Also in Figure 8 the directional characteristic of the microphone without the screen is shown.

The reduction in the response to wind due to the vents with different resistances below that obtained with the vents inoperative is shown in Table I for two values of the wind velocity. It is noted that the response goes through a minimum as the resistance is varied.

A comparison of the screening effectiveness of the Bernouilli screen with that of an ellipsoidal screen, several times larger in volume, is shown by the wind-pressure directional characteristics in Figures 10 and 11. The relative size of the two screens is shown in Figure 12. It is noted that the shielding by the two screens is essentially the same at small angles while the Bernouilli screen is much smaller in size.

The curves in Figure 13 show the alteration in the response of the microphone with baffle at the various frequencies introduced by the Bernouilli and ellipsoidal screens. They do not represent the frequency characteristics of the microphone with the wind screens. Below 1000 cycles per second the screens do not affect the microphone response. The fluctuations at high frequencies may be minimized by increasing the area of the perforated section.

SELECTIVE SIDE-BAND vs. DOUBLE SIDE-BAND TRANSMISSION OF TELEGRAPH AND FACSIMILE SIGNALS

By

J. Ernest Smith, Bertram Trevor, Philip S. Carter
Engineering Department, R.C.A. Communications, Inc.

Summary—*Due to the demand for high-speed transmission facilities and the increased modulation band widths required, an investigation was conducted to determine both theoretically and experimentally the advantages and disadvantages of selective side-band as compared with double side-band transmission of telegraph and facsimile signals.*[1] *The theoretical analysis includes the derivation of the transient and steady state output response of a band pass filter when the modulated carrier frequency corresponds; (a) to the midband and (b) to one of the cut-off frequencies of the filter. The experimental tests include sufficient data to verify the theoretical conclusions.*

This paper will describe the methods of attack and the results obtained from the investigation as well as attempt to set up generalized physical concepts of the effect of frequency, phase and phase-intercept distortion on the output response for this type of applied wave. For recording devices depending upon the wave shape of the received signal, the results of the analysis indicate that selective side-band transmission shows no outstanding advantages as compared to double side-band transmission for telegraph and facsimile signals.

This paper does not consider distortion correction. Where such correction is feasible the results derived here must be modified in amount, but the general characteristics will be the same.

IT IS well known that the characteristics of any transmission medium having constant parameters can be exactly expressed in terms of a four-terminal network. For coherence we shall review briefly the theory of linear passive networks as applied to four-terminal systems having input terminals 1 and 2 and output terminals 3 and 4.

For any single frequency let Z_1 be the image impedance at terminals 1 and 2 where

$$Z_1 = \sqrt{Z_{oc} Z_{sc}}$$

in which Z_{oc} is the impedance between terminals 1 and 2 when ter-

[1] Pure single side-band transmission is not considered in this paper since it is not obtainable in actual networks. Selective side-band transmission as used here refers to the case where the carrier frequency is set at one edge of a filter pass band. The approximation to pure single side-band transmission obviously depends upon the discrimination of the filter frequency characteristic.

minals 3 and 4 are open circuited and Z_{sc} is the impedance between terminals 1 and 2 when terminals 3 and 4 are short circuited.

Correspondingly let Z_2 be the image impedance at terminals 3 and 4. Let I_1 be the input current when a generator of internal impedance Z_1 is applied at the input terminals and I_2 the output current through a load Z_2.

When the terminating impedance equals the image impedance, the image transfer constant P_1 of the network is

$$P_1 = \log_\epsilon \left(\frac{I_1}{I_2} \right) \sqrt{\frac{Z_1}{Z_2}}$$

For the analysis presented later we are interested in symmetrical networks i.e., $Z_1 = Z_2$. For this case we have

$$P_1 = \log_\epsilon \left(\frac{I_1}{I_2} \right) = A(\omega) + j B(\omega)$$

or for resistance terminations

$$A(\omega) + j B(\omega) = \log_\epsilon \left(\frac{E_1}{E_2} \right)$$

where E_1 is the input voltage at terminals 1 and 2 and E_2 is the output voltage at terminals 3 and 4.

$A(\omega)$ is the attenuation constant and may be expressed in decibels as

$$N_{db} = 20 \log_{10} \varepsilon^{A(\omega)}$$

$B(\omega)$ is the phase-shift constant and is ordinarily expressed in the form of a series.

$A(\omega)$ is frequently designated as the insertion loss of the network i.e., it is a comparison between the magnitude of the current or voltage obtained across the load with the network inserted and the current of voltage that would be obtained if the load were connected directly to the energy source. Correspondingly $B(\omega)$ is designated as the insertion-phase shift. *It should be noted that this definition does not apply to a comparison of the input and output currents or voltages of the network except in the special case where the network image impedances are exactly matched by the terminating impedances for all frequencies of the applied wave.*

This ideal matching is seldom obtained in practice. For example, a complex wave as shown across a resistance load will be quite different when the resistance is replaced with a filter network. The discrepancy is due to the fact that the image impedance of the filter is not a constant resistance except for a relatively narrow frequency band. When this frequency band does not include all components of the applied wave a considerable variation of wave form will be observed.

Before presenting a quantitative analysis of network distortion it will be desirable to form some qualitative conclusions that may be expected from linear passive network behavior. Assume the four

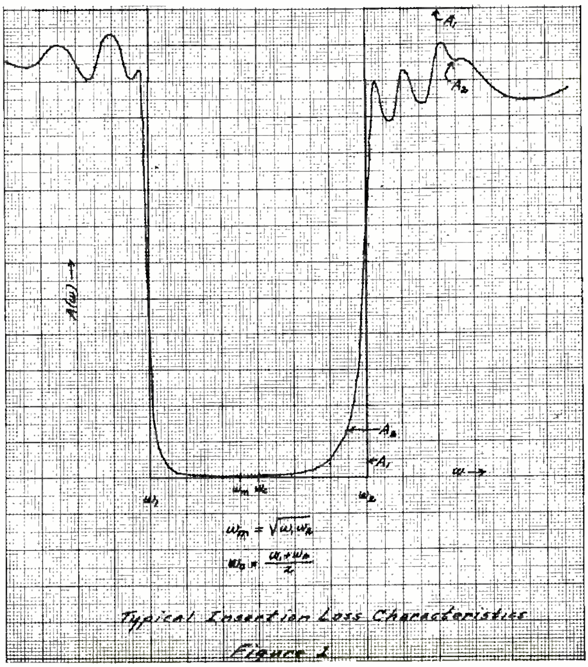

Typical Insertion Loss Characteristics

Figure 1

terminal network to be a band pass filter since this particular filter configuration has the greatest application to multi-channel transmission systems.

Frequency Distortion

If the attenuation constant $A(\omega)$ has the same value for all frequency components of the applied wave, such as curve A_1 Figure 1, the input wave will appear at the output with the same wave form, but of reduced amplitude depending upon the value of $A(\omega)$. If $A(\omega)$ corresponds to the insertion loss of a band-pass filter, such as curve A_2 Figure 1, we know that the attenuation versus frequency characteristic will generally be symmetrical about the geometric mean frequency ω_m of the filter when ω is plotted on a logarithmic scale. We shall use the term mid-frequency or mid-band frequency instead of $\sqrt{\omega_1\omega_2}$ where ω_1 and ω_2 are the lower and upper cut-off frequencies respectively. When a carrier frequency ω_c equal to the midband frequency is modulated by a complex wave we obtain upper and lower side-band components having an arithmetic spacing about ω_c in the frequency spectrum. We are accordingly interested in the insertion-loss characteristic of the band-pass filter with the abscissa ω plotted on an arithmetic scale. The graph of this function will in general be unsymmetrical about ω_c or, more specifically, a band-pass filter attenuates the upper side-band components more than the corresponding components of the lower side-band when the carrier frequency ω_c equals the arithmetic mean of the upper and lower cut-off frequencies.

It is well known that in pure amplitude modulation, the vector resultant of any upper and lower side-band component of the same order must by definition add in phase with the carrier vector at any instant. If one side-band vector is reduced more than its conjugate side band the resultant vector will no longer be in phase with the carrier. The resultant distortion depends upon the number and amplitudes of the side-band components. A recent paper shows this effect for the case of one upper and one lower side-band component.[2] For the extreme cases where one side-band component is reduced to zero, the envelope resulting from the remaining side-band component and the carrier is the same as for two heterodyning frequencies. This suppression of one side band is obtained by shifting ω_c toward one of the cut-off frequencies of the filter. When ω_c and the remaining side-band component approach equal amplitudes the envelope will be a half sine wave i.e., even-order harmonic distortion has been introduced.

A Fourier series analysis of any recurrent voltage wave form shows the complex wave to be the summation of a number of harmonically related sinusoidal and cosinusoidal e.m.f.'s. When the wave group envelope contains abrupt changes of amplitude the number and energy content of the component harmonics are increased. If the band-pass filter attenuated the higher harmonics we would expect an elimination or smoothing out of these abrupt amplitude changes. It is therefore seen that symmetrical loss versus frequency characteristics limit the ability of the filter output response to follow rapid variations in amplitude of the input wave whereas unsymmetrical

---

[2] Edmund A. LaPort "Characteristics of Amplitude Modulated Waves," RCA REVIEW, April 1937.

loss versus frequency characteristics introduce a phase modulation as well.

Phase Distortion

With the advent of high-speed communication circuits, phase distortion and phase-distortion correction have received an increasing amount of study.[3] It is now appreciated that a circuit equalized for frequency distortion alone may not be satisfactory for high-speed telegraph and facsimile transmission where the recording methods depend upon the wave shape of the received signal.

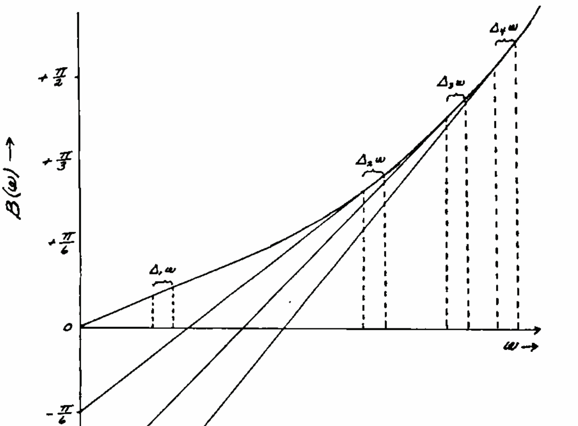

Figure 2.

A Typical Phase/Frequency Curve.

$B(\omega) = B_0 + B_1(\omega) + B_2\omega^2 + \ldots + B_n\omega^n$

Consider a typical phase-frequency function as shown in Figure 2 where $B(\omega)$ may be represented by the power series

$$B(\omega) = B_0 + B_1\omega + B_2\omega^2 + \cdots \quad \cdots + B_n\omega^n.$$

The effect of phase shift on the applied wave group may be most easily visualized by considering each term of the series to represent the phase characteristic of an individual network. The total phase distortion is then obtained by the operation of the networks in tandem.

[3] S. P. Mead, "Phase Distortion and Phase Distortion Correction," *B.S.T.J.*, April 1928.
C. E. Lane, "Phase Distortion in Telephone Apparatus," *B.S.T.J.*, July 1930.

For network N_1 having the phase characteristic B_o we see that B_o is the phase shift of the communication circuit for zero frequency. An applied wave group occupying the frequency band $\triangle_{1\omega}$ of Figure 2 would have the value $B_o = 0$. Assume the applied wave components to be ω, 3ω and 5ω as shown at A in Figure 3. It is seen that these components in the frequency range $\triangle_{1\omega}$ are transmitted without distortion. Similarly no distortion occurs if $B_o = 2\pi$ or any multiple of 2π radians.

If, on the other hand, the applied wave group lies within the frequency band $\triangle_{2\omega}$, the output wave B results. In like manner the

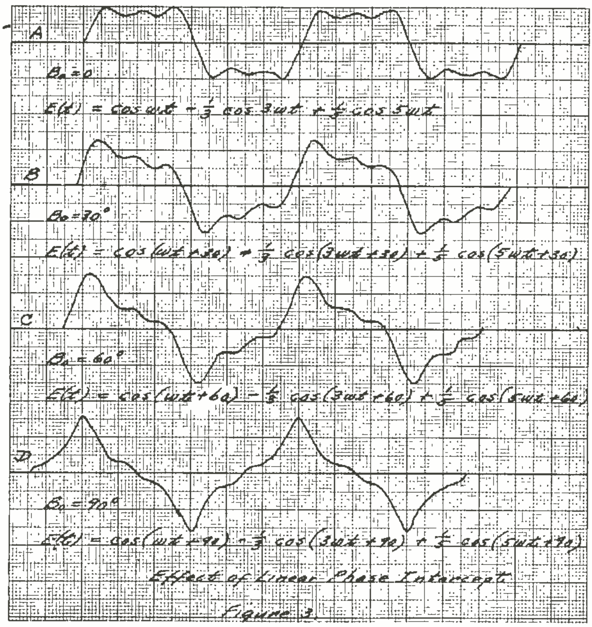

Effect of Linear Phase Intercept
Figure 3.

frequency band $\triangle_{3\omega}$ produces wave C. A maximum distortion occurs when $B_o = \pm \frac{\pi}{2}$ or an odd multiple of $\pm \frac{\pi}{2}$ as shown by wave D, Figure 3. For $B_o = \pi$ radians the output wave will be inverted which is equivalent to reversing the connections of the filter output. B_o is termed the linear phase intercept and it may conveniently be defined as the extension to zero frequency of the tangent of $B(\omega)$ evaluated at some reference frequency which generally will be the carrier frequency in multi-channel systems.

An analysis of phase distortion based on an actual phase function will include the effects of B_o. One important requirement for distortionless transmission—a necessary condition is that $B_0 = 2m\pi$ where m is an integer.

In network N_2 the phase characteristic $B_{1\omega}$ is obviously linear with frequency. Consider an applied wave function such as A of Figure 3, and assume the fundamental frequency is shifted 10 degrees. The third harmonic would then be shifted 30 degrees with respect to its angular velocity or 10 degrees with respect to the fundamental. Likewise, the fifth harmonic is shifted ten degrees with respect to the fundamental. The summation of the three components will produce the applied envelope undistorted except that it has been shifted in the time scale. The

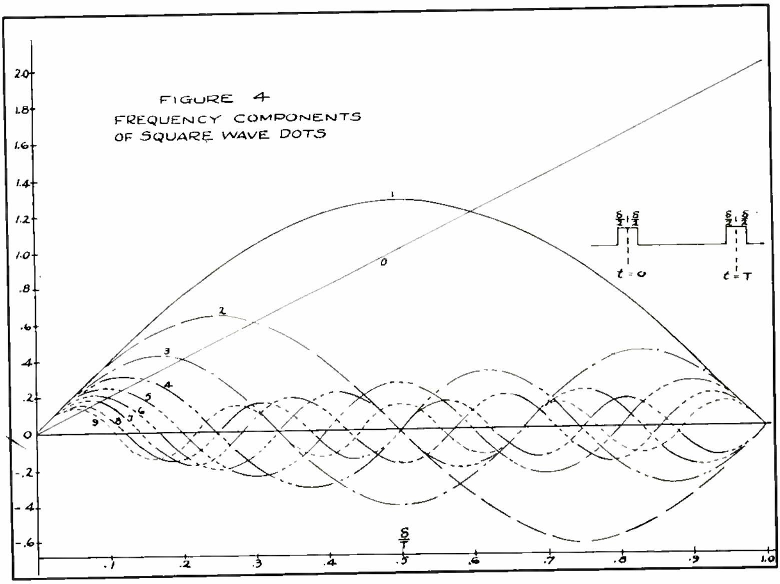

FIGURE 4
FREQUENCY COMPONENTS OF SQUARE WAVE DOTS

$\frac{dB_{1\omega}}{d\omega}$ i.e., the slope of the phase characteristic determines the time of transmission of the wave components through the network. We observe that a linear phase function delays all components equally and no distortion results. The effect of network N_2 therefore is to introduce definite time-of-transmission of the applied wave through the network. We then have the following theorem. If the attenuation and $\frac{dB(\omega)}{d\omega}$ are constant at all frequencies of the applied source and the linear phase intercept is a multiple of 2π, the received wave is a replica of the applied wave delayed by a time proportional to the slope of the phase shift.

The network N_3 having the phase characteristic $B_2\omega^2$ is required to describe the behavior of practical networks and it always introduces distortion. This term is seen to describe a curved phase-frequency function. If $B(\omega)$ has a parabolic locus the aggregate action of networks N_1, N_2 and N_3 can be used to predict exactly the output response. In practice a large group of networks will have an approximately parabolic $B(\omega)$ and Carson has derived a general expression for these conditions.[4] If the radius of curvature of the phase characteristics decreases i.e., the rate of change of slope increases, higher-

Figure 5

Typical Band Pass Filter Phase Characteristic

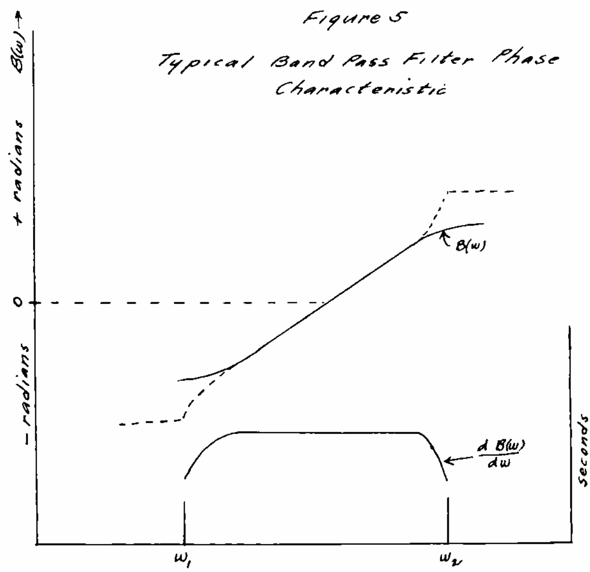

order terms of the power series are necessary to describe adequately $B(\omega)$. The corresponding increase in complexity of a mathematical analysis renders a general solution impracticable. It then becomes necessary to analyze particular phase functions for applied waves chosen to give a true representation of the circuit behavior for its type of transmission.

For a physical picture of the effect of a curved phase characteristic consider Figure 5 which is typical of band-pass filters. For a carrier frequency ω_c equal to the mid-band frequency the time-of-transmission is fixed by the slope of the phase curve. An equal time-of-transmission will be obtained in this filter for upper and lower

[4] J. R. Carson, "Building Up of Sinusoidal Currents in Long Periodically Loaded Lines," *B.S.T.J.*, October 1924.

side-band components adjacent to ω_c since the phase characteristic is linear over this frequency range. However, the side-band components in the neighborhood of the cut-off frequencies ω_1 and ω_2 will arrive at the filter output before the carrier frequency. This is so since the time-of-transmission as determined by the slope of the phase characteristic is less at the cut-off frequencies than at the mid-band frequency. The distortion produced depends upon the relative energy content of these earlier components compared with the main components of the applied wave group.

General Summary

Figure 4 shows the relative amplitudes of the harmonic components of a square-wave dot having duration (δ) compared with the recurrent frequency. For marking intervals between 25 per cent and 75 per cent of the keying cycle $\left(\frac{T}{4} < \frac{\delta}{T} < \frac{3T}{4}\right)$ the lower-order components are seen to possess the greater portion of the square dot energy. This range of δ/T is closely approximated in practice by ordinary telegraph signals. We may therefore make the following general qualitative conclusions. Telegraph transmission through a band-pass filter will not undergo serious phase distortion when the carrier frequency lies *near the mid-band frequency* since the essential frequency components have approximately equal times-of-transmission. Telegraph transmission through a band-pass filter will undergo considerable phase distortion *when the carrier frequency lies near one cut-off frequency of the filter* since the essential signal components are delayed unequally. Advantage is frequently taken of this fact for particular channel characteristics by adjusting ω_c to give cancellations during the code spacing intervals. The improvement, however, depends upon the keying speed and is limited in its application to fixed keying speeds and fixed channels.

In the case of facsimile transmission employing the constant-frequency variable-dot system,[5] the smallest dot transmitted may be used as the criterion of the circuit requirements. In this system the duration of the shortest signal is approximately ten per cent of the recurrence period. For this ratio of δ/T, we observe from Figure 4, that the higher-order signal components contain a much larger proportion of the total signal energy than is obtained for telegraph

[5] J. L. Callahan, J. N. Whitaker and Henry Shore, "Photoradio Apparatus and Operating Technique Improvements," *Proc. I.R.E.*, December 1935.

signals. We may accordingly make the generalization—*facsimile transmission through a band-pass filter will undergo considerable phase distortion when the carrier frequency lies either at the mid-band or at one edge of the filter since unequal TIMES-of transmission occur for the essential signal components in either case.*

The discussion so far presented has been general and qualitative. The aim has been primarily to show the major characteristics of frequency and phase distortion for telegraph and facsimile signals. We shall proceed now to analyze the filter-output response quantitatively. We would like to obtain a complete general solution for suddenly applied square-wave dots of any duration. Unfortunately this involves an integration that has not been evaluated except for idealized filter characteristics. Before taking up the remaining alternative of Fourier series analysis, it will be worth our while to consider this idealized case.

OUTPUT RESPONSE OF AN IDEALIZED BAND-PASS FILTER

We are here interested in learning the effect of an idealized band-pass filter upon the transmission of an isolated dot. The applied wave may be represented mathematically as

$$e(t) = \int_{-\infty}^{\infty} g(\omega)\, d\omega\, \varepsilon^{j\omega t} \qquad (1)$$

$$g(\omega) = \frac{\delta E}{2\pi}\left[\frac{\sin\dfrac{\omega\delta}{2}}{\dfrac{\omega\delta}{2}}\right] \qquad (2)$$

where $e(t)$ represents the time voltage function having a duration of δ seconds and $g(\omega)$, its frequency mate, expresses the amplitude and phase of the frequency components in the complex form. The Fourier integral expression for a single square-wave dot is obtained by substituting equation (2) in equation (1) which gives

$$e(t) = \frac{\delta E}{2\pi}\int_{-\infty}^{\infty} \frac{\sin\dfrac{\omega\delta}{2}}{\dfrac{\omega\delta}{2}}\, d\omega\, \varepsilon^{j\omega t} \qquad (3)$$

To write this expression as the envelope of a carrier frequency ω_c we multiply equation (3) by $\cos \omega_c t$ and define the product as $e_1(t)$. To keep the equation in algebraic form we perform the equivalent operation of multiplying by $\varepsilon^{-j\omega_c t}$ and consider only the real part of the result. By the property of Fourier transforms $g(\omega)$ now becomes $g(\omega - \omega_c)$.[6] We then have

$$e_1(t) = R.P. \left[\frac{\delta E}{2\pi} \int_{-\infty}^{\infty} \frac{\sin(\omega - \omega_c)\frac{\delta}{2}}{(\omega - \omega_c)\frac{\delta}{2}} d\omega \, \varepsilon^{j\omega t} \right] \tag{4}$$

where $e_1(t)$ represents a carrier frequency ω_c amplitude modulated by a single Morse dot. We wish to apply $e_1(t)$ to the input of an idealized band-pass filter and determine the response function $e_2(t)$.

From the theory of linear passive networks we know that $e_2(t)$ will be of the form

$$e_2(t) = e_1(t) \, Y(\omega) \, Z(\omega) \tag{5}$$

where

$Y(\omega)$ = complex transfer admittance of the filter
$Z(\omega)$ = the load impedance function

Suppose we define

$$h(\omega) = Y(\omega) \, Z(\omega) = H(\omega) \, \varepsilon^{-j\theta(\omega)} \tag{6}$$

where

$$\begin{aligned} H(\omega) &= \text{magnitude of } h(\omega) \\ \theta(\omega) &= (\omega - \omega_c) \, t_d \end{aligned} \tag{7}$$

where t_d is the constant time delay determined by the slope of the phase characteristic $\theta(\omega)$. Substituting equations (6), (7), and (4) into equation (5) gives

$$e_2(t) = R.P. \left[\frac{\delta E K}{2\pi} \varepsilon^{j\omega_c t_d} \int_{-\infty}^{\infty} \frac{\sin(\omega - \omega_c)\frac{\delta}{2}}{(\omega - \omega_c)\frac{\delta}{2}} d\omega \, \varepsilon^{j\omega(t - t_d)} \right] \tag{8}$$

[6] G. A. Campbell, "Fourier Integrals for Practical Applications," *B.S.T.J. Monograph B-584.*

Integrating between the cut-off frequencies ω_1 and ω_2 and defining the band width as W, we obtain

$$e_2(t) = R.P. \left[\frac{\delta EK}{\pi} \varepsilon^{j\omega_c t_d} \int_0^{\frac{W}{2}} \frac{\sin(\omega - \omega_c)\frac{\delta}{2}}{(\omega - \omega_c)\frac{\delta}{2}} d\omega \, \varepsilon^{j\omega(t-t_d)} \right] \quad (9)$$

If we let $\omega' = \omega - \omega_c$

then $d\omega' = d\omega$

Substituting in (9) and reducing gives

$$e_2(t) = R.P. \left[\frac{\delta EK}{\pi} \varepsilon^{j\omega_c t} \int_0^{\frac{W}{2}} \frac{\sin \omega' \frac{\delta}{2}}{\omega' \frac{\delta}{2}} \varepsilon^{j\omega'(t-t_d)} \right] \quad (10)$$

Writing the real part and simplifying, we have

$$e_2(t) = \frac{EK}{\pi} \cos \omega_c t \int_0^{\frac{W}{2}} \frac{2 \sin \omega' \frac{\delta}{2} \cos \omega'(t - t_d) \, d\omega'}{\omega'} \quad (11)$$

From trigonometry

$$2 \sin \frac{\omega'\delta}{2} \cos \omega' \,(t - t_d) = \sin \omega' \left(t - t_d + \frac{\delta}{2} \right) - \sin \omega' \left(t - t_d - \frac{\delta}{2} \right)$$

$$= \sin \omega'\delta \,(t' + 1/2) - \sin \omega'\delta \,(t' - 1/2) \quad (12)$$

where $t' = \dfrac{t - t_d}{\delta}$

Substituting in equation (11) and evaluating gives

$$e_2(t) = \frac{EK}{\pi} \left\{ Si \frac{W\delta}{2} (t' + 1/2) - Si \frac{W\delta}{2} (t' - 1/2) \right\} \cos \omega_c t \quad (13)$$

The envelope of the response function is seen to be the difference of two sine integral functions. As would be expected it can be shown that the same envelope response results for an applied square-topped d-c impulse when transmitted through a low-pass filter.[7]

In this analysis we are primarily interested in the manner in which the output response builds up to its steady-state value. The wave front of the output wave is shown pictorially in Figure 6 in which EK is the steady-state amplitude and t_d is the delay time of the filter i.e., it is the time interval between the instant of application at the input and the instant when the output response equals ½ EK. If at

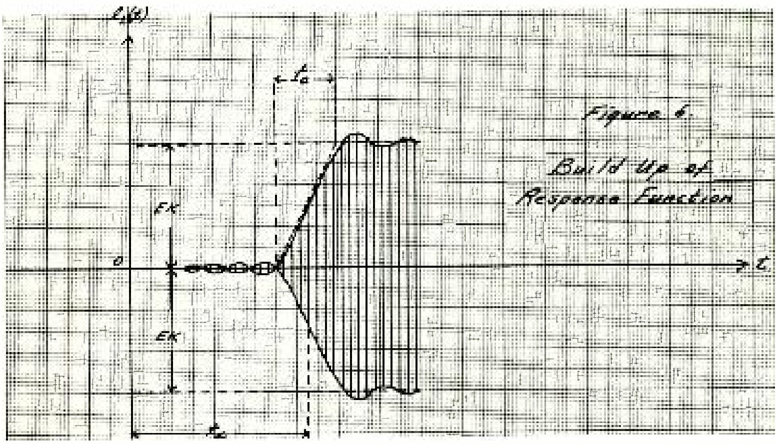

the point $t = t_d$, we draw the tangent to the envelope, then the time interval between the intercepts of this tangent with the time axis and the final value EK is defined as the time of build-up t_a. It will be of interest to determine how t_a varies with the band width W.

We may transform equation (11) to the form

$$e_2(t) = \frac{EK}{\pi}\left[\int_0^{\frac{W}{2}} \frac{\sin \omega'\left\{t - \left(t_d - \frac{\delta}{2}\right)\right\}}{\omega'} d\omega' - \int_0^{\frac{W}{2}} \frac{\sin \omega'\left\{t - \left(t_d + \frac{\delta}{2}\right)\right\}}{\omega'} d\omega'\right] \qquad (14)$$

[7] Guillemin, "Communication Networks," Vol. 2, Chapter 11-Jno., Wiley & Sons.

Differentiating and evaluating for $t = t_a$ gives

$$\frac{d}{dt}\left[e_2(t) \right] = e_2'(t) = \frac{EKW}{2\pi} \tag{15}$$

where $e_2'(t)$ is the slope of the tangent to the output-wave envelope at the point $t = t_a$. Observing Figure 6 it is clear that

$$t_a = \frac{EK}{e_2'(t)}$$

Substituting equation (15) we have

$$t_a = \frac{2\pi}{W} = \frac{1}{f}$$

It should be noted that the build-up time of the envelope to the value EK is actually somewhat longer than t_a due to the non-linearity of the build-up response. A better value obtained empirically for the build-up time is 1.1 t_a.

We have derived a useful reciprocal relation between the build-up time in seconds and the filter band width in cycles. This agrees with the qualitative statement in the introduction that the frequency response of the filter determines the maximum rate of change of the signal envelope that can be reproduced at the output.

In actual networks the insertion loss and insertion phase-shift parameters are not independent. Generally, in fact, when the frequency response approaches the ideal characteristic adverse phase effects result and vice versa. We have therefore assumed for our ideal case conditions which cannot be attained practically.

One other point should not be overlooked in this analysis. At the instant the signal was applied we have assumed a quiescent state in the filter network. This assumption is undoubtedly valid for a large number of possible signal combinations, but it cannot be true for applied signals having very short-spacing intervals such as a succession of 90% dots. For narrow-band widths these spaces will be filled in to some extent in the output response and the build-up time will depend upon the transient state of the network due to the previous signal excitation.

Distortion as a Function of Threshold Level

It has been mentioned previously that the wave forms considered in this paper are voltage functions. The analysis has been on this basis since the transmitting and receiving equipment are voltage-operated devices. It may be well therefore to consider briefly the effect of the terminal equipment on these wave forms.

Figure 7 shows a transmitted and received impulse superimposed. The received impulse has been idealized to a trapezoidal form to simplify analysis. As seen from the figure, if the received trapezoidal wave form were threshold limited at one-half its maximum amplitude, the received dot duration would be equal to δ and no distortion would exist. For threshold settings above or below this value the received dot is lesser or greater than δ.

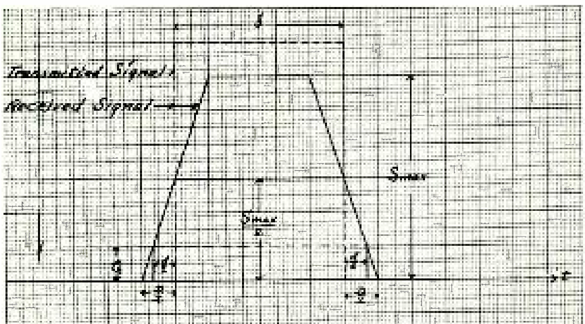

Figure 7
Distortion as a Function of Threshold Level
S_{max} = Maximum signal amplitude
D = Elongation of signal at base
d = Elongation of signal at threshold
δ = Duration of signal transmitted
t_h = Threshold level

In a radio circuit the signal-to-noise ratio and variation of signal amplitude due to fading need not be explicitly considered since, in practice, they determine the threshold level. The noise level merely limits the lowest value of threshold setting whereas the minimum instantaneous signal amplitude limits the highest threshold setting.

Normal radio circuit conditions are such that the threshold level produces an elongation of the signal. From Figure 7 we have the relation

$$\frac{\frac{d}{2}}{\frac{D}{2}} = \frac{\frac{S_{max}}{2} - t_h}{\frac{S_{max}}{2}}$$

or

$$\frac{d}{D} = 1 - 2\left(\frac{t_h}{S_{max}}\right)$$

Defining the ratio of threshold to maximum signal as β and rearranging, we have

$$d = D\ (1 - 2\beta)$$

In order to translate in terms of band width we recall from the previous section that the band width is inversely proportional to the build-up time t_a. Observing again Figure 6, we find that the actual

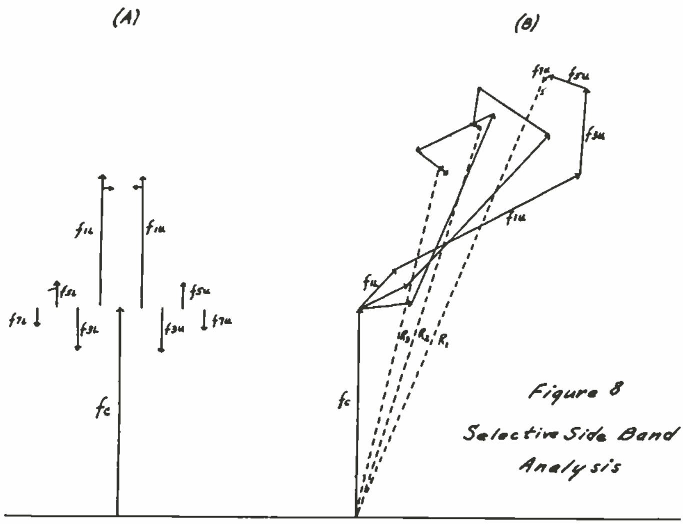

Figure 8
Selective Side Band Analysis

build-up time D is somewhat greater than the value t_a. A good average value has been taken as $D = 1.1\ t_a$. Substituting in the above equation gives

$$d = 1.1\ t_a\ (1 - 2\beta)$$

This relation gives the effective distortion in terms of band width and ratio of threshold level to maximum signal amplitude. It is of interest to note that threshold limiting cannot produce greater distortion than is present in the incoming wave form so long as sufficient band width is available to allow some flat top in the received wave and the wave is symmetrically shaped. If the wave is unsymmetrical as produced by adverse phase characteristics, voltage-operated receivers may record an entirely different response.

Analysis of Recurrent Square-Wave Dots

We have shown the method of analyzing the idealized filter-output response for applied transient functions by means of a Fourier integral expression. When a similar expression is written for an actual filter having neither ideal phase or frequency characteristics, the expression unfortunately cannot be integrated and very little definite information is obtainable heuristically. Since we are interested in a comparison of selective side-band transmission and double side-band transmission, we must know the output wave shape accurately for the two cases. In order to derive this information theoretically we must utilize the remaining alternative of Fourier series

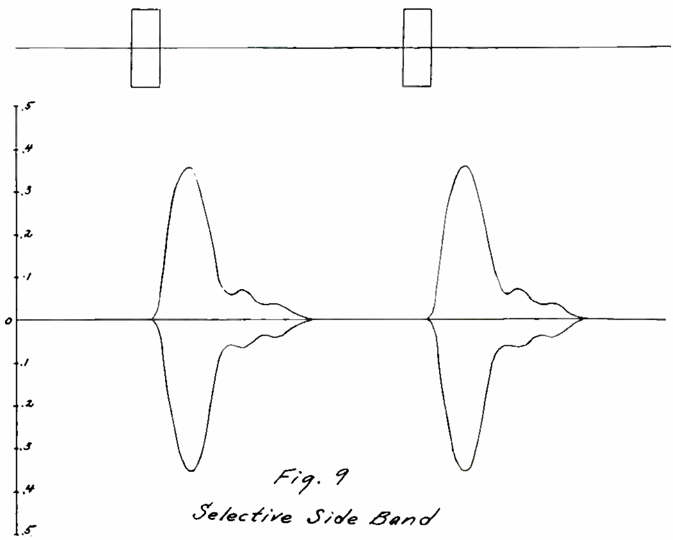

Fig. 9
Selective Side Band

analysis for recurrent applied functions. It is then necessary that we choose recurrent functions typical of the transmitted signal and, as far as possible, select those representative of the most difficult signal combinations required to be transmitted by the circuit. It is well known, for example, that recurrent functions could be chosen that would produce much more favorable results than would be realized in practice.

The Fourier series method of analysis may be outlined briefly in the following three steps:

(1) Determine the amplitude and phase relationships of the Fourier components of the applied wave.

(2) Measure the frequency and phase characteristics of the transmission channel under consideration.

(3) Apply the channel characteristics to the components of step (1) and add vectorially to obtain the envelope of the received response.

This method is long and tedious, but it may be simplified by proper organization of the required data. To illustrate the method we shall present a section of the analysis employed in this paper. It was stated previously that the constant-frequency variable-dot facsimile scanner produces square-wave dots of constant repetition frequency and of variable duration. The amplitude of the frequency components of a

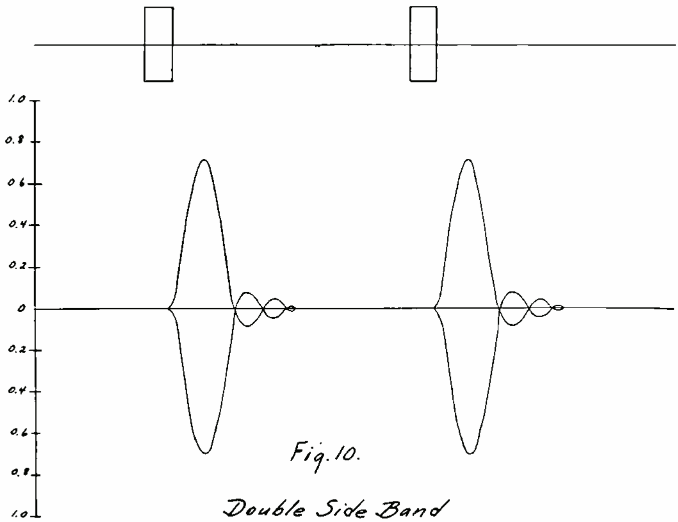

Fig. 10.

Double Side Band

square-wave recurring dot may be expressed mathematically by the relation

$$A_n = \frac{\delta E}{T} \left[\frac{\sin \dfrac{n\pi\delta}{T}}{\dfrac{n\pi\delta}{T}} \right]$$

where

A_n = amplitude of the "n"th harmonic
δ = duration of marking impulse
T = period of the recurrence frequency

This relation has been put in an interesting graphical form for δ/T ratios between 0 and 1. (See Figure 4.) The straight line represents the amplitude of A_0 or the d-c component.

Practical operating considerations in constant-frequency variable-dot facsimile transmission may limit the values of δ/T between 10% and 90%. Observing Figure 4, it is apparent that if we analyze the received response for applied square dots having the δ/T ratios of 10%, 50%, and 90% we will have chosen the extreme signal-wave groups that will be obtained in the actual facsimile transmission.

As in the case of the transient analysis, we shall consider the transmission medium to be a band-pass filter. The phase and frequency characteristics of the filter are shown in Figure 15. Suppose we apply a keyed tone to the filter and analyze the output response. Let the tone frequency be 870 cycles which is modulated by a 50% square wave having a recurrence frequency of 20 c.p.s. From Figure 4 the

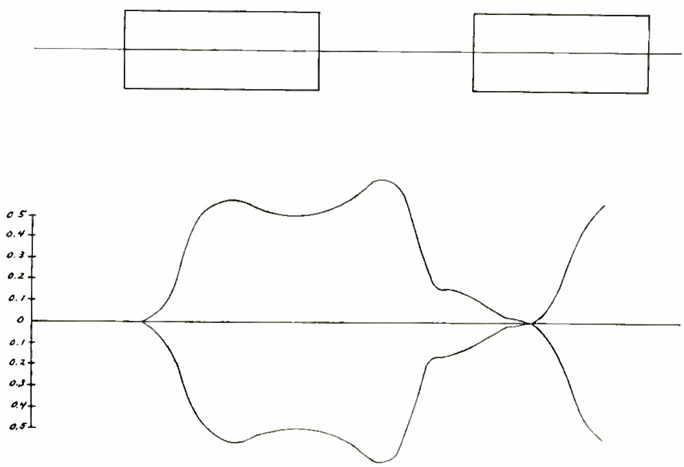

Fig. 11.
Selective Side Band

Fourier components of the applied wave are seen to be as shown in Figure 8A for the time instant t equal to zero. (f_{nu}) represents the "n"th component of the upper side-band and similarly (f_{nl}) represents the corresponding lower side-band component. The usual convention is employed that the upper side-band vectors rotate in a counter-clockwise direction whereas the lower side-band components rotate in a clockwise direction. Actually, of course, Figure 8A should have an infinite number of side-band components, but we are dealing with a finite filter pass band that will eliminate the higher-order components in any case.

According to Step 2 of the general method we must now apply the filter characteristics to these components. The filter characteristics are tabulated below with the phase shift considered to be zero for the tone or sub-carrier frequency. For this example only five components and the sub-carrier need be considered since the filter loss reduces the other components to negligible values.

FILTER CHARACTERISTICS

	Frequency	Percentage of amplitude passed by Filter	Phase shift	Amplitude of component at filter output
f_c	870 cycles	50%	0 degrees	1.0
f_{1l}	850 "	21%	—34 "	.27
f_{1u}	890 "	78%	63 "	1.0
f_{3u}	930 "	100%	184 "	.42
f_{5u}	970 "	89%	289 "	.23
f_{7u}	1010 "	26%	417 "	.05

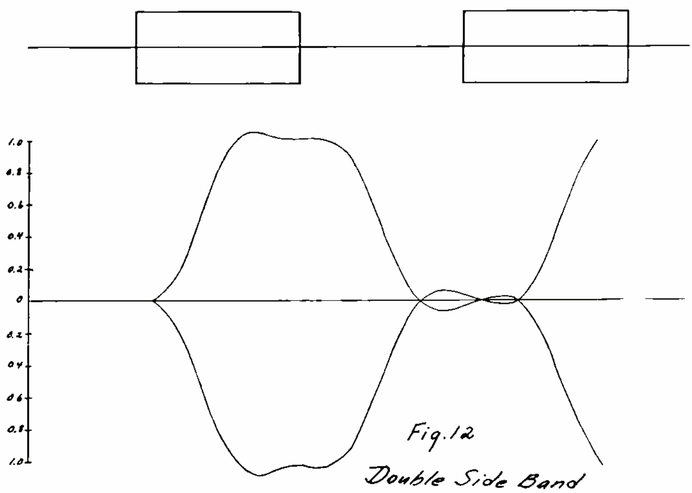

Fig. 12
Double Side Band

Setting up these several vectors with the amplitude and phase relations given by the table and the original vector relationship given by A of Figure 8, we may obtain the envelope amplitude for the time $t = 0$ by measuring the resultant of these vectors. This is shown by the dotted line R_1 in Figure 8B. By allowing all vectors except the carrier to rotate twenty fundamental degrees in their normal directions we obtain the envelope amplitude R_2. In this way we may obtain the complete envelope shape by plotting the resultants R_1, R_2, R_3, etc., for the entire modulation cycle. For this example, taking twenty-degree increments we need 17 points to plot the cycle. This envelope when completed represents the filter-output response for single side-band transmission. If we had set the tone frequency at the mid-band

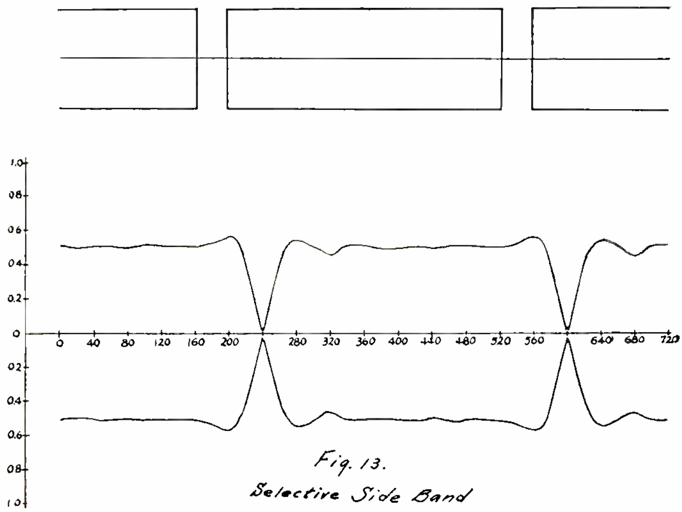

Fig. 13.
Selective Side Band

of the filter, we would have obtained the output response for double side-band transmission.

Using the method outlined above, we have derived the output response of the filter for the three applied waves mentioned. Figure 9 shows the received wave for an applied signal having a δ/t ratio of 10% when the tone frequency is 870 cycles. Figure 10 shows the corresponding result when the tone frequency equals the mid-band frequency. The applied signal is indicated at the top of the illustration in each case. Several interesting facts are brought out by these figures. While both selective and double side-band transmission pro-

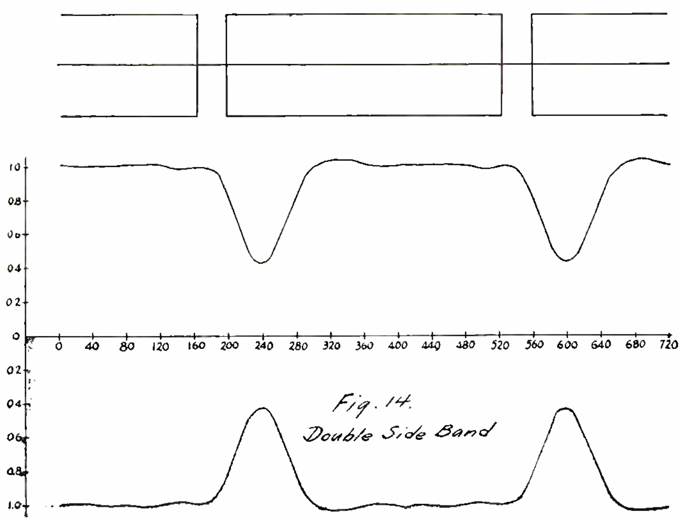

Fig. 14.
Double Side Band

duce considerable elongation as we predicted in the introduction, the selective side-band response has the greater distortion. Observing the ordinates for the received response which are plotted on the basis of unity for the applied signal amplitude, we see that the selective side-band response amplitude is only about half that of the double side band. Remembering that our receiver is a voltage-limiting device, it is apparent that threshold limiting will produce a closer approxima-

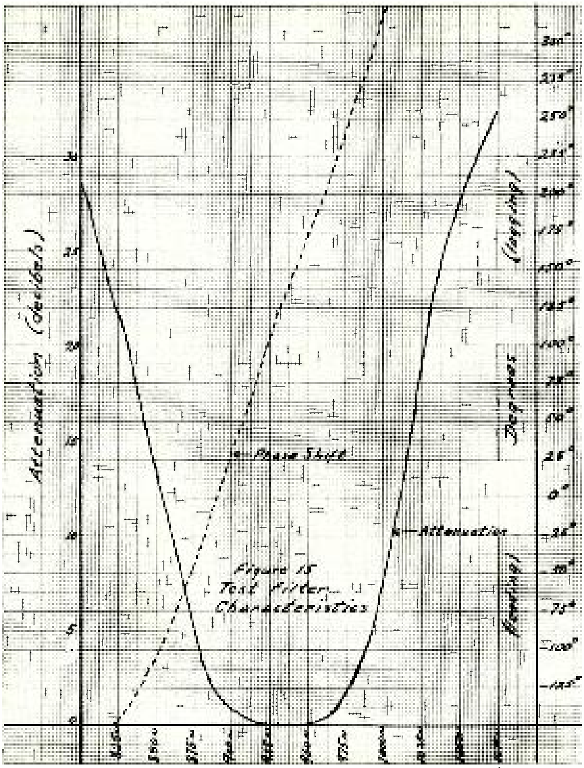

tion to the original signal for double side-band reception than for selective side band. Another point of practical value is that the threshold setting is not so critical and less variation in the marking length will be obtained due to fading of the signal. We may also state that, since the band width is identical for the two cases, the noise level will be the same and, therefore, double side-band transmission will give a better signal-to-noise ratio by a factor of nearly 2:1.

Observing Figures 11 and 12 for the δ/T ratio of 50% we find that the same conclusions are true. In fact for this case, the double side-band response can be made undistorted when the threshold level is set at one half of the maximum signal amplitude. Unfortunately, as stated in an earlier section, the threshold level is determined by the degree of fading and the noise level for that signal. We can safely say, however, that double side-band transmission gives the more favorable response.

For the 90% marking interval shown in Figures 13 and 14, the advantages of double side band are more questionable. While less

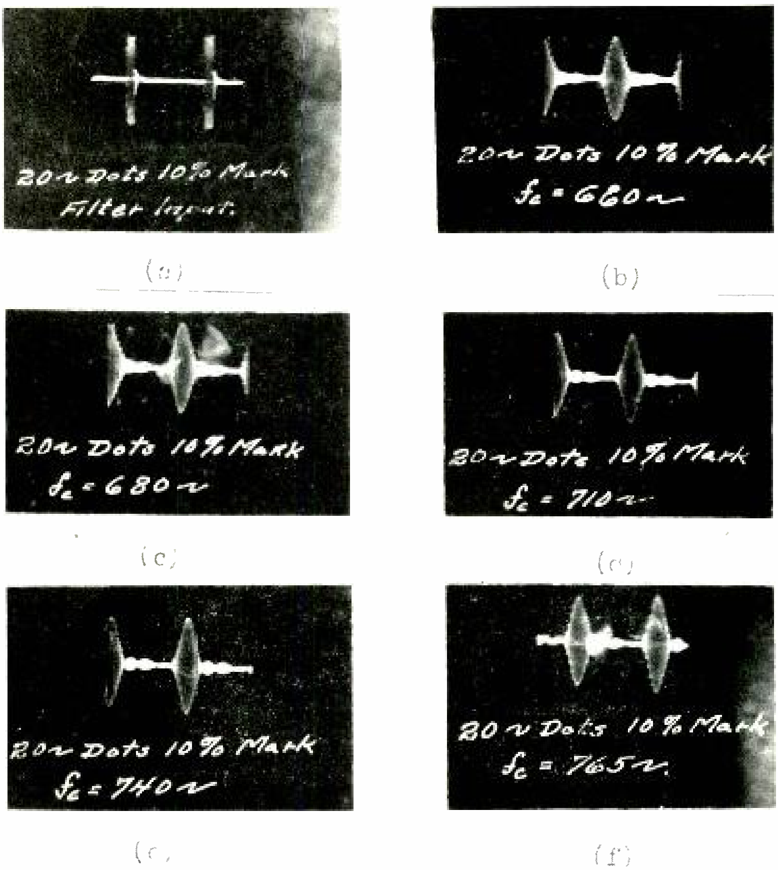

Fig. 16

elongation is obtained than in selective side-band transmission the signal fills in at about 40% of its maximum amplitude. We notice that a greater amplitude is still obtained for double side band. Considered from the standpoint that the radio path generally elongates the signal we may say that the two cases have about equal merit.

Figures 16 to 20 inclusive show the experimental results obtained when transmitting various applied signals through a band-pass filter similar in characteristics to the one used in our theoretical analysis.

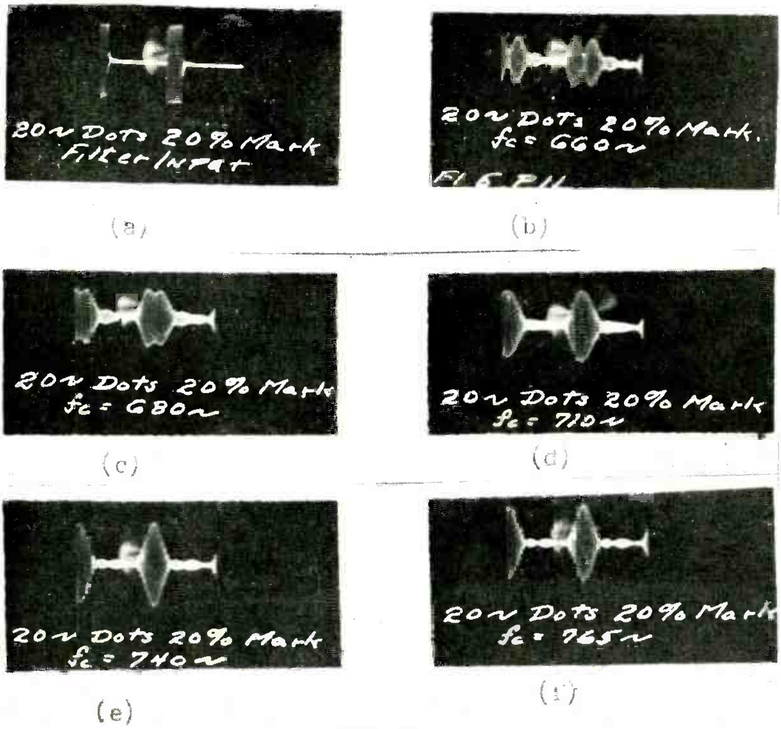
20~ Dots 20% Mark
Filter Input
(a)
20~ Dots 20% Mark.
fc = 660~
(b)
20~ Dots 20% Mark
fc = 680~
(c)
20~ Dots 20% Mark
fc = 710~
(d)
20~ Dots 20% Mark
fc = 740~
(e)
20~ Dots 20% Mark
fc = 765~
(f)

Fig. 17

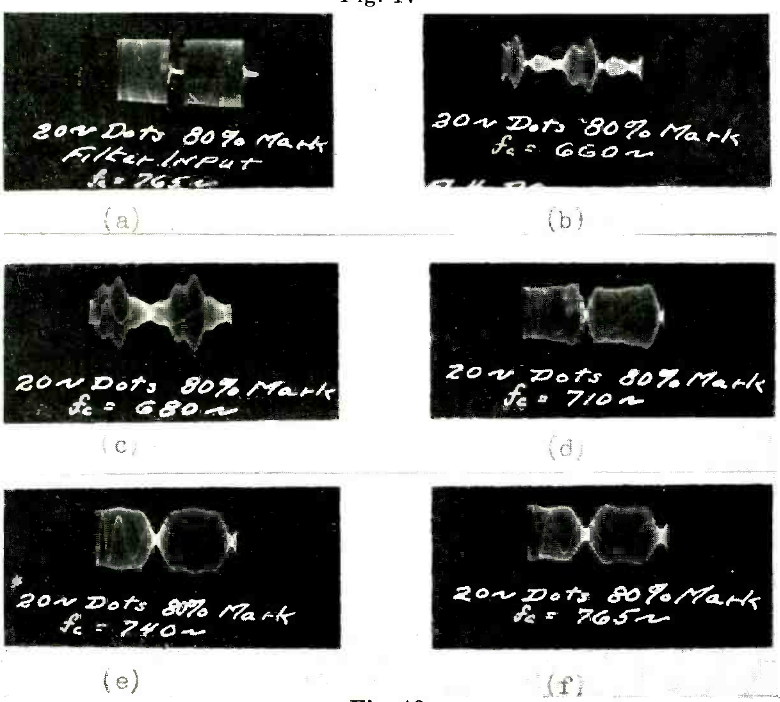
20~ Dots 80% Mark
Filter Input
(a)
30~ Dots 80% Mark
fc = 660~
(b)
20~ Dots 80% Mark
fc = 680~
(c)
20~ Dots 80% Mark
fc = 710~
(d)
20~ Dots 80% Mark
fc = 740~
(e)
20~ Dots 80% Mark
fc = 765~
(f)

Fig. 18

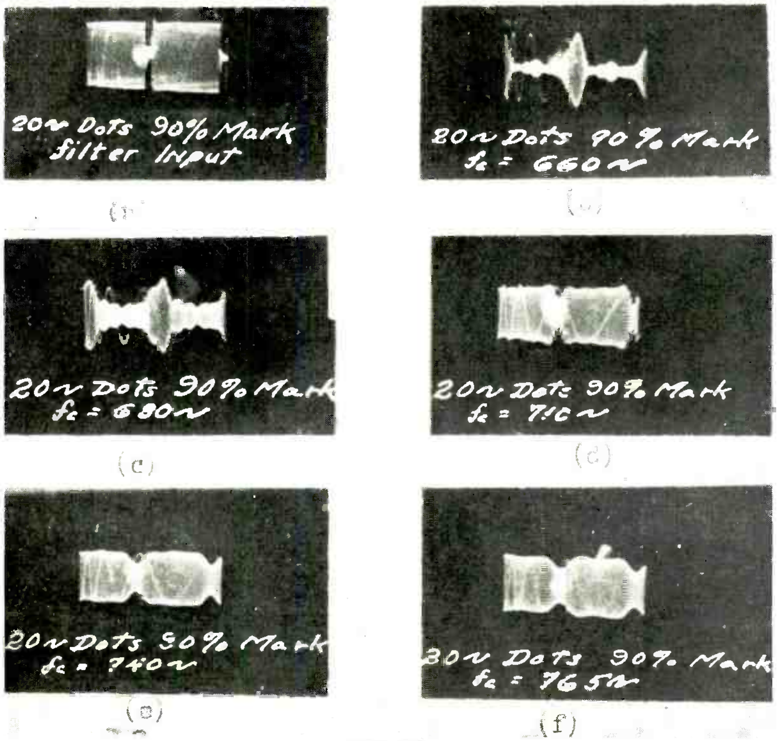
20~ Dots 90% Mark
filter Input
(a)
20~ Dots 90% Mark
fc = 660~
(b)
20~ Dots 90% Mark
fc = 680~
(c)
20~ Dots 90% Mark
fc = 710~
(d)
20~ Dots 90% Mark
fc = 740~
(e)
30~ Dots 90% Mark
fc = 765~
(f)

Fig. 19

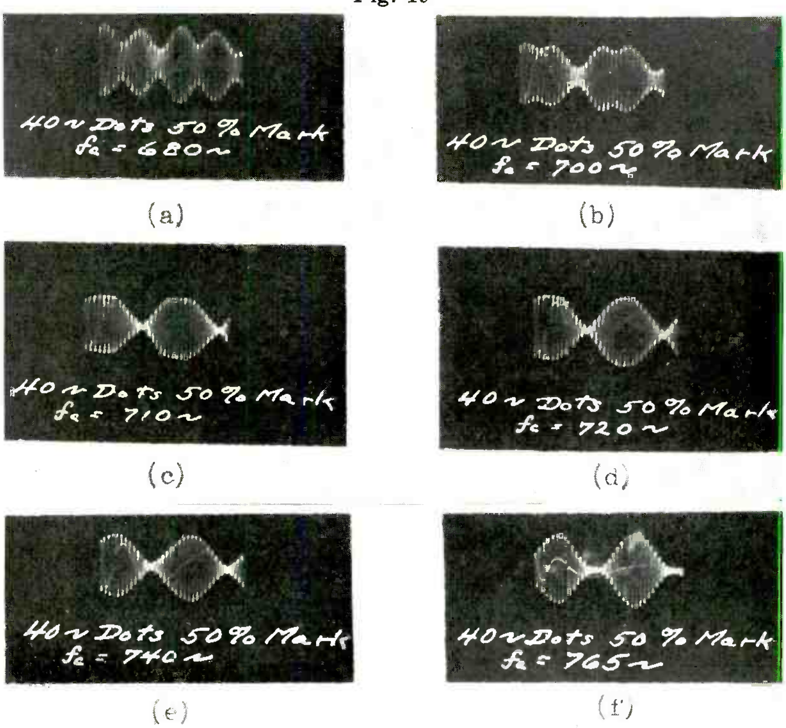
40~ Dots 50% Mark
fc = 680~
(a)
40~ Dots 50% Mark
fc = 700~
(b)
40~ Dots 50% Mark
fc = 710~
(c)
40~ Dots 50% Mark
fc = 720~
(d)
40~ Dots 50% Mark
fc = 740~
(e)
40~ Dots 50% Mark
fc = 765~
(f)

Fig. 20

The applied wave is shown by picture (a) of each figure. The tone is then moved in frequency increments toward the arithmetic mid-band of the filter as depicted by pictures (b), (c), (d) and (e) for each figure. Picture (f) shows the response for each case when the tone is set at the arithmetic mid-frequency of the filter.

A study of these pictures verifies the theoretical analysis just presented. It also demonstrates several important facts concerning the intermediate carrier settings between selective side-band and double side-band transmission.

We are thus led to the conclusion that the theoretical analysis and experimental measurements which we have made have failed to show any outstanding advantages for selective side-band as compared to double side-band transmission for telegraph and facsimile signals. This conclusion is on the basis that the filter-band width is the same for both cases. If, as they are sometimes compared, double side-band transmission were allowed twice the band width utilized for the selective side-band transmission, we can definitely predict that the selective side-band response will be inferior. The use of selective side-band transmission requires greater stability of the tone-carrier frequency due to the steep slope of the filter characteristic. This is evident from the figures (b) of the photographs. Furthermore, in multi-channel operation, selective side-band transmission produces greater cross-talk in the adjacent channels. For the particular filters considered in this analysis, the increase in cross-talk amounted to 8 decibels.

It should be understood that the conclusions of this paper are predicated on the basis of threshold limiting at the receiver in accordance with the present practice for telegraph and facsimile transmissions. They do not apply to the transmission of music or speech since these signals may be reproduced satisfactorily with much greater phase and frequency distortion than is permissible in facsimile or television transmission.

ACKNOWLEDGMENT

The authors wish to express their appreciation to Messrs. C. H. Taylor, H. H. Beverage, J. L. Callahan, C. W. Hansell, and H. O. Peterson of the R.C.A. Communications Engineering Department, whose support and assistance have made this work possible.

TENSOR ANALYSIS AND ITS APPLICATION TO EQUIVALENT CIRCUITS[1]

BY

D. W. EPSTEIN

RCA Manufacturing Company, Inc., Camden, N. J.

Summary—*A brief introduction to the tensor concept is presented. This concept is then applied to the determination of a group of networks having the same input impedance at all frequencies as a given network. A particular case is worked out as an example. The tensor concept is also applied to the determination of a group of networks having the same transfer impedance with respect to any mesh as a given network. A particular example is also worked out for this case. It is shown that in order that a group of networks have the same transfer impedance as a given network, it is necessary that they also have the same input impedance as the given network.*

INTRODUCTION

TENSOR analysis is used in physics because it permits the statement of physical laws in terms which are independent of the system of coordinates. Thus if a physical law is stated as a tensor equation, the equation is true no matter in what system of coordinates one chooses to make his measurements.

The use of the tensor concept for the solution of problems in electrical engineering has been extolled by Kron in a series of articles[2] on the application of tensor analysis to rotating machinery. It is the object of this paper to present a brief review of the tensor concept and to apply it to equivalent circuit theory.

TENSORS

The first task is to define a tensor. The concept of a tensor is a generalization of that of a vector and hence a vector is a special case of a tensor. The procedure to be followed is to review the basic concept of a vector and then generalize it to more complex tensors.

The usual well known definition of a vector as a directed quantity is insufficient except for very elementary work. For analytical work, especially in cases requiring more than three "dimensions" the very meaning of "directed quantity" loses its significance and a more workable definition of a vector is necessary. A suitable definition of a vector may be obtained by utilizing the fact that a vector is a quantity independent of the type of "coordinate system" in which it may be

[1] Manuscript received December 30, 1937.

[2] "The Application of Tensors to the Analysis of Rotating Electrical Machinery" by Gabriel Kron—*G. E. Review*. This was an extensive series of articles beginning on Page 181 (April 1935). The most recent article at the time of writing this paper was Page 594 (December 1937).

convenient to consider it. Thus, for convenience a vector is usually visualized in a rectangular system of coordinates, and the projections of the vector on the coordinate axes are taken as its components. Measurements are then performed in this system of coordinates. Or, if more convenient, the vector is decomposed into components in a spherical, cylindrical, or any other system of coordinates. It should be clear from physical considerations that the particular system of coordinates used is merely a convenience and does not, in any way, affect the vector. However, the physical concept of a vector is a vaguely conceived entity which is independent of any system of coordinates. In order to specify a vector analytically it is usual to associate the vector with a system of coordinates (or a system of measurement) and its components (or measure numbers) in this system of coordinates. The terms "system of coordinates" and "components of a vector", which shall be adhered to in this paper, are usually associated with a definite geometrical picture. For analytical purposes it may be more convenient to substitute such terms as "a system of measurement" and "measure numbers".

As stated above, although a vector is independent of the system of coordinates, it is customary to associate it with a system of coordinates. How then may a vector be defined to be useful in analytical work? The definition must contain the property that a vector is independent of any system of coordinates, and yet to be useful it must be defined in terms of components in a system of coordinates. Such a definition follows: Given any three[3] numbers A^1, A^2, A^3,[4] associated with a system of coordinates (X_1, X_2, X_3) or (X, Y, Z) then if these numbers become $A^{1'}$, $A^{2'}$, $A^{3'}$ when transformed to a new system of coordinates (X_1', X_2', X_3') such that

$$
\begin{aligned}
A^{1'} &= \frac{\partial X_1'}{\partial X_1} A^1 + \frac{\partial X_1'}{\partial X_2} A^2 + \frac{\partial X_1'}{\partial X_3} A^3 = \sum_{\alpha=1}^{3} \frac{\partial X_1'}{\partial X_\alpha} A^\alpha \\
A^{2'} &= \frac{\partial X_2'}{\partial X_1} A^1 + \frac{\partial X_2'}{\partial X_2} A^2 + \frac{\partial X_2'}{\partial X_3} A^3 = \sum_{\alpha=1}^{3} \frac{\partial X_2'}{\partial X_\alpha} A^\alpha \qquad (1) \\
A^{3'} &= \frac{\partial X_3'}{\partial X_1} A^1 + \frac{\partial X_3'}{\partial X_2} A^2 + \frac{\partial X_3'}{\partial X_3} A^3 = \sum_{\alpha=1}^{3} \frac{\partial X_3'}{\partial X_\alpha} A^\alpha
\end{aligned}
$$

then the three numbers A^1, A^2, A^3 are defined as the components of a contravariant vector.

[3] For the sake of simplicity the discussion here is limited to three dimensions or three independent variables.

[4] An upper suffix *does not stand for an exponent,* but is merely used to indicate various A's.

This definition of a vector is useful in analytical work since the transformation equations (1) guarantee that the vector whose components are the three numbers A^1, A^2, A^3 in (X_1, X_2, X_3) and $A^{1'}$, $A^{2'}$, $A^{3'}$ in (X_1', X_2', X_3') is independent of the system of coordinates, and yet the definition is made in terms of coordinate systems. Analytically, therefore, a contravariant vector is a set of three numbers (A^1, A^2, A^3) different in different coordinate systems, but related by equations (1). However, the relations given by equations (1) are not the only relations that may be used to define a vector. If a set of three numbers A_1, A_2, A_3 in coordinate system (X_1, X_2, X_3) becomes A_1', A_2', A_3' in the coordinate system (X_1', X_2', X_3') where

$$A_1' = \frac{\partial X_1}{\partial X_1'} A_1 + \frac{\partial X_2}{\partial X_1'} A_2 + \frac{\partial X_3}{\partial X_1'} A_3 = \sum_{\alpha=1}^{3} \frac{\partial X_\alpha}{\partial X_1'} A_\alpha$$

$$A_2' = \frac{\partial X_1}{\partial X_2'} A_1 + \frac{\partial X_2}{\partial X_2'} A_2 + \frac{\partial X_3}{\partial X_2'} A_3 = \sum_{\alpha=1}^{3} \frac{\partial X_\alpha}{\partial X_2'} A_\alpha \qquad (2)$$

$$A_3' = \frac{\partial X_1}{\partial X_3'} A_1 + \frac{\partial X_2}{\partial X_3'} A_2 + \frac{\partial X_3}{\partial X_3'} A_3 = \sum_{\alpha=1}^{3} \frac{\partial X_\alpha}{\partial X_3'} A_\alpha$$

then the set of numbers (A_1, A_2, A_3) is defined as a covariant vector. Both equations (1) and (2) guarantee that the vectors defined in terms of their components shall be independent of coordinate systems. There seem to be no other relations which will guarantee this property.

The transformation equations (1) and (2) are identical in the case of transformation from one rectangular system of coordinates to another. Hence if only rectangular systems are considered, as is done in elementary analysis, the difference between covariant and contravariant vectors disappears. In oblique coordinates there is a difference between contravariant and covariant vectors. Contravariant vectors are indicated by superscripts and covariant vectors by subscripts. Vectors such as velocity and current are contravariant because they transform according to equation (1), while the gradient of a potential and electromotive force are covariant because they transform according to equation (2).

A vector as just defined is a tensor of the first rank. The number of components necessary to specify the vector represents the number of dimensions (or independent variables) used in describing the vector. In the above definition only three dimensions were used, but the definition of a vector as given by equations (1) and (2) is easily extended to apply to any number of dimensions. There are some physical concepts such as stress, strain, and impedance which *in general* require nine components in three dimensional systems and n^2 components in n dimensional systems and a system of coordinates in order to be specified analytically. Like vectors such quantities are also independent of the coordinate system in which it is convenient to consider them. Such quantities are called tensors of the second rank, and are defined analytically as follows: if a set of nine numbers A^{11}, A^{12}, A^{13}, A^{21}, A^{22}, A^{23}, A^{31}, A^{32}, A^{33} when transformed to a new set of coordinates become $A^{11'}$, $A^{12'}$, $A^{13'}$, $A^{21'}$, $A^{22'}$, $A^{23'}$, $A^{31'}$, $A^{32'}$, $A^{33'}$ where

$$A^{\mu\nu'} = \sum_{\alpha=1}^{3} \sum_{\beta=1}^{3} \frac{\partial X_{\mu}'}{\partial X_{\alpha}} \frac{\partial X_{\nu}'}{\partial X_{\beta}} A^{\alpha\beta} \qquad \begin{matrix} \mu = 1, 2, 3 \\ \nu = 1, 2, 3 \end{matrix} \tag{3}$$

then the quantities $A^{\alpha\beta}$ constitute the components of a contravariant tensor of the second rank. Similarly covariant tensors of the second rank transform according to the nine relations

$$A_{\mu\nu}' = \sum_{\alpha=1}^{3} \sum_{\beta=1}^{3} \frac{\partial X_{\alpha}}{\partial X_{\mu}'} \frac{\partial X_{\beta}}{\partial X_{\nu}'} A_{\alpha\beta} \qquad \begin{matrix} \mu = 1, 2, 3 \\ \nu = 1, 2, 3 \end{matrix} \quad . \tag{4}$$

Finally mixed tensors of the second rank transform according to the nine relations

$$A_{\mu}{}^{\nu'} = \sum_{\alpha=1}^{3} \sum_{\beta=1}^{3} \frac{\partial X_{\alpha}}{\partial X_{\mu}'} \frac{\partial X_{\nu}'}{\partial X_{\beta}} A_{\alpha}{}^{\beta} \qquad \begin{matrix} \mu = 1, 2, 3 \\ \nu = 1, 2, 3 \end{matrix} \quad . \tag{5}$$

Equations (3), (4), and (5) seem to be the only transformations which guarantee that tensors of the second rank defined in terms of their components shall be independent of coordinate systems.

It is to be noted that each of the equations (3), (4), and (5) consist of nine equations with nine terms on the right-hand side of each. As is the case with tensors of the first rank the three types of tensors of the second rank become identical for transformations from one rectangular system of coordinates to another.

It is customary in tensor analysis to adopt the convention that whenever a literal suffix appears twice in a term that term is to be summed for values of the suffix that is indicated. Thus instead of writing equation (1) as

$$A^{\mu'} = \sum_{\alpha=1}^{3} \frac{\partial X_{\mu}'}{\partial X_{\alpha}} A^{\alpha} \qquad \mu = 1, 2, 3 \tag{1}$$

it is written, according to this convention, as

$$A^{\mu'} = \frac{\partial X_{\mu'}}{\partial X_a} A^{\alpha} \qquad \mu = 1, 2, 3 \qquad (1)$$

Similarly equations (2), (3), (4), and (5) are written as

$$A_{\mu'} = \frac{\partial X_a}{\partial X_{\mu'}} A_a \qquad \mu = 1, 2, 3 \qquad (2)'$$

$$A^{\mu\nu'} = \frac{\partial X_{\mu'}}{\partial X_a} \frac{\partial X_{\nu'}}{\partial X_B} A^{\alpha\beta} \qquad \mu, \nu = 1, 2, 3 \qquad (3)'$$

$$A_{\mu\nu'} = \frac{\partial X_a}{\partial X_{\mu'}} \frac{\partial X^{\beta}}{\partial X_{\nu'}} A_{aB} \qquad \mu, \nu = 1, 2, 3 \qquad (4)'$$

$$A_{\mu}^{\nu'} = \frac{\partial X_a}{\partial X_{\mu'}} \frac{\partial X_{\nu'}}{\partial X_B} A_a^{\beta} \qquad \mu, \nu = 1, 2, 3 \qquad (5)'$$

There are some concepts which require 27 and 81 components for specification in a three dimensional system and n^3 and n^4 components respectively in an n dimensional system. Such quantities are called tensors of the third and fourth rank respectively. They also are classified as covariant, contravariant, and mixed and are defined by transformations which are generalizations of equations (3)′, (4)′, and (5)′. The relation between the number of components and the type of quantity may be summarized as follows:

Quantity	Number of components required for specification in n dimensions
tensor of zero rank-scalar	$n^0 = 1$
tensor of first rank-vector	$n^1 = n$
tensor of second rank	n^2
tensor of mth rank	n^m

Two rules of tensor analysis which are important for this paper and which follow from the above definitions of a tensor are:

1. The sum of two tensors of the same rank and of the same covariant and contravariant character is a tensor of that rank and character.
2. The product of two tensors such as A^{μ} and $B_{\mu\nu}$ is $A^{\mu} B_{\mu\nu} = C\nu$, i.e., the covariance suffix and contravariance suffix cancel each other.

Application of Tensor Concept to Equivalent Circuits

In terms of tensors Ohm's Law is written as

$$e_\alpha = Z_{\alpha\beta}\, i^\beta \qquad \alpha, \beta = 1, 2, 3, \cdots n \tag{6}$$

where the voltage tensor e_α is a covariant tensor of the first rank, the current tensor i^β is a contravariant tensor of the first rank, and the impedance tensor $Z_{\alpha\beta}$ is a covariant tensor of the second rank. The physics of the set of equations (6) is recognized as soon as it is written out in full. Thus,

$$\begin{aligned} e_1 &= Z_{11}i^1 + Z_{12}i^2 + Z_{13}i^3 + \cdots + Z_{1n}i^n \\ e_2 &= Z_{21}i^1 + Z_{22}i^2 + Z_{23}i^3 + \cdots + Z_{2n}i^n \\ e_n &= Z_{n1}i^1 + Z_{n2}i^2 + Z_{n3}i^3 + \cdots + Z_{nn}i^n \end{aligned} \tag{6}$$

from which it is seen that equation (6) represents an n mesh network, where the mesh currents are the components of the contravariant tensor i^β, the mesh voltages are the components of the covariant tensor e_α and the self and mutual mesh impedances are the components of the covariant tensor of the second rank $Z_{\alpha\beta}$. The tensor $Z_{\alpha\beta}$ written as the sum of three tensors is

$$Z_{\alpha\beta} = R_{\alpha\beta} + pL_{\alpha\beta} + \frac{1}{p} S_{\alpha\beta}$$

where $R_{\alpha\beta}$ is the resistance tensor, $L_{\alpha\beta}$ is the inductance tensor, $S_{\alpha\beta}$ is the stiffness or capacitance tensor and p and $\frac{1}{p}$ are the operators indicating $\frac{d}{dt}$ and $\int dt$ respectively. It is worth noting that the number of meshes corresponds to the number of dimensions. Equation (6) corresponds, therefore, to a tensor equation in an n dimensional system.

For the application of tensor analysis to equivalent circuits consider the problem of the determination of a group of two-terminal networks equivalent at all frequencies to a given two-terminal network. Referring to Figure 1, the problem is to determine a group of networks equivalent to it, i.e., having the same input impedance at all frequencies. In terms of tensor analysis the problem may be restated as: to transform the currents $i^1, i^2, i^3, \cdots, i^n$ of the given n mesh network of Figure 1, to any other set of currents $i^{1'}, i^{2'}, i^{3'}, \cdots i^{n'}$ with the stipulations that applied voltage and input current remain the same. Let such a transformation be

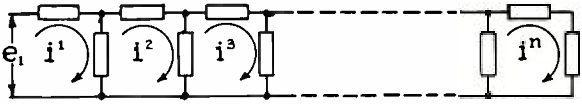

Fig. 1

$$
\begin{aligned}
i^1 &= i^{1'} \\
i^2 &= a_{21}i^{1'} + a_{22}i^{2'} + a_{23}i^{3'} + \cdots + a_{2n}i^{n'} \\
i^3 &= a_{31}i^{1'} + a_{32}i^{2'} + a_{32}i^{3'} + \cdots \quad \cdots + a_{3n}i^{n'} \\
&\cdot \\
&\cdot \\
&\cdot \\
&\cdot \\
i^n &= a_{n1}i^{1'} + a_{n2}i^{2'} + a_{n3}i^{3'} + \cdots + a_{nn}i^{n'}
\end{aligned}
\tag{7}
$$

where the a's are arbitrary constants. This transformation leaves the old input current the same as the new, but it makes the old mesh currents linear combinations of the new mesh currents. This transformation corresponds to a transformation of coordinates and the i's correspond to the X's of the first part of the paper.

Since the voltage tensor is covariant it transforms according to equation (2), i.e.,

$$e_{\mu'} = e_a \frac{\partial i^\alpha}{\partial i^{\mu'}} \qquad \alpha, \mu = 1, 2, 3, \cdots, n.$$

or written out in full

$$
\begin{aligned}
e_1' &= e_1 \frac{\partial i^1}{\partial i^{1'}} + e_2 \frac{\partial i^2}{\partial i^{1'}} + e_3 \frac{\partial i^3}{\partial i^{1'}} + \cdots + e_n \frac{\partial i^n}{\partial i^{1'}} \\
e_2' &= e_1 \frac{\partial i^1}{\partial i^{2'}} + e_2 \frac{\partial i^2}{\partial i^{2'}} + e_3 \frac{\partial i^3}{\partial i^{2'}} + \cdots + e_n \frac{\partial i^n}{\partial i^{2'}} \\
&\cdot \\
&\cdot \\
&\cdot \\
&\cdot \\
e_n' &= e_1 \frac{\partial i^1}{\partial i^{n'}} + e_2 \frac{\partial i^2}{\partial i^{n'}} + e_3 \frac{\partial i^3}{\partial i^{n'}} + \cdots + e_n \frac{\partial i^n}{\partial i^{n'}}
\end{aligned}
\tag{8}
$$

However, it was assumed in the circuit of Figure 1 that the only component of the tensor e_a that does not vanish is e_1, hence equations (8) reduced to

$$
\begin{aligned}
e_1' &= e_1 \frac{\partial i^1}{\partial i^{1'}} \\
e_2' &= e_1 \frac{\partial i^1}{\partial i^{2'}} \\
&\cdot \\
&\cdot \\
&\cdot \\
e_n' &= e_1 \frac{\partial i^1}{\partial i^{n'}} \quad .
\end{aligned}
\tag{9}
$$

Further, in order that the applied voltages remain the same it is necessary that $e_1' = e_1$ and $e_2' = e_3' = \cdot \cdot \cdot = e_n' = 0$. Hence it is necessary that

$$\frac{\partial i^1}{\partial i^{1'}} = 1 \qquad \frac{\partial i^1}{\partial i^{2'}} = \frac{\partial i^1}{\partial i^{3'}} = \cdot \cdot \cdot \cdot = \frac{\partial i^1}{\partial i^{n'}} = 0 \quad .$$

It is seen that the above conditions are fulfilled by the transformation equation (7).

The problem now is to determine how the circuit constants may change under the transformation (7). This is determined by the fact that $R_{\alpha\beta}$, $L_{\alpha\beta}$, and $S_{\alpha\beta}$ are covariant tensors of the second rank and hence transform according to equation (4)′, i.e.,

$$
\begin{aligned}
R_{\mu\nu}' &= R_{\alpha\beta} \frac{\partial i^\alpha}{\partial i^{\mu'}} \frac{\partial i^\beta}{\partial i^{\nu'}} \\
L_{\mu\nu}' &= L_{\alpha\beta} \frac{\partial i^\alpha}{\partial i^{\mu'}} \frac{\partial i^\beta}{\partial i^{\nu'}} \\
S_{\mu\nu}' &= S_{\alpha\beta} \frac{\partial i^\alpha}{\partial i^{\mu'}} \frac{\partial i^\beta}{\partial i^{\nu'}} \quad .
\end{aligned}
\tag{10}
$$

Writing out the resistance tensor in full (the others are identical in form) there results

$$R_{11}' = R_{11} \frac{\partial i^1}{\partial i^{1'}} \frac{\partial i^1}{\partial i^{1'}} + R_{12} \frac{\partial i^1}{\partial i^{1'}} \frac{\partial i^2}{\partial i^{1'}} + \cdot \cdot \cdot \cdot \cdot \cdot + R_{nn} \frac{\partial i^n}{\partial i^{1'}} \frac{\partial i^n}{\partial i^{1'}}$$

$$R_{12}' = R_{11}\frac{\partial i^1}{\partial i^{1'}}\frac{\partial i^1}{\partial i^{2'}} + R_{12}\frac{\partial i^1}{\partial i^{1'}}\frac{\partial i^2}{\partial i^{2'}} + \cdots + R_{nn}\frac{\partial i^n}{\partial i^{1'}}\frac{\partial i^n}{\partial i^{2'}}$$

$$\vdots \qquad (11)$$

$$R_{nn}' = R_{11}\frac{\partial i^1}{\partial i^{n'}}\frac{\partial i^1}{\partial i^{n'}} + R_{12}\frac{\partial i^1}{\partial i^{n'}}\frac{\partial i^2}{\partial i^{n'}} + \cdots + R_{nn}\frac{\partial i^n}{\partial i^{n'}}\frac{\partial i^n}{\partial i^{n'}}$$

From equations (7) and (11) and the fact that $R_{mn} = R_{nm}$, it then follows that

$$R_{11}' = R_{11} + 2a_{21}R_{12} + a_{21}^2 R_{22} + 2a_{31}R_{13} + 2a_{21}a_{31}R_{23} + a_{31}^2 R_{33} + \cdots + a_{n1}^2 R_{nn}$$

$$R_{12}' = a_{22}R_{12} + a_{21}a_{22}R_{22} + a_{32}R_{13} + a_{21}a_{32}R_{23} + a_{31}a_{22}R_{23} + a_{31}a_{32}R_{33} + \cdots + a_{n1}a_{n2}R_{nn}$$

$$R_{22}' = a_{22}^2 R_{22} + 2a_{22}a_{32}R_{23} + a_{32}^2 R_{33} + \cdots + a_{n2}^2 R_{nn}$$

$$R_{13}' = a_{23}R_{12} + a_{21}a_{23}R_{22} + a_{33}R_{13} + a_{21}a_{33}R_{23} + a_{31}a_{23}R_{23} + a_{31}a_{33}R_{33} + \cdots + a_{n1}a_{n3}R_{nn}$$

$$R_{23}' = a_{22}a_{23}R_{22} + a_{22}a_{33}R_{23} + a_{32}a_{23}R_{32} + a_{32}a_{33}R_{33} + \cdots + a_{n2}a_{n3}R_{nn}$$

$$R_{33}' = a_{23}^2 R_{22} + 2a_{23}a_{33}R_{23} + a_{33}^2 R_{33} + \cdots \cdots + a_{n3}R_{nn}$$

$$\vdots$$

$$R_{nn}' = a_{2n}^2 R_{22} + \cdots \cdots + a_{nn}^2 R_{nn}\ . \qquad (12)$$

By assigning various suitable values to the arbitrary constants denoted by the various a's in equation (7) one obtains from equation (12) the values of resistance, inductance, and stiffness (or capacity) for any number of circuits having the same impedance as the given circuit of Figure 1.

A simple example will illustrate the method. Given the two-terminal network shown in Figure 2(a) it is desired to find one or more networks having the identical input impedance at all frequencies as the network of Figure 2(a).

Since this circuit has only two meshes, n of the previous equations is 2 and equations (12) reduced to

$$\begin{aligned} L_{11}' &= L_{11} + 2a_{21} L_{12} + a_{21}^2 L_{22} \\ L_{12}' &= a_{22} L_{12} + a_{21} a_{22} L_{22} \\ L_{22}' &= a_{22}^2 L_{22} \end{aligned} \tag{13}$$

$$\begin{aligned} S_{11}' &= S_{11} + 2a_{21} S_{12} + a_{21}^2 S_{22} \\ S_{12}' &= a_{22} S_{12} + a_{21} a_{22} S_{22} \\ S_{22}' &= a_{22}^2 S_{22} \end{aligned} \tag{14}$$

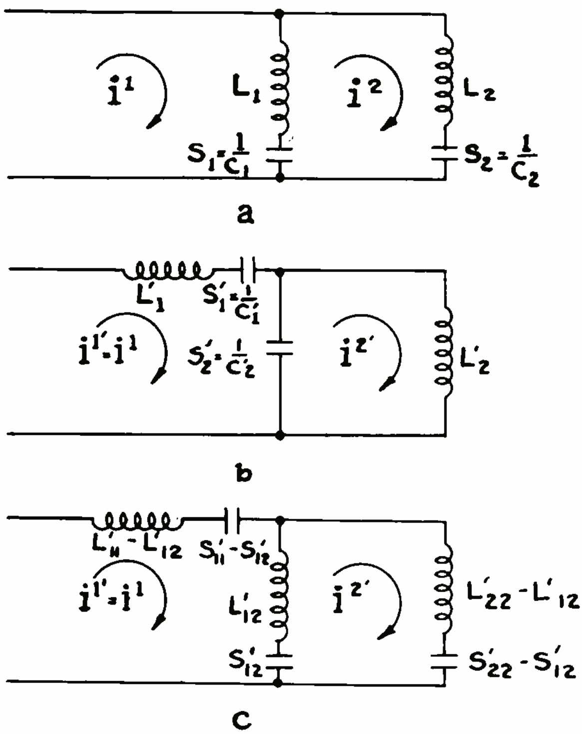

Fig. 2

Various networks having the primed values of inductances and stiffness are then obtained by assigning suitable values to the arbitrary constants a_{21} and a_{22}.

As a numerical example let

$$a_{21} = -0.5 \quad \text{and} \quad a_{22} = -0.1$$

Further let

$$L_1 = 1 \qquad L_2 = 1$$

$$S_1 = 2 \qquad S_2 = 3$$

then

$$L_{11} = L_{12} = L_1 = 1 \qquad L_{22} = L_1 + L_2 = 2$$

$$S_{11} = S_{12} = S_1 = 2 \qquad S_{22} = S_1 + S_2 = 5$$

Inserting these numbers into equations (13) and (14) there results that

$$L_{11}' = .5 \qquad S_{11}' = 1.25$$

$$L_{12}' = 0 \qquad S_{12}' = 0.05$$

$$L_{22}' = 0.02 \qquad S_{22}' = 0.05$$

The primed circuit which has the identical impedance as the unprimed circuit of Figure 2(a) is shown in Figure 2(b) where (since $L'_{12} = 0$)

$$L_1' = L_{11}' = 0.5 \qquad S_1' = S_{11}' - S_{12}' = 1.20$$

$$L_2' = L_{22}' = 0.02 \qquad S_2' = S_{12}' = S_{22}' = 0.05$$

Equations (13) and (14) which apply to any two-mesh network of inductance and capacity may also be used for the following purpose. Given the networks of Figure 2(a) and Figure 2(b) determine the relation between the circuit constants in order that they have identical input impedance. To solve this problem it is necessary to determine a_{21} and a_{22}. This may be accomplished by noting two relations such as

$$L_{12}' = 0 = a_{22}L_{12} + a_{21}a_{22}L_{22} \tag{16}$$

$$S_{12}' = S_{22}' = a_{22}^2 S_{22} = a_{22}S_{12} + a_{21}a_{22}S_{22} \,. \tag{17}$$

From (16) it immediately follows that

$$a_{21} = -\frac{L_{12}}{L_{22}} = -\frac{L_1}{L_1 + L_2} \tag{18}$$

and inserting (18) into (17) there results that

$$a_{22} = \frac{S_{12} - \dfrac{L_{12}}{L_{22}} S_{22}}{S_{22}} = \frac{S_1}{S_1 + S_2} - \frac{L_1}{L_1 + L_2} . \qquad (19)$$

From the values of a_{21} and a_{22} as given by equation (18) and (19) the circuit constants of the two-terminal network shown in Figure 2(b) is determined which is equivalent at all frequencies to the network shown in Figure 2(a). Thus,

$$L_1' = \frac{L_1 L_2}{L_1 + L_2}$$

$$L_2' = \frac{(L_2 S_1 - L_1 S_2)^2}{(S_1 + S_2)^2 \, (L_1 + L_2)} \qquad (20)$$

$$S_1' = \frac{S_1 S_2}{S_1 + S_2}$$

$$S_2' = \frac{(L_2 S_1 - L_1 S_2)^2}{(S_1 + S_2) \, (L_1 + L_2)^2} .$$

In general the group of networks equivalent at all frequencies to the given network Figure 2(a) is from equations (13) and (14) and is shown in Figure 2(c). Figure 2(c) represents a large number of networks if both positive and negative circuit elements are used.

Another type of problem which may be solved with the aid of the tensor concept is the determination of a group of two-terminal networks having the same transfer impedance at all frequencies as a given network. In terms of tensors the problem may be restated as follows:

Referring to Figure 1 it is desired to transform the contravariant current tensor to another set of mesh currents (to another set of coordinates) whereby the components of the tensor in terms of the old mesh currents $i^1, i^2, i^3, \cdots i^n$ transform to $i^{1'}, i^{2'}, i^{3'}, \cdots i^{n'}$ with the conditions that $e_1' = e_1$, $e_2' = e_3' = \cdots = e_n' = 0$ and $i^m = i^{m'}$.

From the condition that the applied voltage remain unaltered and from equations (8) and (9) it follows that

$$\frac{\partial i^1}{\partial i^{1'}} = 1, \quad \frac{\partial i^1}{\partial i^{2'}} = \frac{\partial i^1}{\partial i^{3'}} = \cdots \frac{\partial i^1}{\partial i^{n'}} = 0,$$

and hence $i^1 = i^{1'}$. Since the transfer impedance of the mth mesh is to be unchanged, that is, $i^m = i^{m'}$ the transformation equations for the currents become

$$
\begin{aligned}
i^1 &= i^{1'} \\
i^2 &= a_{21}i^{1'} + a_{22}i^{2'} + a_{23}i^{3'} + \cdots + a_{2m}i^{m'} + \cdots + a_{2n}i^{n'} \\
i^3 &= a_{31}i^{1} + a_{32}i^{2'} + a_{33}i^{3'} + \cdots + a_{3m}i^{m'} + \cdots + a_{3n}i^{n'} \\
&\;\;\vdots \\
i^m &= \qquad\qquad\qquad\qquad i^{m'} \\
&\;\;\vdots \\
i^n &= a_{n1}i^{1'} + a_{n2}i^{2'} + a_{n3}i^{3'} + \cdots + a_{nm}i^{m'} + \cdots + a_{nn}i^{n'}. \qquad (21)
\end{aligned}
$$

The first equation of the set (21) shows that in order to obtain equivalent networks with regard to transfer impedance it is necessary that they are also equivalent with regard to input impedance.

The circuit constants of the group of networks having the same transfer impedance as the given network are thus determined from equations (12) (upon letting $a_{m1} = a_{m2} = \cdots = a_{m(m-1)} = 0$, $a_{mm} = 1$, $a_{m(m+1)} = a_{m(m+2)} = \cdots = a_{mn} = 0$).

As an example consider the 3 mesh shown in Figure 3(a). It is desired to find a group of networks having the same transfer impedance in the third mesh. For this case equations (21) and (12) reduce to

$$
\begin{aligned}
i^1 &= i^{1'} \\
i^2 &= a_{21}i^{1'} + a_{22}i^{2'} + a_{23}i^{3'} \qquad (22) \\
i^3 &= \qquad\qquad\qquad i^{3'}
\end{aligned}
$$

and

$$
\begin{aligned}
R_{11}' &= R_{11} + 2a_{21}R_{12} + a_{21}^2 R_{22} \\
R_{12}' &= a_{22}R_{12} + a_{21}a_{22}R_{22} \\
R_{22}' &= a_{22}^2 R_{22} \\
R_{13}' &= a_{23}R_{12} + a_{21}a_{23}R_{22} + R_{13} + a_{21}R_{23} \qquad (23)
\end{aligned}
$$

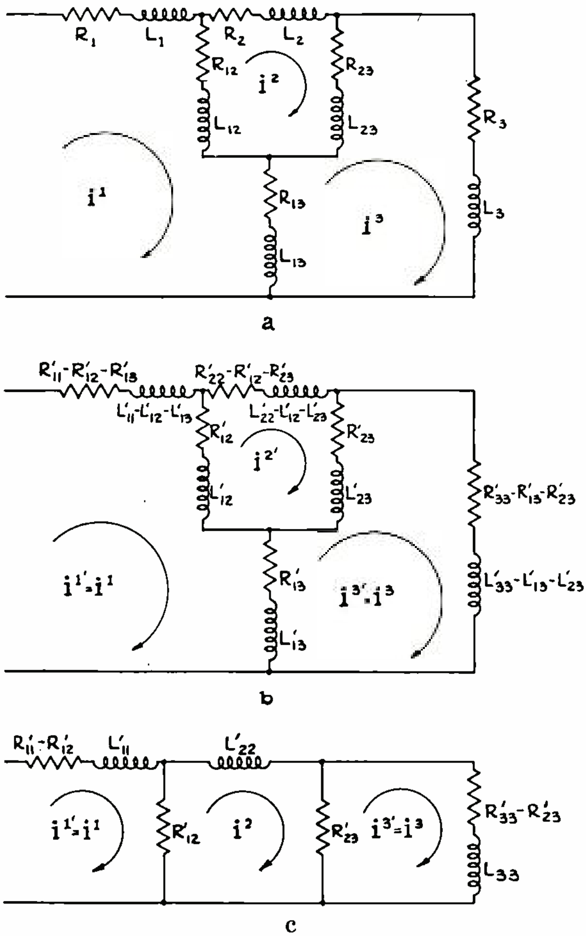

Fig. 3

$$
\begin{aligned}
R_{23}' &= a_{22}a_{23}R_{22} + a_{22}R_{23} \\
R_{33}' &= a_{23}^2\, R_{22} + 2a_{23}R_{23} + R_{33} \\
L_{11}' &= L_{11} + 2a_{21}L_{12} + a_{21}^2\, L_{22} \\
L_{12}' &= a_{22}L_{12} + a_{21}a_{22}L_{22} \\
L_{22}' &= a_{22}^2\, L_{22} \\
L_{13}' &= a_{23}L_{12} + a_{21}a_{23}L_{22} + L_{13} + a_{21}L_{23} \\
L_{23}' &= a_{22}a_{23}L_{22} + a_{22}L_{23} \\
L_{33}' &= a_{23}^2\, L_{22} + 2a_{23}L_{23} + L_{33}\ .
\end{aligned}
\qquad (24)
$$

respectively. In general the group of networks having the same transfer impedance in the third mesh (and also the same input impedance) as the given network of Figure 3(a) is by equations (23) and (24) shown in Figure 3(b).

As a numerical illustration let

$$a_{21} = -0.1 \qquad a_{22} = -0.2 \qquad a_{23} = -0.1.$$

Further let

$$\begin{aligned} R_1 &= 1 & L_1 &= 2.5 \\ R_{12} &= 10 & L_{12} &= 2.5 \\ R_2 &= 30 & L_2 &= 20 \\ R_{13} &= 1.5 & L_{13} &= .25 \\ R_{23} &= 10 & L_{23} &= 2.5 \\ R_3 &= 11 & L_3 &= 2.5 \end{aligned}$$

then

$$\begin{aligned} R_{11} &= 12.5 & L_{11} &= 5.25 \\ R_{12} &= 10 & L_{12} &= 2.5 \\ R_{22} &= 50 & L_{22} &= 25 \\ R_{13} &= 1.5 & L_{13} &= .25 \\ R_{23} &= 10 & L_{23} &= 2.5 \\ R_{33} &= 12.5 & L_{33} &= 5.25. \end{aligned}$$

Inserting these numbers into equations (23) and (24) there results that

$$\begin{aligned} R_{11}' &= 11 & L_{11}' &= 5 \\ R_{12}' &= 1 & L_{12}' &= 0 \\ R_{22}' &= 2 & L_{22}' &= 1 \\ R_{13}' &= 0 & L_{13}' &= 0 \\ R_{23}' &= 1 & L_{23}' &= 0 \\ R_{33}' &= 11 & L_{33}' &= 5. \end{aligned}$$

Figure 3(c) shows the network.

To determine the relations between the circuit constants of Figures 3(a) and 3(c) in order that they have identical input and transfer (with respect to the third mesh) impedances at all frequencies, it is necessary to determine the three arbitrary constants a_{21}, a_{22}, and a_{23}. This is accomplished by noting three relations such as

$$L_{12}' = a_{22}L_{12} + a_{21}a_{22}L_{22} = 0 \tag{25}$$

$$L_{23}' = a_{22}a_{23}L_{22} + a_{22}L_{23} = 0 \tag{26}$$

$$\begin{aligned} R_{22}' = R_{12}' + R_{23}' = a_{22}R_{12} + a_{21}a_{22}R_{22} + a_{22}a_{23}R_{22} \\ + a_{22}R_{23} = a_{22}^2 R_{22} \,. \end{aligned} \tag{27}$$

From equations (25) and (26) it immediately follows that

$$a_{21} = -\frac{L_{12}}{L_{22}}$$

$$a_{23} = -\frac{L_{23}}{L_{22}}$$

and inserting these into (27) there results that

$$a_{22} = \frac{R_{12} + R_{23}}{R_{22}} - \frac{L_{12} + L_{23}}{L_{22}} \,.$$

These values of a_{21}, a_{22}, and a_{23} inserted into equations (23) and (24) yield the required relations.

It is worth noting, in conclusion, that the application of the transformation equations of tensors to electric circuits is by no means limited to the cases discussed in this paper. For example, they may be simply used for determining networks in which the mesh currents are any given linear functions of the mesh currents of a given network.

OUR CONTRIBUTORS

WILLIAM A. R. BROWN attended the Massachusetts Institute of Technology and in 1916 entered the marine service of the Marconi Company. From 1921 to 1924 he was employed as transmitter engineer at RCA transoceanic stations, and from 1924 to 1927 at the WJZ broadcast station. He became Assistant Station Engineer of the WEAF broadcast station in 1927, and in 1928 was transferred to the technical staff of the National Broadcasting Company. Mr. Brown has conducted extensive correlation studies of short-wave transmission and solar activity. He is an associate member of I.R.E. and of A.I.E.E.

PHILIP S. CARTER received his A.B. degree in Mechanical Engineering from Stanford University in 1918. From May to December, 1918, he was in the Signal Corps of the United States Army, and from 1919 to 1921 was in the employ of the General Electric Company. Since 1921 he has been with the Radio Corporation of America and R.C.A. Communications, Inc., Engineering Department. Mr. Carter is an associate member of the Institute of Radio Engineers.

DAVID W. EPSTEIN received a B.S. degree in engineering physics from Lehigh University in 1930, an M.S. in 1934, and a D.Sc. in electrical engineering in 1937 from the University of Pennsylvania. Since joining RCA in 1930 he has been in the Research Department of the RCA Victor Division, RCA Manufacturing Company. Dr. Epstein is a member of the American Physical Society and an associate member of the Institute of Radio Engineers.

FRANK MASSA received a B.S. degree in electrical engineering in 1927, he held a Swope Fellowship in 1927-1928, and received his M.S. degree in electrical engineering at the Massachusetts Institute of Technology in 1928. He was a research engineer for the Victor Talking Machine Company in 1928-1929, and since then an electroacoustic research engineer for the RCA Manufacturing Company at Camden, N. J. Mr. Massa is a Fellow, Acoustical Society of America, and an associate member of the Institute of Radio Engineers.

LEON S. NERGAARD received his B.S. degree in electrical engineering from the University of Minnesota in 1927, following which he joined the General Electric Company serving in the Research Laboratory and Vacuum Tube Engineering Department until 1930. After receiving an M.S. degree in electrical engineering at Union College in 1930, he spent three years as teaching assistant in the department of physics at the University of Minnesota, from which institution he received his Ph.D. degree in 1935. Since 1933 he has been in the RCA Radiotron research laboratory. Dr. Nergaard is a member of Sigma Xi, the American Physical Society, and I.R.E.

WILLIAM D. PHELPS received the A.B. degree from DePauw University in 1929; the M.S. degree from the University of Oklahoma in 1931, and the Ph.D. degree from the University of Iowa in 1934. He was instructor in physics at the University of Iowa from 1931 to 1933, following which he served a year as research assistant and another year as research associate in physics at the same University. Since January, 1935, he has been a research physicist in the RCA Victor Division of the RCA Manufacturing Company. Dr. Phelps is a member of Sigma Xi and of the American Acoustical Society.

J. ERNEST SMITH, a native of Missouri, received a B.A. degree in mathematical physics from Jamestown College in 1932, and in the following year was a graduate scholar of the California Institute of Technology. He served as instructor in communication engineering at RCA Institutes from 1934 to 1938. Since 1935 he has been in the Central Office Laboratory of the Engineering Department of R.C.A. Communications, Inc.

BROWDER J. THOMPSON received a B.S. degree in electrical engineering from the University of Washington in 1925. From 1926 to 1931 he was engaged in vacuum tube research and development for the General Electric Company at Schenectady. From 1931 to the present he has been in charge of the Research Section, Research and Engineering Department, Radiotron Division, RCA Manufacturing Company, Harrison, N. J., engaged in television, ultra-short-wave, and other tube research problems. In 1936 Mr. Thompson was awarded the Morris Liebmann Memorial Prize by the Institute of Radio Engineers for important contributions to the ultra-short-wave field of radio. He is a Fellow of the Institute of Radio Engineers and a member of the American Physical Society.

BERTRAM TREVOR received his E.E. degree from Cornell University in 1928, and in the same year joined the Research and Development Division of R.C.A. Communications, Inc., where he has since remained. He is an associate member of the Institute of Radio Engineers.